Copyright Warning & Restrictions

The copyright law of the United States (Title 17, United States Code) governs the making of photocopies or other reproductions of copyrighted material.

Under certain conditions specified in the law, libraries and archives are authorized to furnish a photocopy or other reproduction. One of these specified conditions is that the photocopy or reproduction is not to be "used for any purpose other than private study, scholarship, or research." If a, user makes a request for, or later uses, a photocopy or reproduction for purposes in excess of "fair use" that user may be liable for copyright infringement,

This institution reserves the right to refuse to accept a copying order if, in its judgment, fulfillment of the order would involve violation of copyright law.

Please Note: The author retains the copyright while the New Jersey Institute of Technology reserves the right to distribute this thesis or dissertation

Printing note: If you do not wish to print this page, then select "Pages from: first page # to: last page #" on the print dialog screen

COMBINED FEEDFORWARD-FEEDBACK CONTROL OF A FLUIDIZED-BED REACTOR

BY

REGINALD EUGENE MITCHELL

A THESIS

PRESENTED IN PARTIAL FULFILLMENT OF

THE REQUIREMENTS FOR THE DEGREE

OF

MASTER OF SCIENCE IN CHEMICAL ENGINEERING

AT

NEWARK COLLEGE OF ENGINEERING

Newark, New Jersey
1970

APPROVAL OF THESIS

COMBINED FEEDFORWARD-FEEDBACK

CONTROL OF A FLUIDIZED-BED REACTOR

BY

REGINALD EUGENE MITCHELL

FOR

DEPARTMENT OF CHEMICAL ENGINEERING

NEWARK COLLEGE OF ENGINEERING

BY

FACULTY COMMITTEE

APPROVED :_____

_____

_____

NEWARK, NEW JERSEY

JUNE, 1970

ABSTRACT

Feedforward control, feedback control, and combined feedforward-feedback control were studied on an analog computer to evaluate their effectiveness in controlling a fluidized-bed reactor used for the decomposition of cumene. Proportional, proportional-integral, proportional-derivative, and proportional-integral-derivative modes of control were investigated. Step changes in set-point and load were used as disturbances. The Ziegler-Nichols method and the process reaction curve method of Cohen and Coon were compared in determining values of K_c, T_i, and T_d which gave optimum control of the fluidized-bed reactor.

Control equation were obtained from the block diagrams of the systems and solved on an EAI TR-20 Analog Computer.

It was found that tighter control of the fluidized-bed reactor was maintained when feedforward control was combined with feedback control for all modes of control studied. The Cohen and Coon reaction curve method and the Ziegler-Nichols method resulted in values of K_c, T_i, and T_d which gave equally good control.

TABLE OF CONTENTS

LIST OF FIGURES

CONTENTS (Con't)

LIST OF TABLES

INTRODUCTION

Significant advances have been made in the area of controlling chemical reactors. The conventional feedback system and the newer feedforward system have afforded fairly good control of a chemical reactor. These reactor systems have been affected by changes in load and set-point. In a feedback system the manipulated variable is responsive to changes in the control variable whereas in a feedforward system the manipulated variable is responsive to the disturbance rather than to the changes in the control variable. It should be pointed out that feedforward control systems allow for perfect control of the control variable since corrective action is taken before any affect is made to this variable. However, all transfer functions must be known exactly and all potential disturbances must be known. For feedback control all potential disturbances need not be known, but the control variable is affected by load and set-point changes. Hence, these two systems supplementing each other should bring about tighter control of a chemical reactor.

A study of the design of a combination feedforward-feedback control system for a continuous flow stirred tank reactor was presented in the EAI Bulletin No. ALAC64075,(3). It was concluded that combination feedforward-feedback systems controlled better those processes displaying large lag times. It is the purpose of this paper to investigate combined feedforward feedback control of a fluidized-bed reactor used for the decomposition of cumene.

A study of frequency response of gas mixing in a fluidized-

bed reactor was done by Barnstone and Harriott,(1). Several models were presented to explain gas mixing and reaction kinetics in a fluidized-bed. These models were based on the two-phase theory of fluidization. The differences in the models were attributed to the amount of weight placed on mixing in the dense phase. The two extremes, perfect mixing in the dense phase and plug flow in the dense phase, both resulted in an empirical transfer function to describe the system. It consisted of a distant time delay equal to the time it takes for a bubble to rise from the bottom to the surface of the bed. The response was first order and had a time constant equal to the holdup time of the bed,(1). Such a transfer function is denoted by:

$$G_p(s) = e^{-T_o s}/(T_1 s + 1) \qquad (1)$$

Here T_o is the bubble time delay, T_1 is the holdup time, and s is the Laplace transform variable.

According to the time-shift theorem of Perlmutter,(8), multiplication by $e^{-T_o s}$ in the s domain is the counterpart of a simple displacement in the time domain. However, in this study an approximation to $e^{-T_o s}$ was used to test its effect in simulation. Accounting for this term in computing the transient response of a control system is quite difficult. For this reason considerable work has been done on the computer simulation of the transportation lag. The transfer function describing this lag in terms of the complex frequency s is given by:

$$G(s) = e^{-T_o s} \qquad (2)$$

where T_o is the delay time constant. Expansion of this function into the Maclaurin series form results in:

$$G(s) = 1 - T_o s + \frac{(T_o s)^2}{2!} - \frac{(T_o s)^3}{3!} + \frac{(T_o s)^4}{4!} - \ldots + \ldots \qquad (3)$$

Holst (7) presents Padé-approximations which give the best values of this series expansion. In defining the Padé-approximation to $e^{-T_o s}$ Holst presents two polynomials whose ratio is given by:

$$F_{a,b} = \frac{N_{a,b}(x)}{D_{a,b}(x)} = \frac{N_o + N_1 x + N_2 x^2 + \ldots N_a x^a}{D_o + D_1 x + D_2 x^2 + \ldots D_b x^b} \qquad (4)$$

By choosing the orders a and b, and selecting the appropriate values for the coefficients N_o and D_o, the Padé-approximation is completely defined. Holst gives methods of obtaining the coefficients in $N_{a,b}(x)$ and $D_{a,b}(x)$ in his paper for the normal type of Padé-approximation where a=b=c, and the reduced type where a= b- 1. Results of the first twelve normal and reduced Padé-approximations are tabulated in the paper (7).

As an example of the accuracy of this approximation consider the second order Padé-approximation, a = b = 2.

$$F_{2,2}(x) = \frac{12 - 6x + x^2}{12 + 6x + x^2} \qquad (5)$$

This gives the first five terms of the Maclaurin series exactly and a final term $R_{2,2}(x)$ equal to :

$$R_{2,2}(x) = -\frac{x^5}{144} - \frac{x^7}{1728} \ldots \qquad (6)$$

The final terms of the Maclaurin series, $M_{2,2}(x)$ are

$$M_{2,2}(x) = -\frac{x^5}{120} + \frac{x^6}{720} \ldots \qquad (7)$$

The higher the order of the approximation, the more exact the value of $F_{a,b}$ is to the Maclaurin series. Figures 1 and 2 show that step responses for the Padé-approximations approach a perfect step response with increasing order.

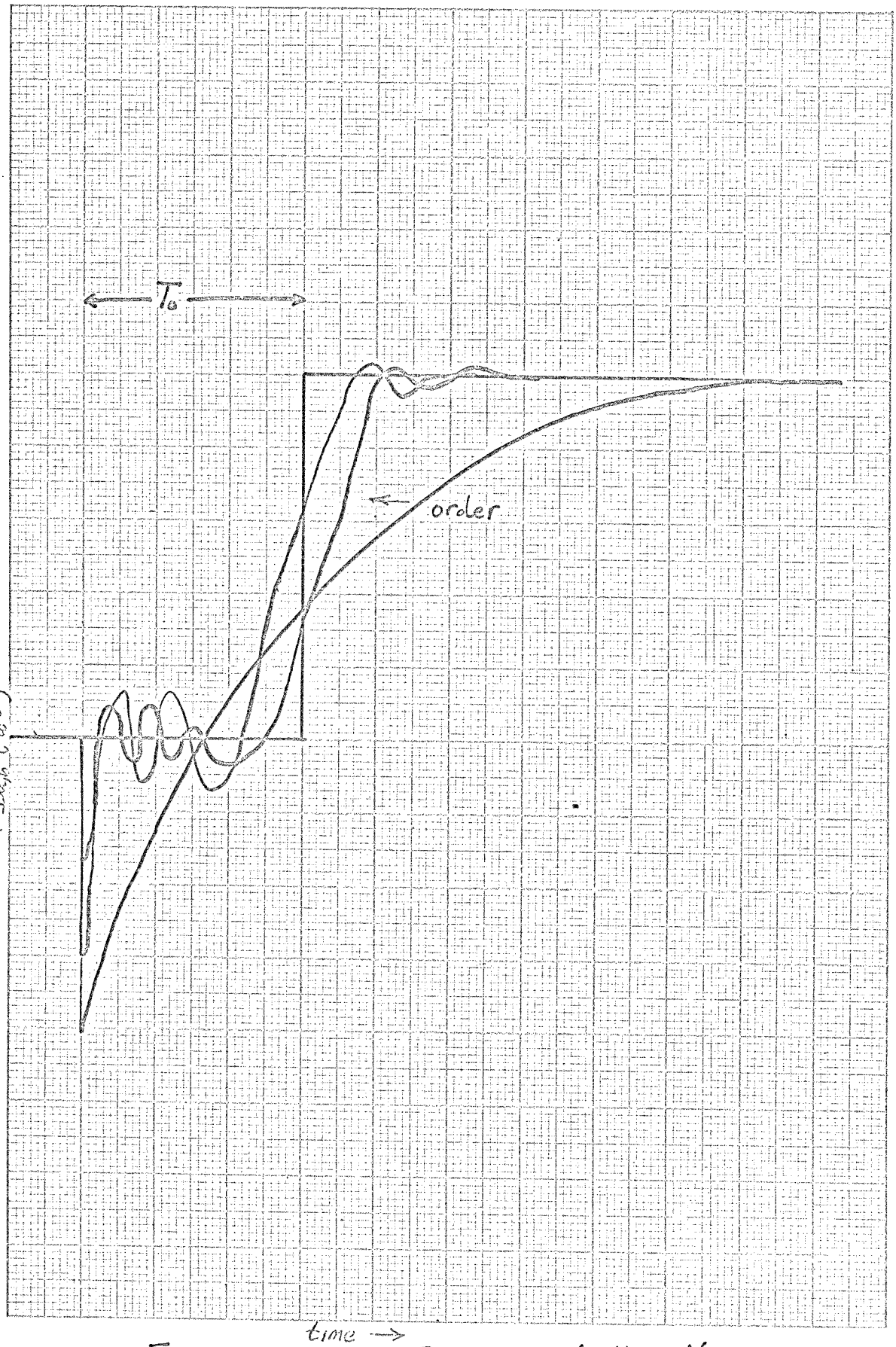

FIGURE 1 STEP RESPONSE of the Normal type Padé-approximation

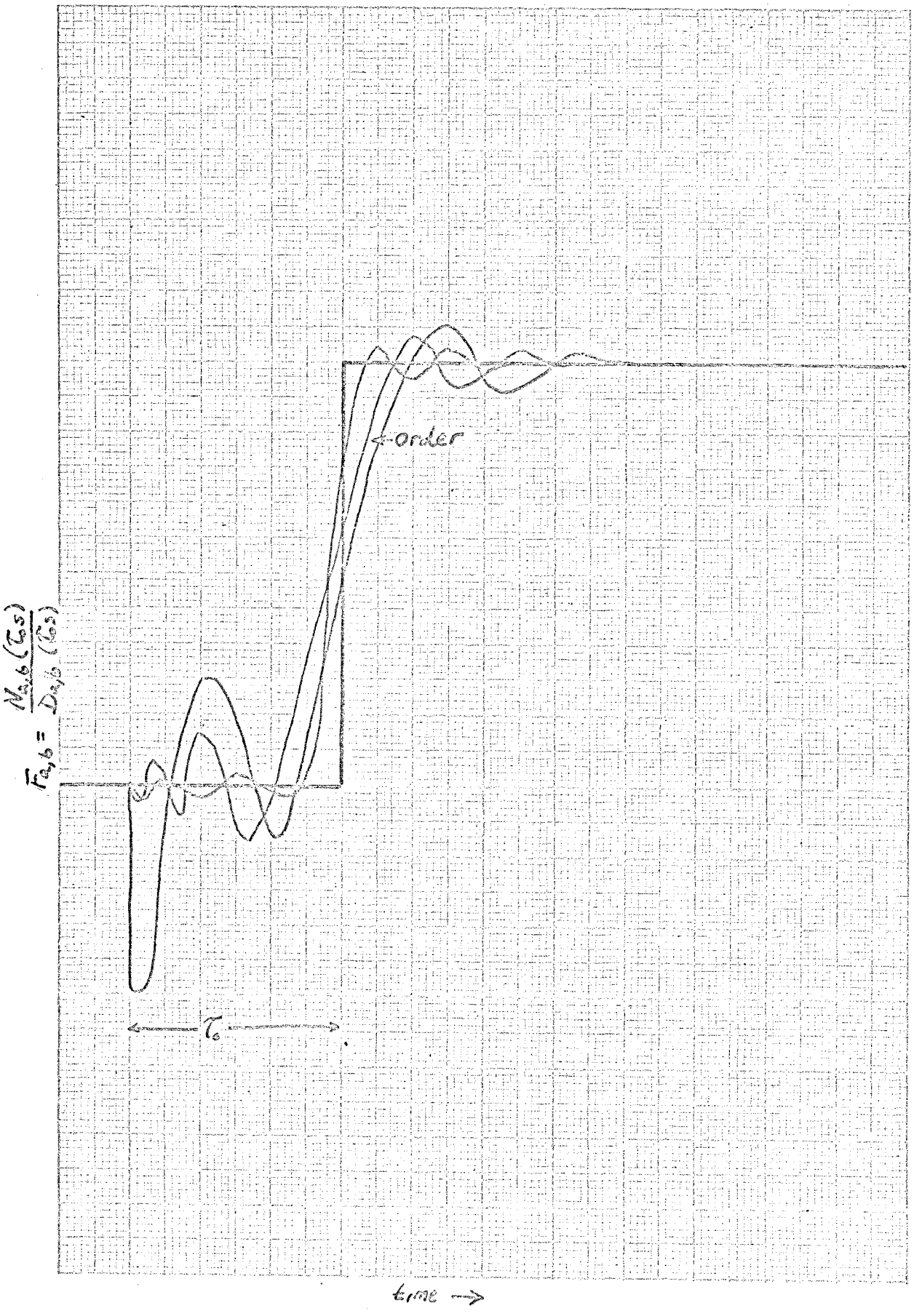

FIGURE 2 STEP RESPONSE of the Reduced type Padé Approximation

With this series expression for the time delay, it is now possible to simulate $e^{-T_o s}$ on an analog computer. Holst presents analog computer circuits for Padé-approximations of order c and reduced types of order b. See the Appendix (Fig.38), for the analog computer circuit of a second order Padé-approximation.

PROCEDURE EMPLOYED

Transient responses of the various systems were obtained and compared graphically. Steps employed in obtaining the transient response were as follows:

1. A signal flow block diagram was made of the system.
2. A control equation of the form

   $$Y(s) = G\ X(s)$$

   was obtained by block diagram algebra.
3. All blocks were evaluated.
4. The resulting equations were solved using an analog computer.
5. The resulting curves were compared.

The analog computer employed was an Electronics Associates, Inc. TR-20 computer.

THEORETICAL ANALYSIS

Reactor system:

The reactor system employed is the fluidized-bed described by Echigoya et al (5), in their paper concerning reaction conversion rates in fluidized-beds. The first order gas phase catalytic cracking reaction of cumene was carried out using silica alumina FCC catalyt. The reaction taking place is :

$$C_6H_5{\cdot}C_3H_7 = C_6H_6 + C_3H_6$$

One hundred- seventy five grams of the silica alumina FCC catalyst (average particle size range from 100-150 mesh), were heat treated to 600°C and fed to a three inch i.d., 3.15 inch high bed. The system was maintained at 450°C and one atmosphere, conditions at which secondary reactions did not occur. Cumene was diluted to a mole ratio of ten times with hydrogen and fed to the reactor at a rate of ten times the catalyst weight. The linear velocity of the gas flow was maintained at seven times the minimum fluidization velocity, (u_{mf} = 0.23 cm/sec).

Pertinent data concerning the reactor system is given in Table I. A schematic diagram of the reactor system is given in Figure 3.

TABLE I

REACTOR SYSTEM

Cross-sectional area of bed = A = 5.26×10^{-2} ft.

Total pressure = Π = 1 atmosphere

Temperature = 450°C

Mole fraction of cumene in feed stream = $y_c = 0.1$

Concentration of cumene in feed stream = $C_c = 1.051 \times 10^{-4}$ lbmoles/ft^3

Feed rate of cumene = F = 1.75 moles/hr

Volumetric flow rate of cumene = x(o) = 1.02×10^{-3} ft^3/sec

Superficial linear velocity = $7u_{mf} = w_o = 0.05275$ ft/sec

Superficial volumetric velocity = $v_o = 2.78 \times 10^{-3}$ ft^3/sec

Transportation delay time = $T_1 = 5$ sec.

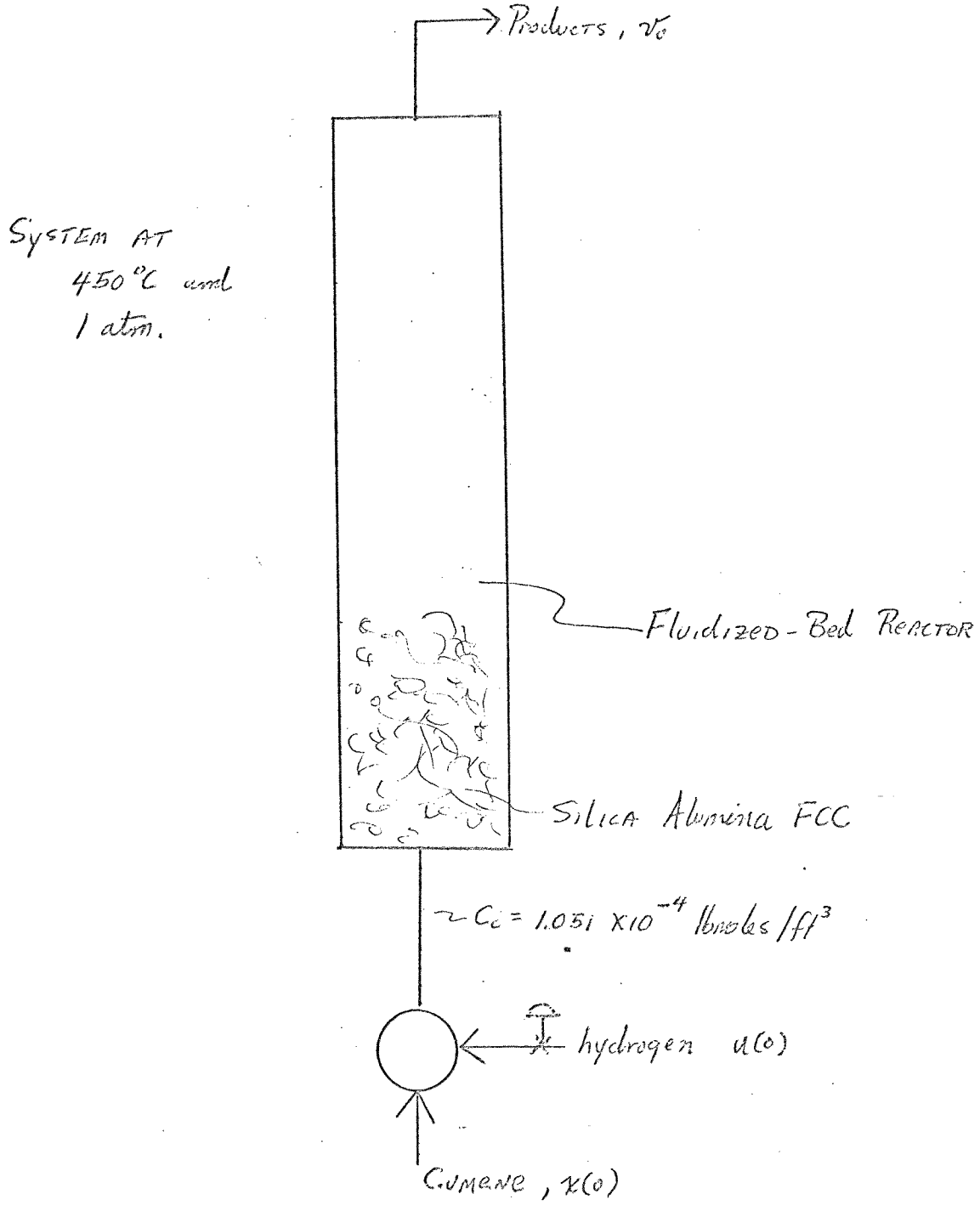

FIGURE 3 : Schematic Diagram of Reactor System

Block diagrams:

Figure 4 gives the block diagram for the feedforward control system. Utilizing block diagram algebra:

$$P(s) = R(s) - H_1 U(s) \tag{8}$$

$$X(s) = G_f(s)G_v K_x P(s) = G_f(s)G_v K_x R(s) - H_1 U(s) \tag{9}$$

$$Z(s) = G_f(s)G_v K_x [R(s) - H_1 U(s)] + K_u U(s) \tag{10}$$

$$Y_{ff}(s) = G_f(s)G_v K_x G_p(s) R(s) + [K_u - H_1 G_f(s) G_v K_x] G_p(s) U(s) \tag{11}$$

Figure 5 gives the block diagram for feedback control. From block diagram algebra:

$$E(s) = R(s) - H_2 Y_{fb}(s) \tag{12}$$

$$X(s) = K_x G_v G_c(s) E(s) = K_x G_v G_c(s) [R(s) - H_2 Y_{fb}(s)] \tag{13}$$

$$Z(s) = K_x G_v G_c(s) R(s) - K_x G_v G_c(s) H_2 Y_{fb}(s) + K_u U(s) \tag{14}$$

$$Y_{fb}(s) = K_x G_v G_c(s) G_p(s) R(s) - K_x G_v G_c(s) H_2 G_p(s) Y_{fb}(s) + G_p(s) K_u U(s) \tag{15}$$

Rearranging,

$$Y_{fb}(s) = \frac{K_x G_v G_c(s) G_p(s) R(s) + G_p(s) K_u U(s)}{1 + K_x G_v G_c(s) H_2 G_p(s)} \tag{16}$$

Figure 6 shows the block diagram for the combined feedforward-feedback control system. Employing block diagram algebra:

$$V(s) = R_f(s) - H_1 U(s) \tag{17}$$

$$F(s) = G_f(s) V(s) = G_f(s) R_f(s) - G_f(s) H_1 U(s) \tag{18}$$

$$E(s) = R(s) - H_2 Y_{fffb}(s) \tag{19}$$

$$M(s) = G_c(s) R(s) - H_2 G_c(s) Y_{fffb}(s) \tag{20}$$

$$P(s) = G_f(s) R_f(s) - H_1 G_f(s) U(s) + G_c(s) R(s) - H_2 G_c(s) Y_{fffb}(s) \tag{21}$$

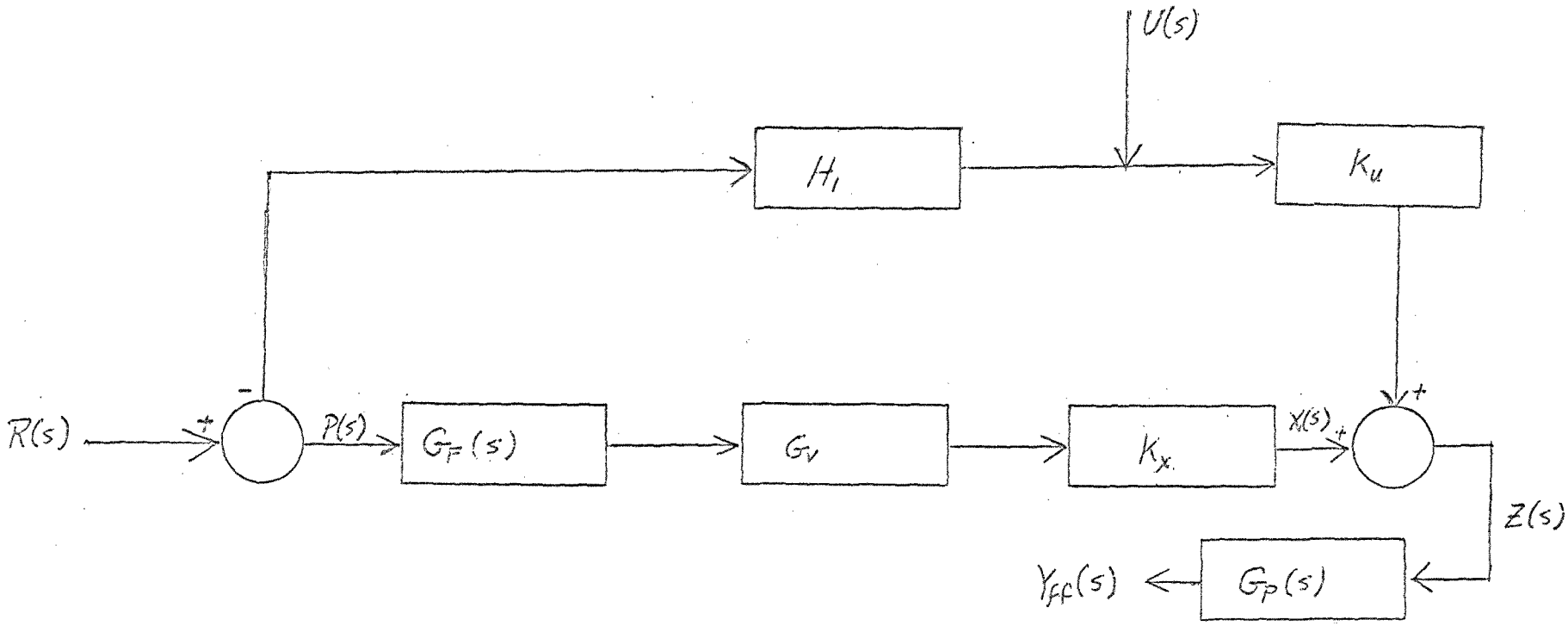

FIGURE 4 FEEDFORWARD SYSTEM : BLOCK DIAGRAM.

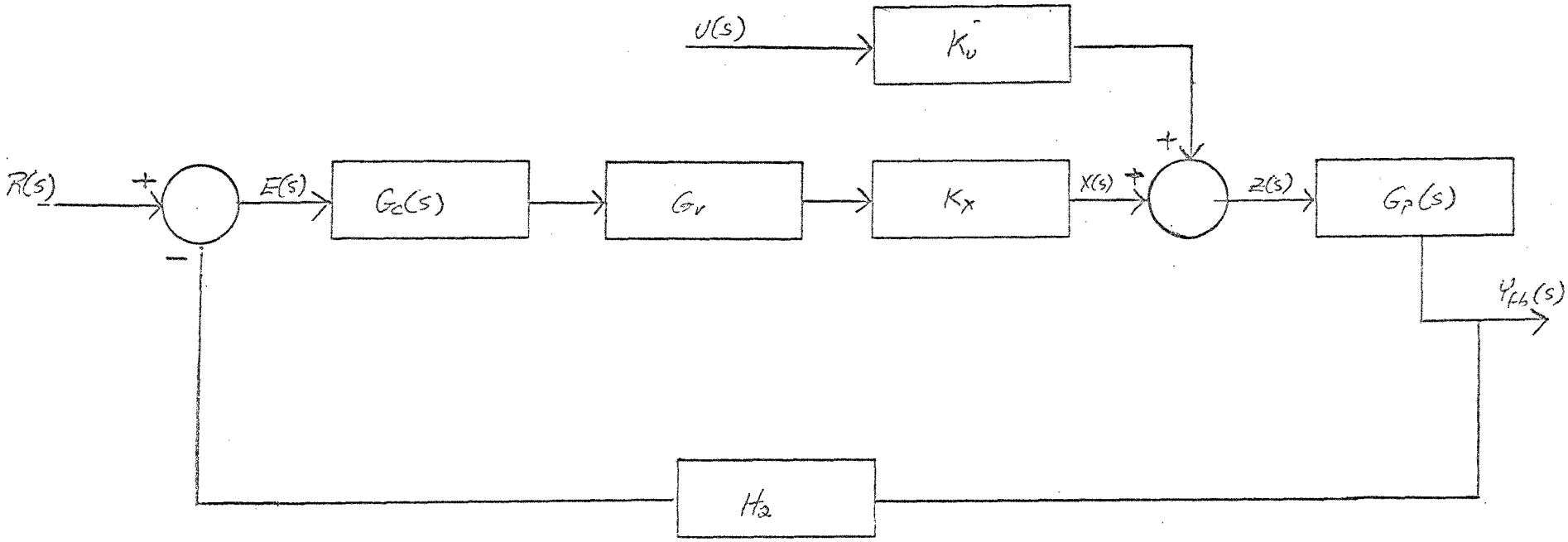

FIGURE 5 Feedback Control System : Block Diagram

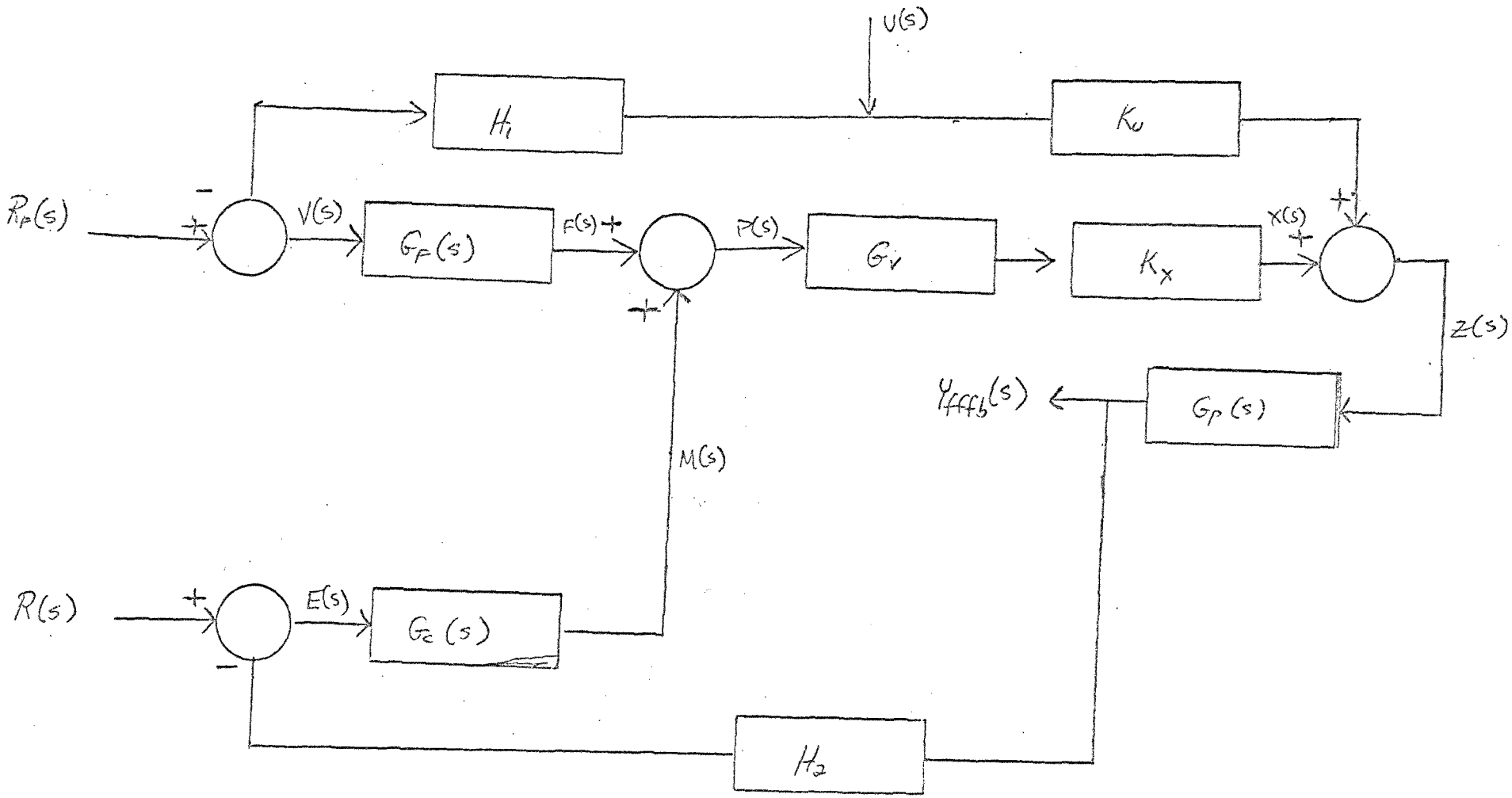

FIGURE 6 FEEDFORWARD FEEDBACK SYSTEM : BLOCK DIAGRAM

$$X(s) = K_x G_v G_f(s) R_f(s) - K_x G_v H_1 G_f(s) U(s) + K_x G_v G_c(s) R(s) - K_x G_v H_2 G_c(s) Y_{fffb}(s) \quad (22)$$

$$Z(s) = K_x G_v G_f(s) R_f(s) - K_x G_v H_1 G_f(s) U(s) + K_x G_v G_c(s) R(s) + K_u U(s) - K_x G_v H_2 G_c(s) Y_{fffb}(s) \quad (23)$$

$$Y_{fffb}(s) = K_x G_v G_f(s) G_p(s) R_f(s) - K_x G_v G_f(s) H_1 G_p(s) U(s) + K_x G_v G_c(s) G_p(s) R(s) - K_x G_v H_2 G_c(s) G_p(s) Y_{fffb}(s) + K_u G_p(s) U(s) \quad (24)$$

Rearranging,

$$Y_{fffb}(s) = \frac{K_x G_v G_p(s) \left[G_f(s) R_f(s) + G_c(s) R(s) \right]}{1 + K_x G_v H_2 G_c(s) G_p(s)} + \frac{\left[K_x G_v G_f(s) H_1 + K_u \right] G_p(s) U(s)}{1 + K_x G_v H_2 G_c(s) G_p(s)} \quad (25)$$

Equations 11, 16 and 25 are the control equations used to obtain the transient responses of the reactor system.

Evaluation Of Transfer Functions:

As stated earlier the process transfer function $G_p(s)$ is the function derived by Barnstone and Harriott(1). Thus

$$G_p(s) = \frac{e^{-T_o s}}{T_1 s + 1} \tag{1}$$

The units of the solvent flow rate, u(t), and the cumene flow rate x(t) are not immediately compatible. From this viewpoint the blocks K_x and K_u are essentially conversion factors (8). To evaluate these blocks, a material balance was taken at the entrance to the fluidized-bed.

$$\frac{\rho}{M} x = z(u + x) \tag{26}$$

where ρ and M are the density and molecular weight of the cumene. Linearization results in

$$\hat{z} = \left(\frac{\partial z}{\partial x}\right)_o x + \left(\frac{\partial z}{\partial u}\right)_o u \tag{27}$$

$$Z(s) = \left(\frac{\partial z}{\partial x}\right)_o X(s) + \left(\frac{\partial z}{\partial u}\right)_o U(s) \tag{28}$$

Let

$$K_x = \left(\frac{\partial z}{\partial x}\right)_o \text{ and } \quad K_u = \left(\frac{\partial z}{\partial u}\right)_o \tag{29}$$

Then

$$Z(s) = K_x X(s) + K_u U(s) \tag{30}$$

By direct calculations the partial derivatives can be found to be

$$K_x = \left(\frac{\partial z}{\partial x}\right)_o = \frac{\rho}{M} \frac{u(o)}{[u(o) + x(o)]^2} = \frac{y_a \overline{\Pi}}{RT} \frac{u(o)}{[u(o) + x(o)]^2} \tag{31}$$

$$K_u = \left(\frac{\partial z}{\partial u}\right)_o = \frac{\rho}{M} \frac{x(o)}{[u(o) + x(o)]^2} = \frac{y_a \overline{\Pi}}{RT} \frac{x(o)}{[u(o) + x(o)]^2} \tag{32}$$

Blocks H_1, H_2, and G_v were selected as follows.

$$H_1 = 12\text{psi}/2v_o$$

$$H_2 = 12\text{psi}/\ C_c$$

$$G_v = y_c v_o/\ 12\text{psi}$$

The maximum deflection of the pressure signal was assumed to be 12psi.

The transfer function for the feedforward controller is denoted by $G_f(s)$. Its value is chosen so that any disturbance in the solvent flow rate, u(t), would not affect the control variable y(t). This means that for R(s) = 0.0, the coefficient of U(s) in the control equation for feedforward and combined feedforward-feedback control must be zero. Thus,

$$K_u G_p(s) - K_x G_v G_f(s) H_1 G_p(s) = 0.0 \qquad (33)$$

or

$$G_f(s) = K_u/H_1 G_v K_x \qquad (34)$$

The feedforward controller transfer function is denoted by $G_c(s)$. The modes of control investigated are proportional, proportional-integral, proportional-derivative, and proportional-integral-derivative. The transfer function of each are given below:

$$\text{P:}\quad G_c(s) = K_c$$

$$\text{PI:}\quad G_c(s) = K_c(1 + 1/T_i s)$$

$$\text{PD:}\quad G_c(s) = K_c(1 + T_d s)$$

$$\text{PID:}\quad G_c(s) = K_c(1 + 1/T_i s + T_d s)$$

Here K_c is the proportional gain; T_i, the integral time constant; and T_d the derivative time constant. In general proportional control results in a response having maximum offset but little if any oscillation. The response to PI control has no offset but a large period of oscillation. PD control gives a response having little offset and a shorter period of oscillation than PI. PID control has a response which dis-

plays the "no offset" characteristic of PI control and the "short period of oscillation" characteristic of PD control.

Step changes in the set-point and load were arbitrarily chosen. The solvent flow rate, u(t), was doubled, that is,

$$U(s) = 2u(o)/s.$$

The step change in set-point was selected to be 3psi, that is

$$R(s) = 3psi/s.$$

Ultimate Controller Settings

The Ziegler-Nichols method and the Cohen and Coon reaction curve method of determining those values of K_c, T_i, and T_d which gave optimum control were compared. The Ziegler-Nichols settings are derived by determining the ultimate gain, K_u and the ultimate period, P_u. The ultimate gain is defined as:

$$K_u = 1/A \tag{35}$$

where A is the gain at the crossover frequency w_{co}. The ultimate period is defined as:

$$P_u = 2\ /w_{co} \tag{36}$$

Table II gives the Ziegler-Nichols controller settings for various modes of control. The ultimate gain and period for the system employed in this study were found to be

$$P_u = 3.37 \text{ sec/cycle}$$
$$K_u = 12$$

Derivation of these values is given in Appendix I. The ultimate controller settings from the Ziegler-Nichols method were:

P: $K_c = 6.0$

PI: $K_c = 5.4$, $T_i = 3.11$

PID: $K_c = 7.2$, $T_i = 1.86$, $T_d = .466$

The Cohen and Coon reaction curve method assumes the process transfer function to have the form

$$G_p(s) = K_p e^{-T_d s}/(1 + Ts) \tag{37}$$

Cohen and Coon derived theoretical values of the controller settings which would give minimum offset and minimum area under the load re-

TABLE II

Ziegler-Nichols Controller Settings

Type of control	$G_c(s)$	K_c	T_i	T_d
Proportional	K_c	$0.5K_u$		
Proportional-Integral	$K_c(1 + 1/T_i s)$	$0.45K_u$	$P_u/1.2$	
Proportional-Integral-Derivative	$K_c(1 + 1/T_i s + T_d s)$	$0.6K_u$	$P_u/2.0$	$P_u/8.0$

sponse curve. The values of the settings found are given below.

Proportional:

$$K_c = \frac{1}{K_p}\frac{T}{T_d}(1 + T_d/3T) \tag{38}$$

Proportional-Integral:

$$K_c = \frac{1}{K_p}\frac{T}{T_d}(9/10 + T_d/12T) \tag{39}$$

$$T_i = T_d(30 + 3T_d/T)/(9 + 20T_d/T) \tag{40}$$

Proportional-Derivative:

$$K_c = \frac{1}{K_p}\frac{T}{T_d}(5/4 + T_d/6T) \tag{41}$$

$$T_d = T_d(6 - 2T_d/T)/(22 + 3T_d/T) \tag{42}$$

Proportional-Integral-Derivative:

$$K_c = \frac{1}{K_p}\frac{T}{T_d}(4/3 + T_d/4T) \tag{43}$$

$$T_i = T_d(32 + 6T_d/T)/(13 + 8T_d/T) \tag{44}$$

$$T_d = T_d(4)/(11 + 2T_d/T) \tag{45}$$

The values T_d, K_p, and T are derived as follows, (2):

1. Apply a small step change M in the manipulated variable to the opened control loop and record the measured variable versus time. A typical curve is shown in Figure 7.
2. A tangent is drawn to the inflection point. The intercept with the abscissa is the apparent dead time T_d.
3. The slope S, of this tangent is B_u/T, therefore

$$T = B_u/S$$

where B_u is the final value reached.

4. The gain K_p is given by

$$K_p = B_u/M$$

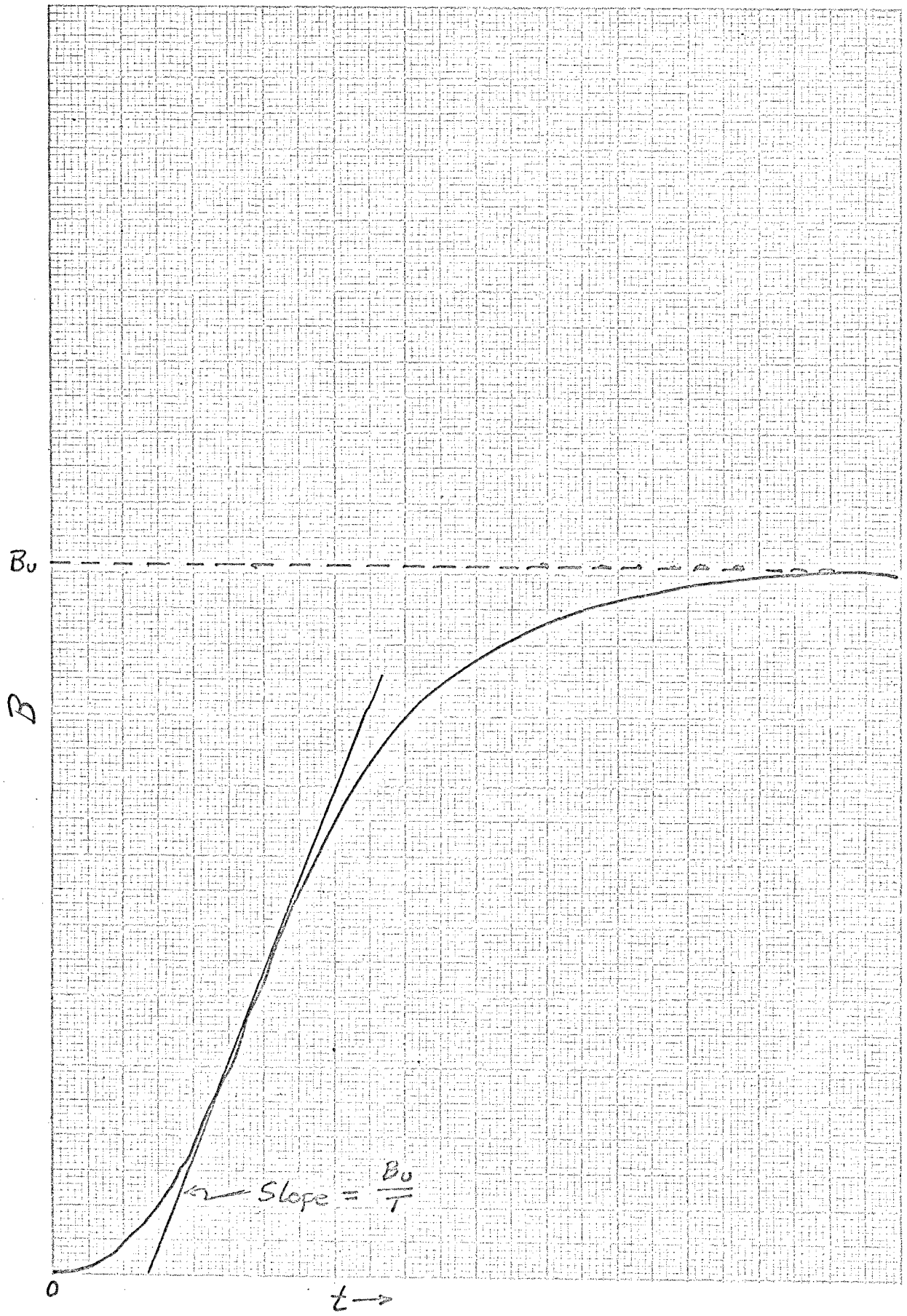

FIGURE 7 TYPICAL PROCESS REACTION CURVE

In this case the process transfer function was the same as that assumed by Cohen and Coon. Thus,

$$K_p = 1.0$$

$$T_d = 1.0$$

$$T = 5.0$$

These resulted in controller settings as follows:

P; $K_c = 5.333$

PI: $K_c = 5.5833$

$T_i = 2.355$

PD: $K_c = 6.4166$

$T_d = 0.248$

PID: $K_c = 6.916$

$T_i = 2.27$

$T_d = 0.351$

DISCUSSION OF RESULTS

Transient responses of the variously controlled systems are given in Figures 8 through 37. It was observed that for any mode of control, combined feedforward-feedback control systems seem to control the fluidized-bed reactor better than either of the systems alone.

Figures 8 through 11 show the transient responses for feedforward control. It seems that offset occurs with changes in load even though corrective action is taken before the measured variable is affected. This is probably because the disturbance might be overflowing the system. That is, the disturbance might be too large for the ideal controller to control properly. If this was the case, the response curve shown is the uncontrolled response to a step change in load partially affected by the ideal controller. Figures 10 and 11 show the response curves for the same systems as do Figures 8 and 9, except here the lag time term was omitted in the process transfer function. The only apparent difference in the curves is that the curves of Figures 10 and 11 are shifted to the left an amount equal to T_o, the system lag time. Since it was observed that this was the only affect T_o had on the system, it was omitted from the process transfer function because of the difficulty met in trying to scale the analog computer circuit with this term present.

Figures 12 through 19 are the transient responses for the system employing feedback control. As expected, proportional and proportional-derivative modes of control exhibited offset, and proportional-integral and proportional-integral-derivative modes exhibited periods

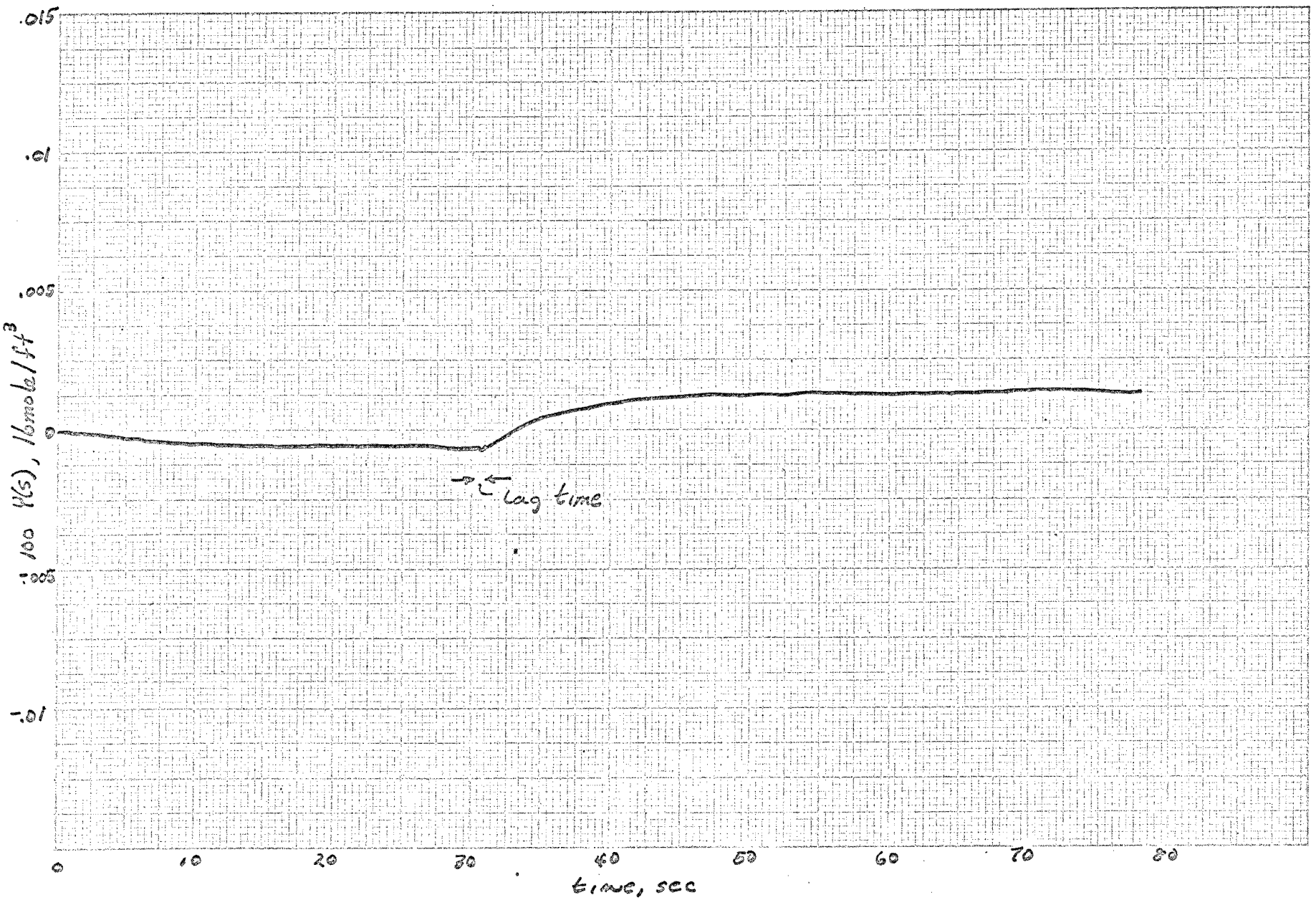

Figure 8 Transient Response for Feedforward Control
Change in set-point

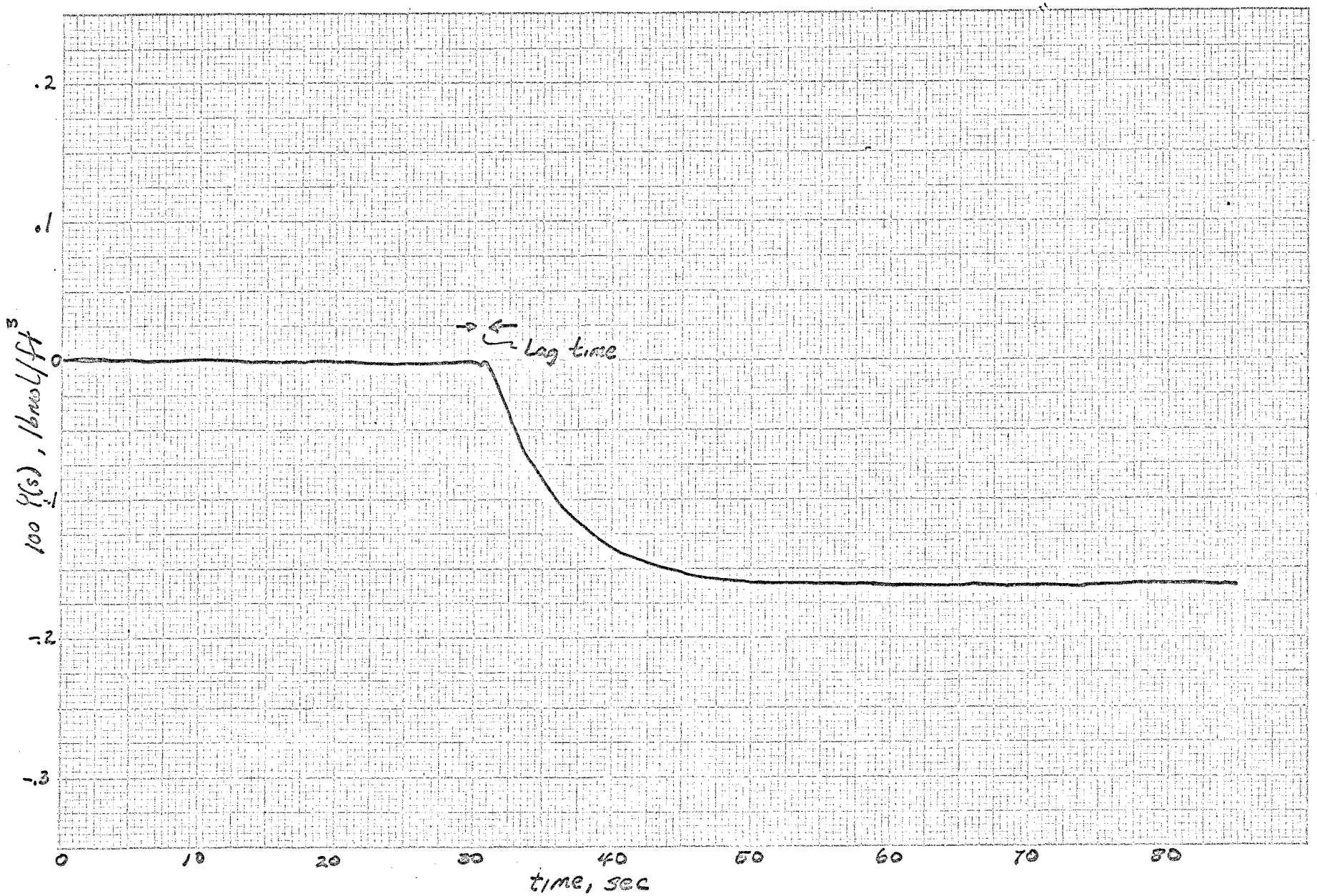

Figure 9 TRANSIENT RESPONSE for Feedforward CONTROL
Change IN LOAD

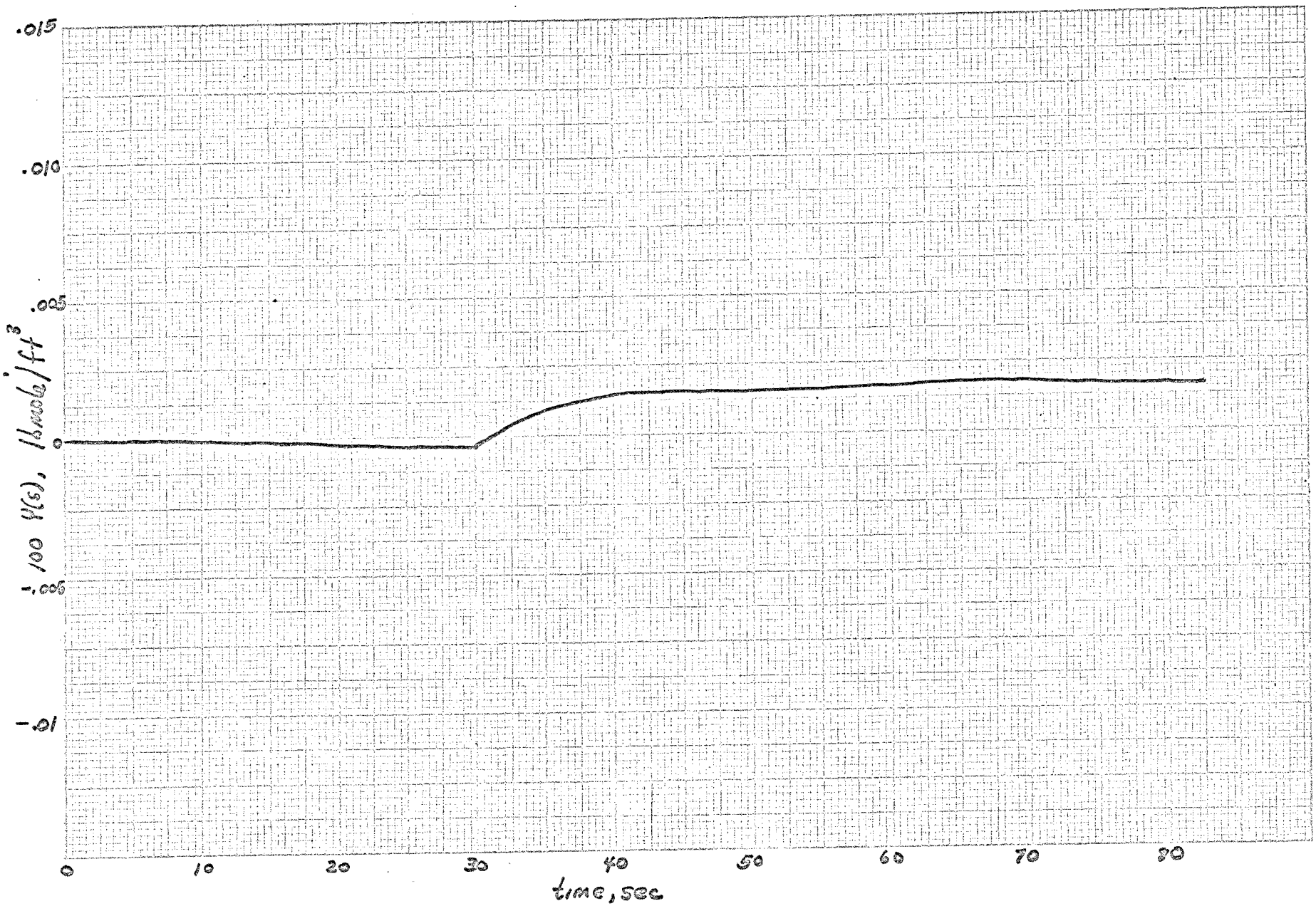

Figure 10 Transient Response for Feedforward Control: Lag term omitted; Change in set-point

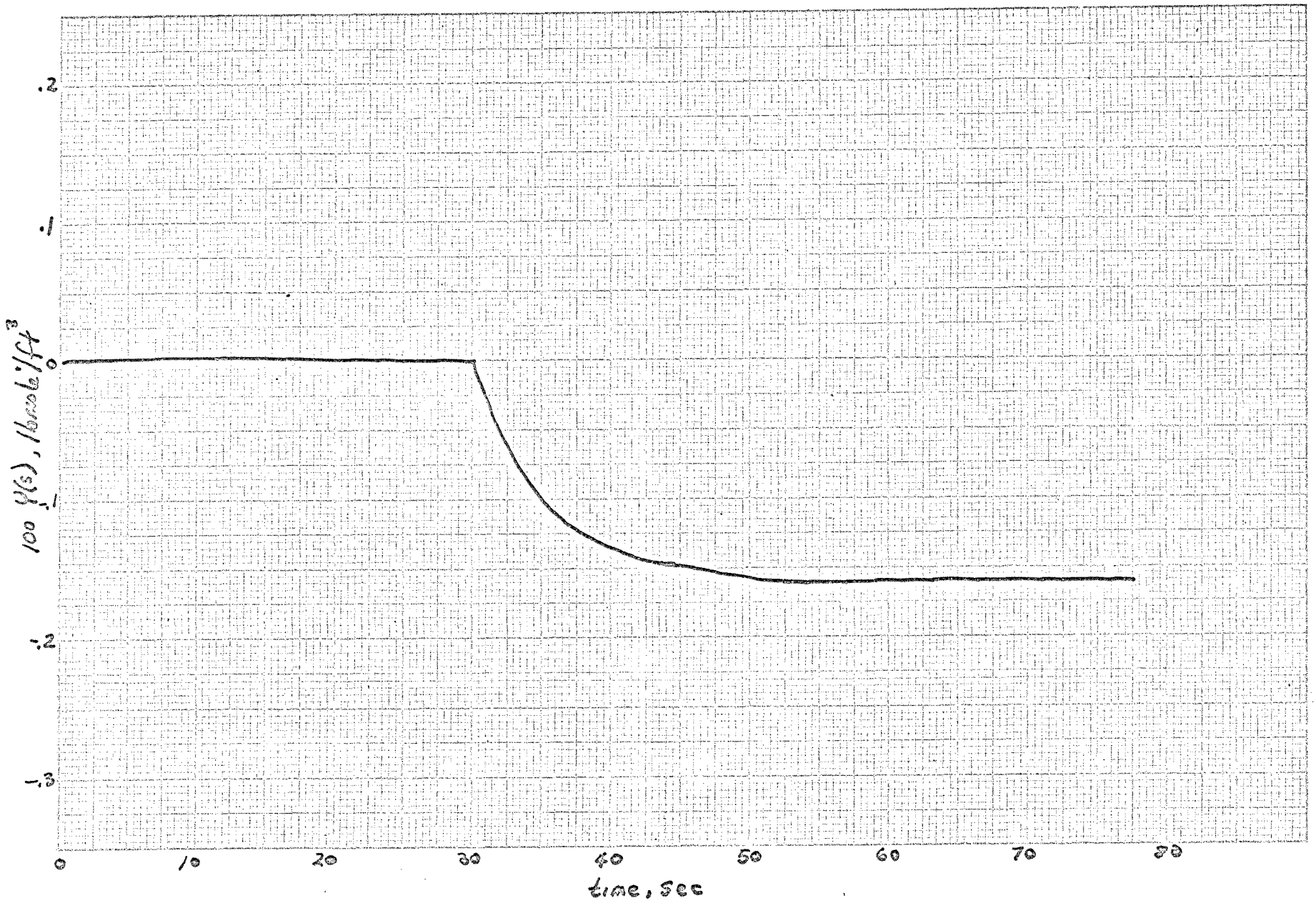

Figure 11 TRANSIENT RESPONSE for Feedforward CONTROL: Lag term omitted, Change IN Load.

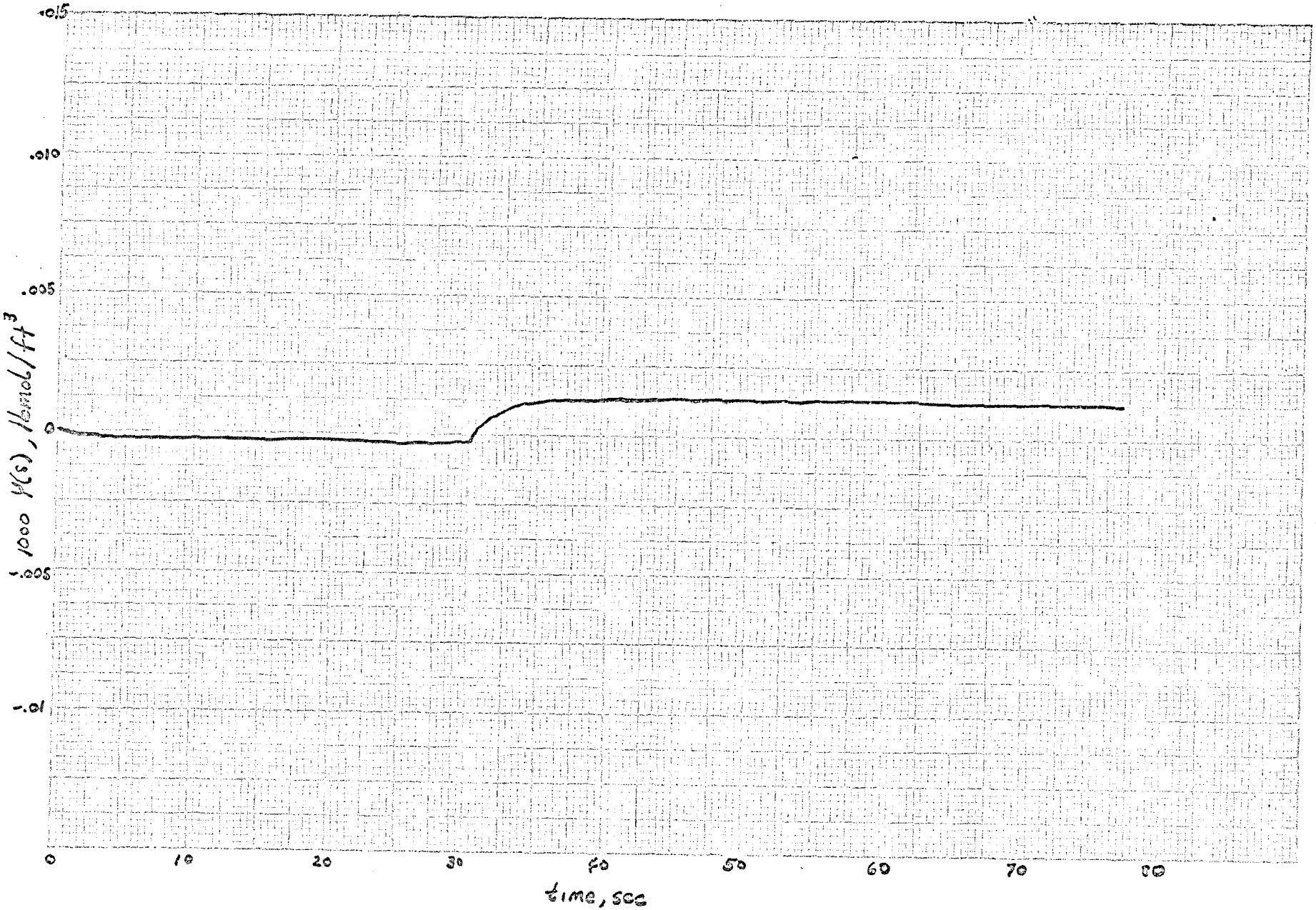

FIGURE 12 TRANSIENT RESPONSE FOR FEEDBACK CONTROL, PROPORTIONAL $K_c = 4$
CHANGE IN SET-POINT

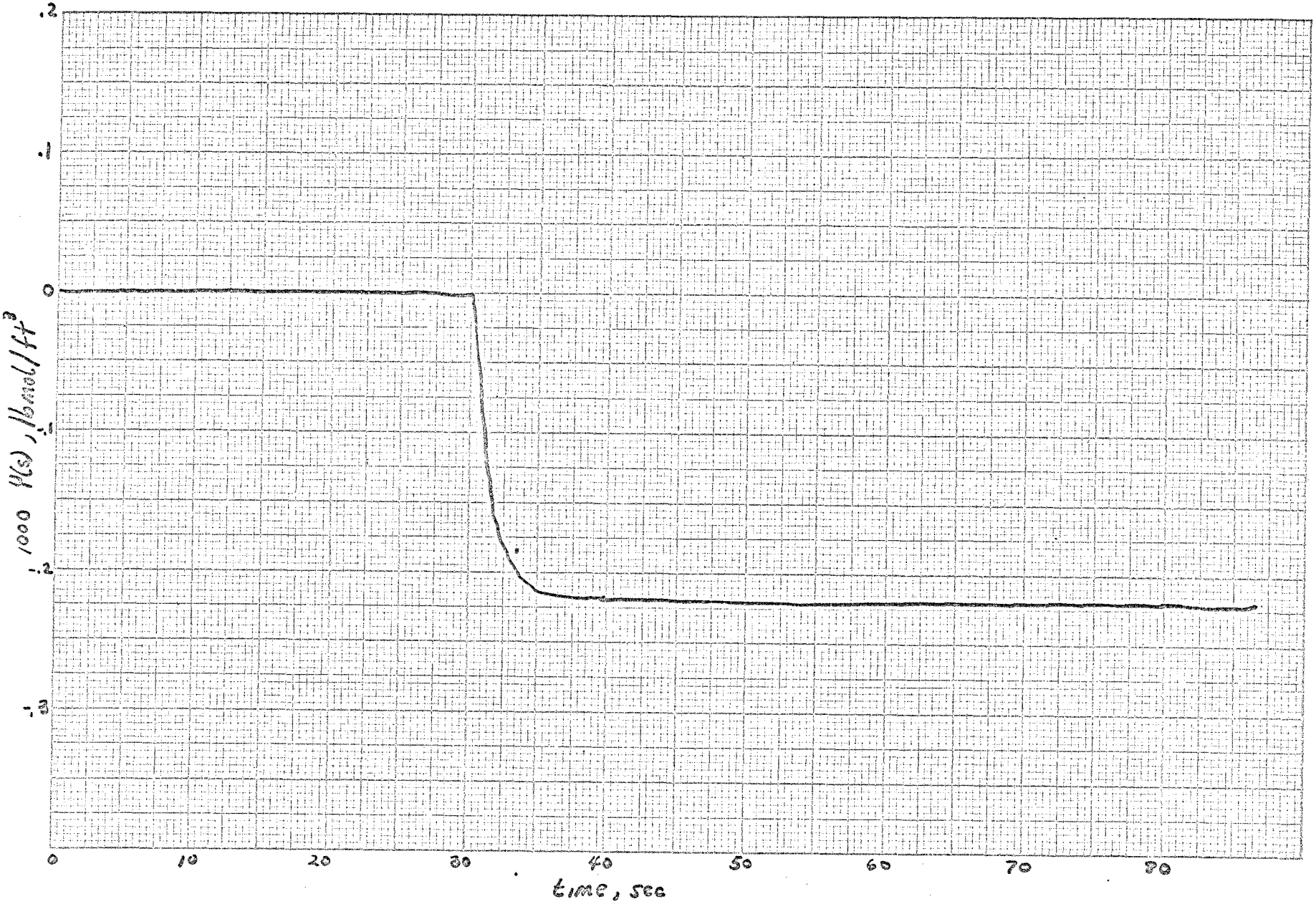

Figure 13 TRANSIENT RESPONSE for Feedback CONTROL, PROPORTIONAL, $K_c = 4$
CHANGE IN LOAD

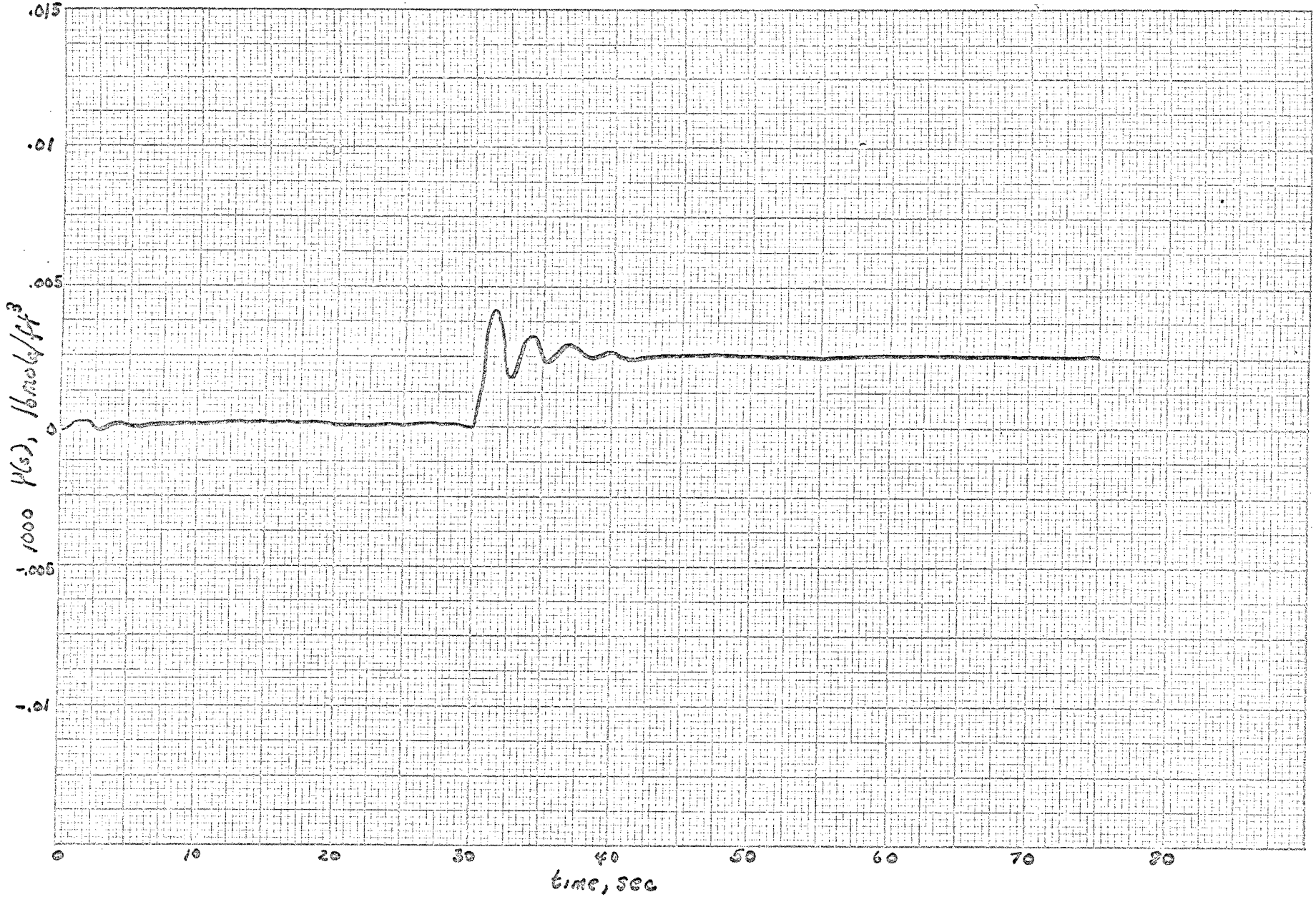

Figure 14 Transient Response for Feedback Control, PI $K_c = 4$ $\tau_I = .1$
Change in set-point

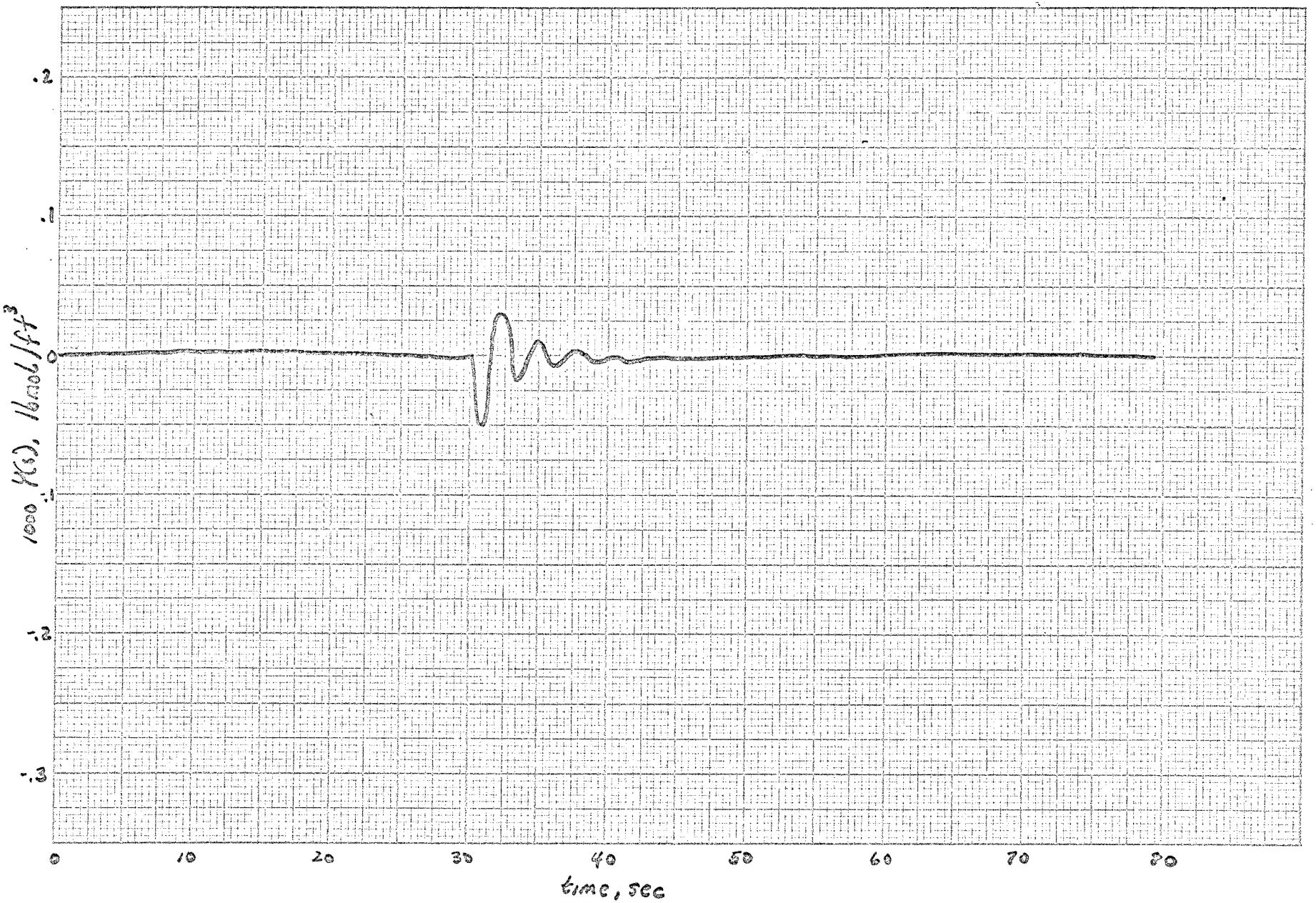

Figure 16 TRANSIENT RESPONSE FOR Feedback CONTROL, PI $K_c=4$ $\tau_I=.1$
Change IN load

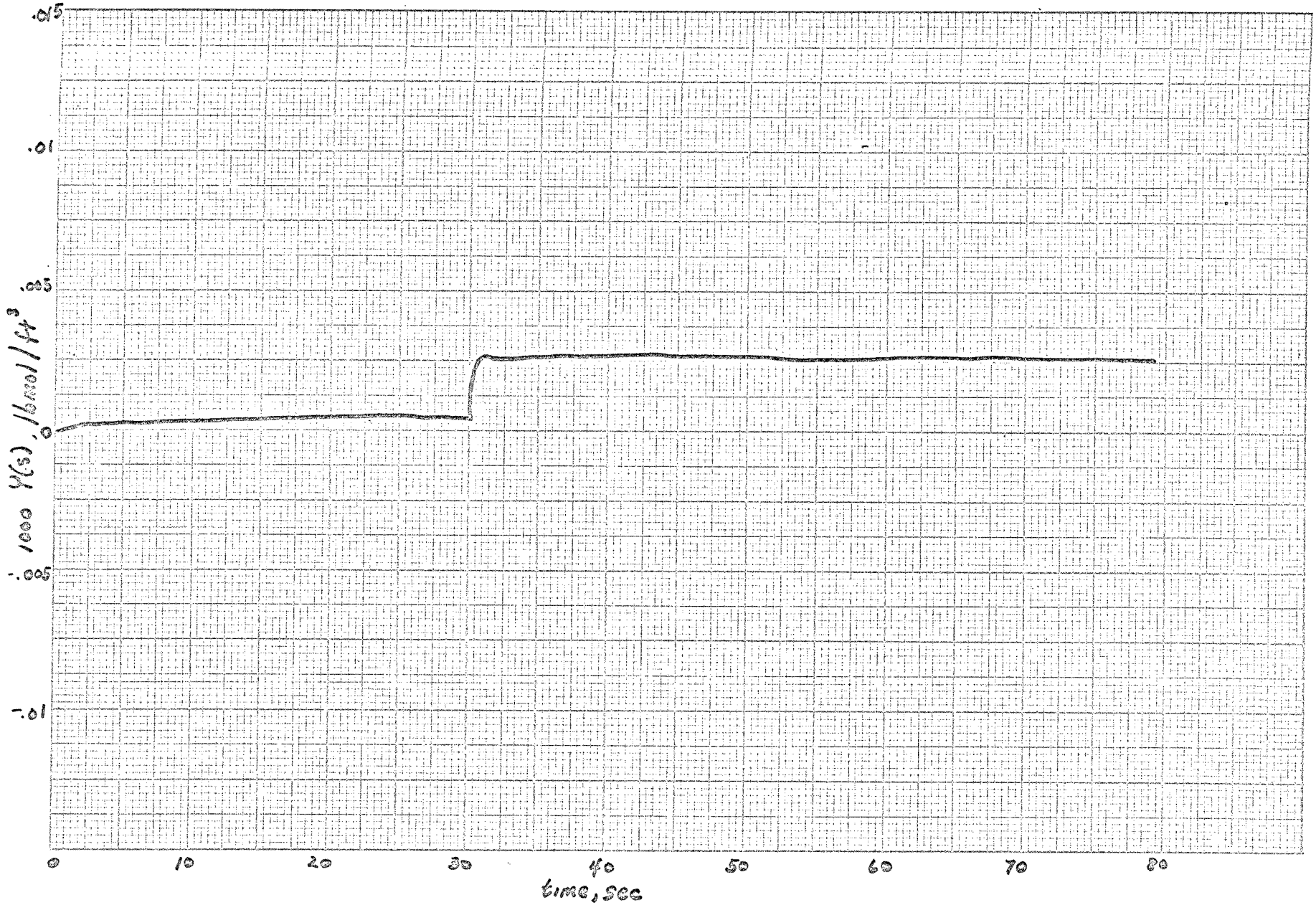

Figure 16 Transient Response for Feedback Control, PD $K_c=4$ $\tau_s = 10$
Change in set-point

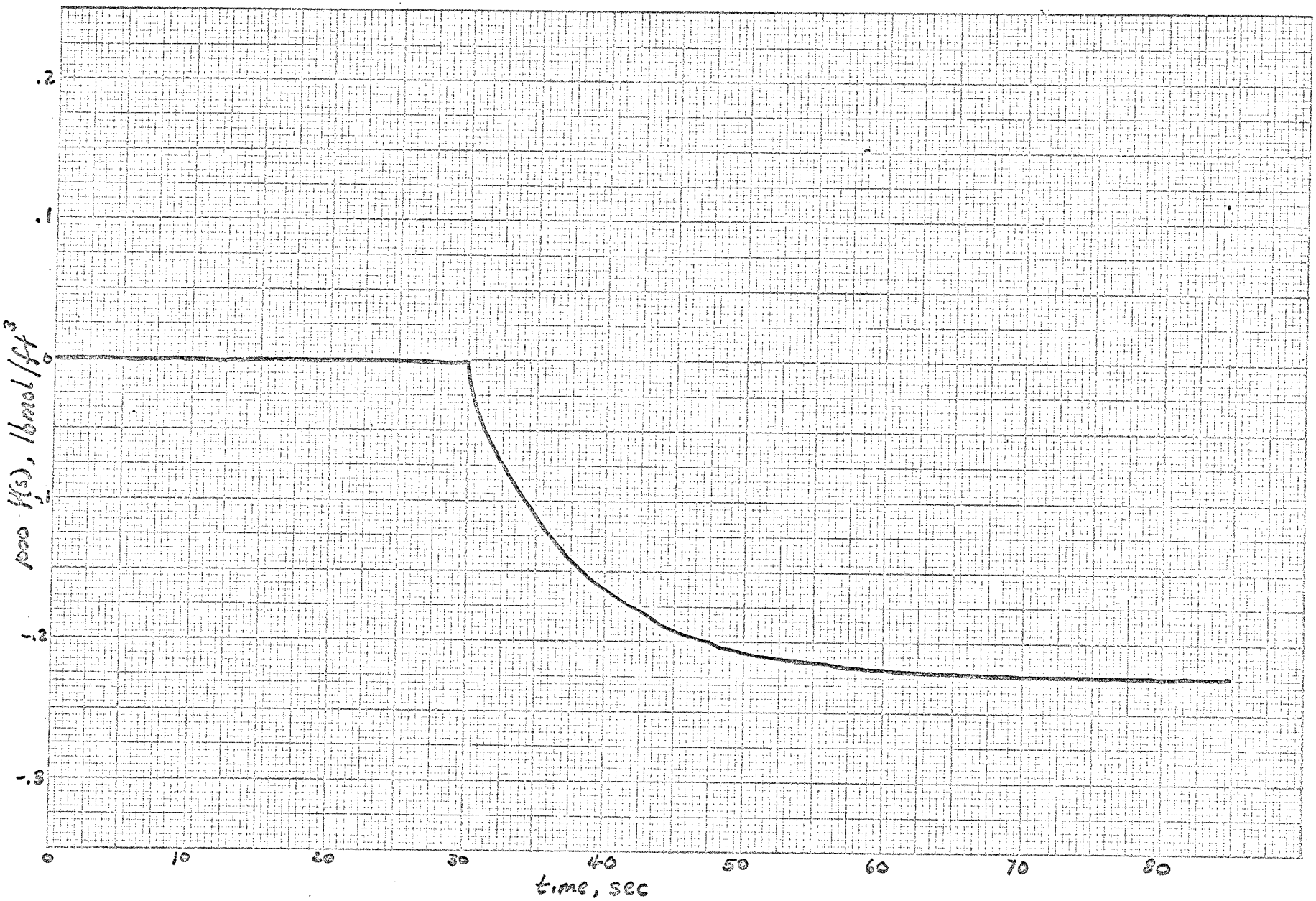

FIGURE 17 TRANSIENT RESPONSE FOR FEEDBACK CONTROL, PD: $K_c = 4$ $\tau_d = 10$
CHANGE IN LOAD

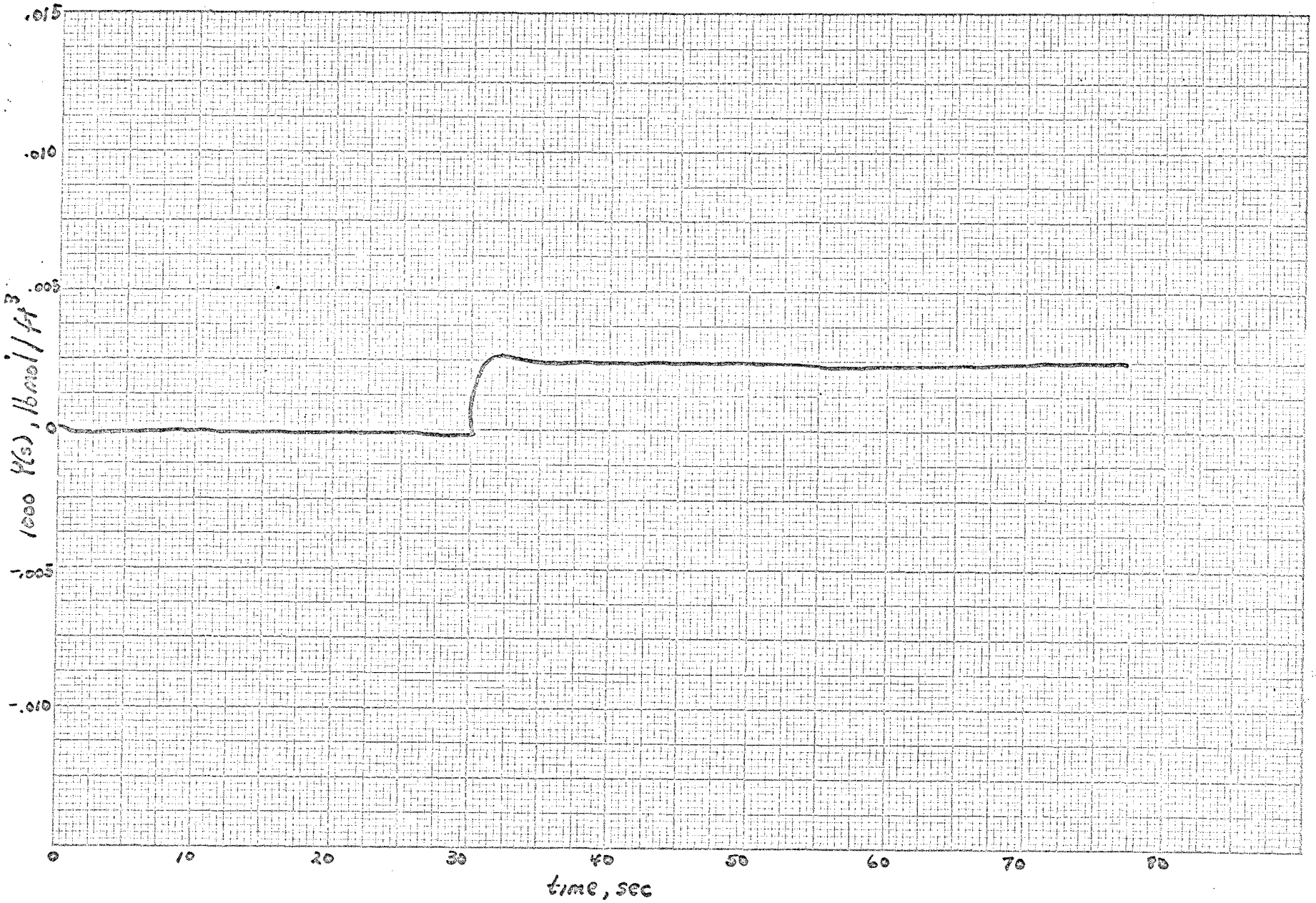

FIGURE 18 TRANSIENT RESPONSE for Feedback CONTROL, PID: $K_c = 4$ $\tau_I = .1$ $\tau_D = 10$
Change in set-point

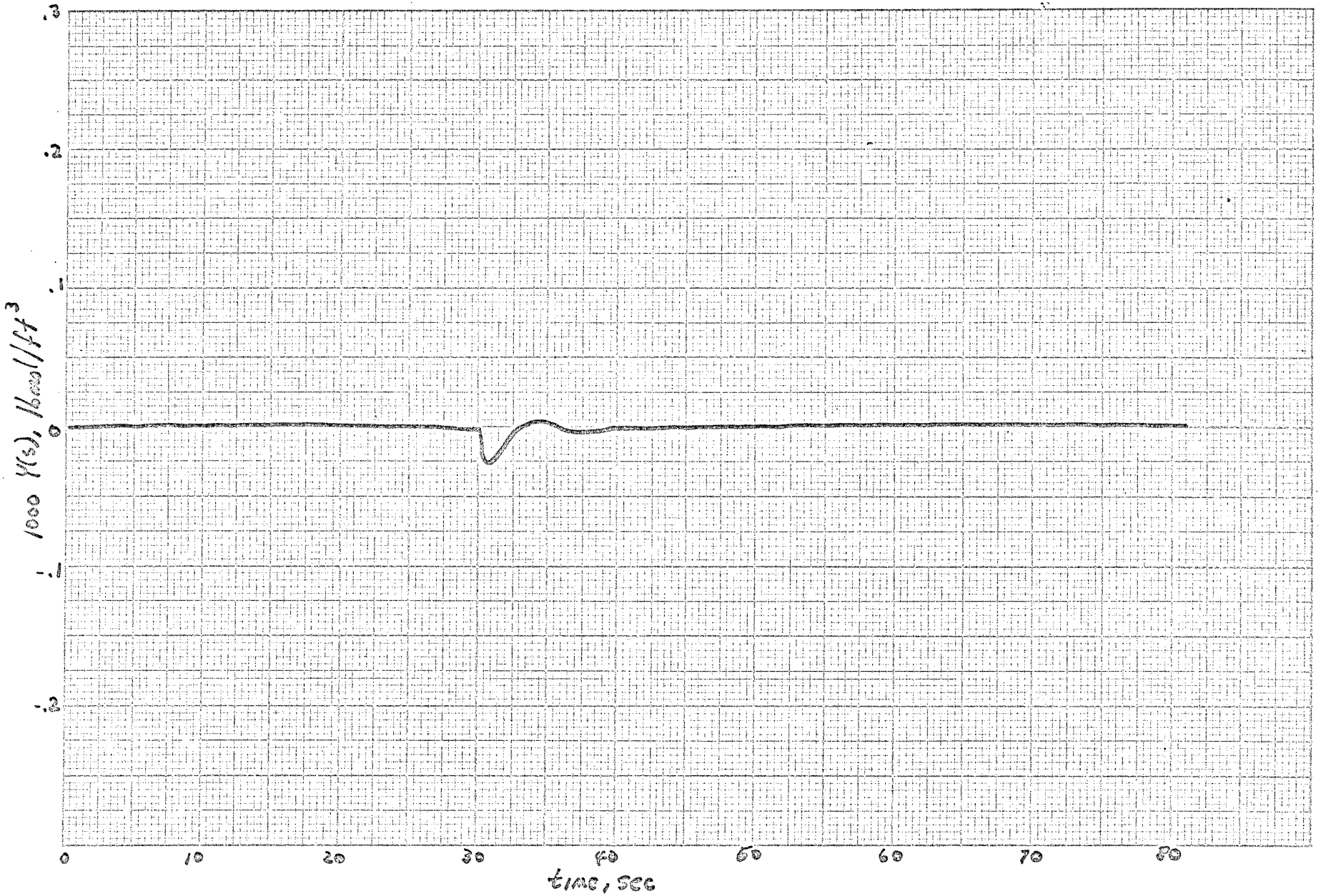

Figure 19 Transient Response for Feedback Control, PID: $K_c = 4$, $\tau_I = .1$ $\tau_d = 10$ Change in Load.

of oscillation. It is observed that as K_c decreases this period of oscillation increases. Thus a higher value of K_c, (which is equivalent to a lower proportional band), means that the system will come into control sooner, although deviation from the final value will be greater.

Figures 20 through 31 show the transient response for the system employing combined feedforward feedback control. Offset in the proportional and proportional-derivative modes of control is not as great as in feedback and the period of oscillation in proportional-integral and proportional-integral-derivative modes is not as long. Also deviation from the final value is not as great as in feedback control. The first 30 seconds in each of the figures corresponds to the initial disturbance due to the step change in the set-point of the ideal controller.

Figures 32 through 37 show the responses for the combined feedforward-feedback control system when using the Ziegler-Nichols ultimate controller settings and the Cohen and Coon ultimate settings. Little difference is seen. At these ultimate settings oscillation and deviation from the final value are minimal.

In the Appendix (Figures 46 through 66) appear Bode Diagrams of the above systems. These futher support the above statements.

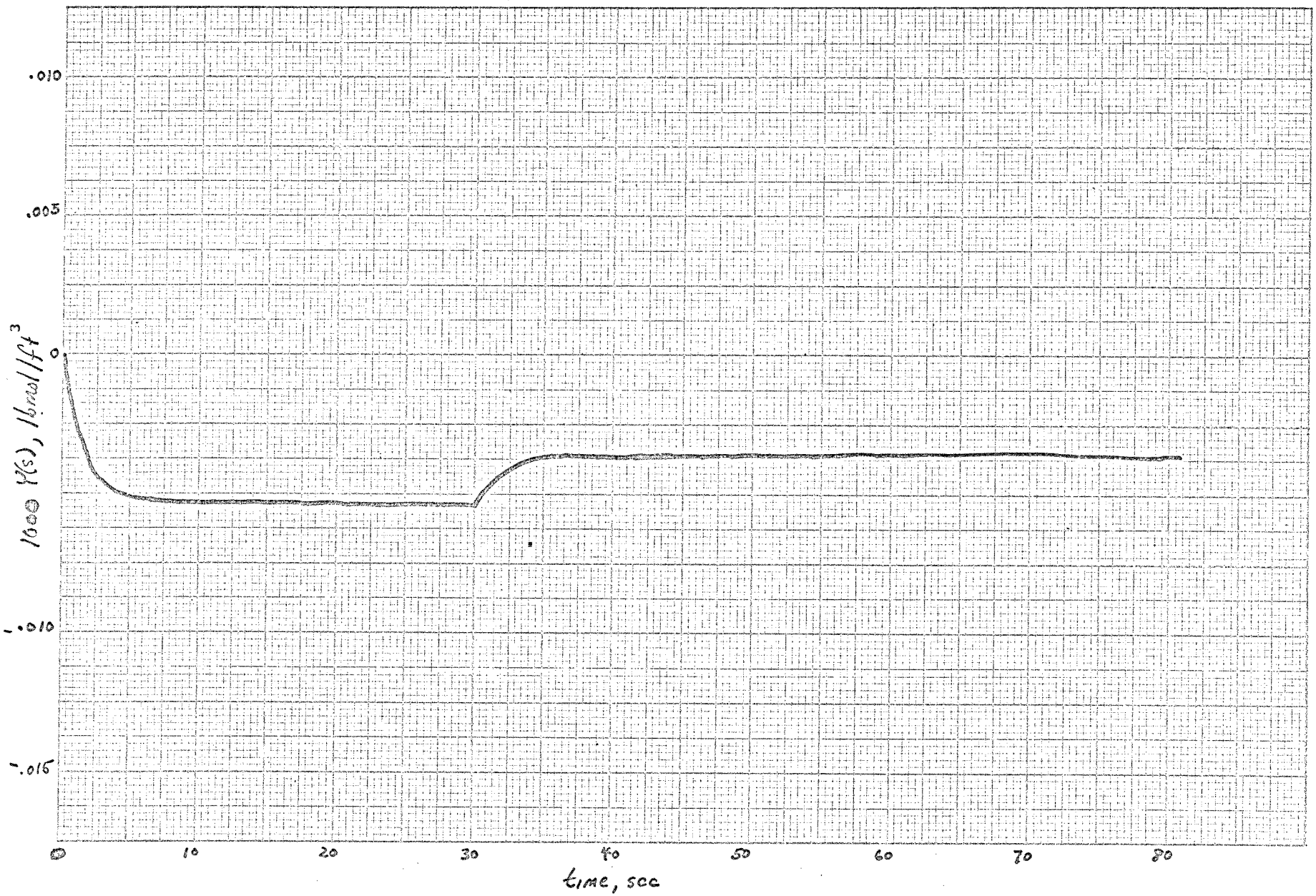

FIGURE 20 TRANSIENT RESPONSE FOR FEEDFORWARD-FEEDBACK CONTROL, PROPORTIONAL $K_c = 4$. CHANGE IN SET-POINT

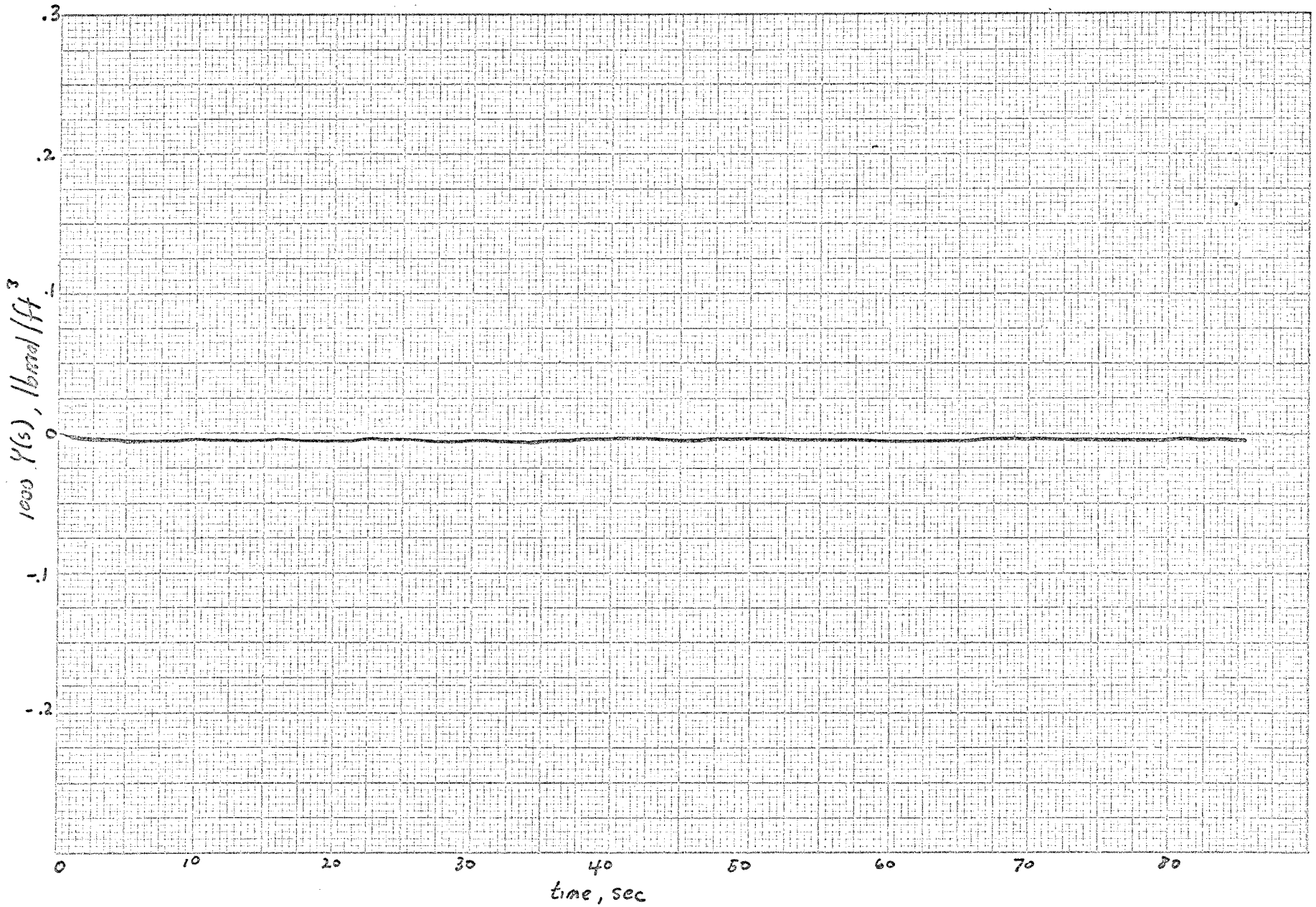

FIGURE 21 TRANSIENT RESPONSE FOR FEEDFORWARD-FEEDBACK CONTROL, PROPORTIONAL $K_c=4$ CHANGE IN LOAD.

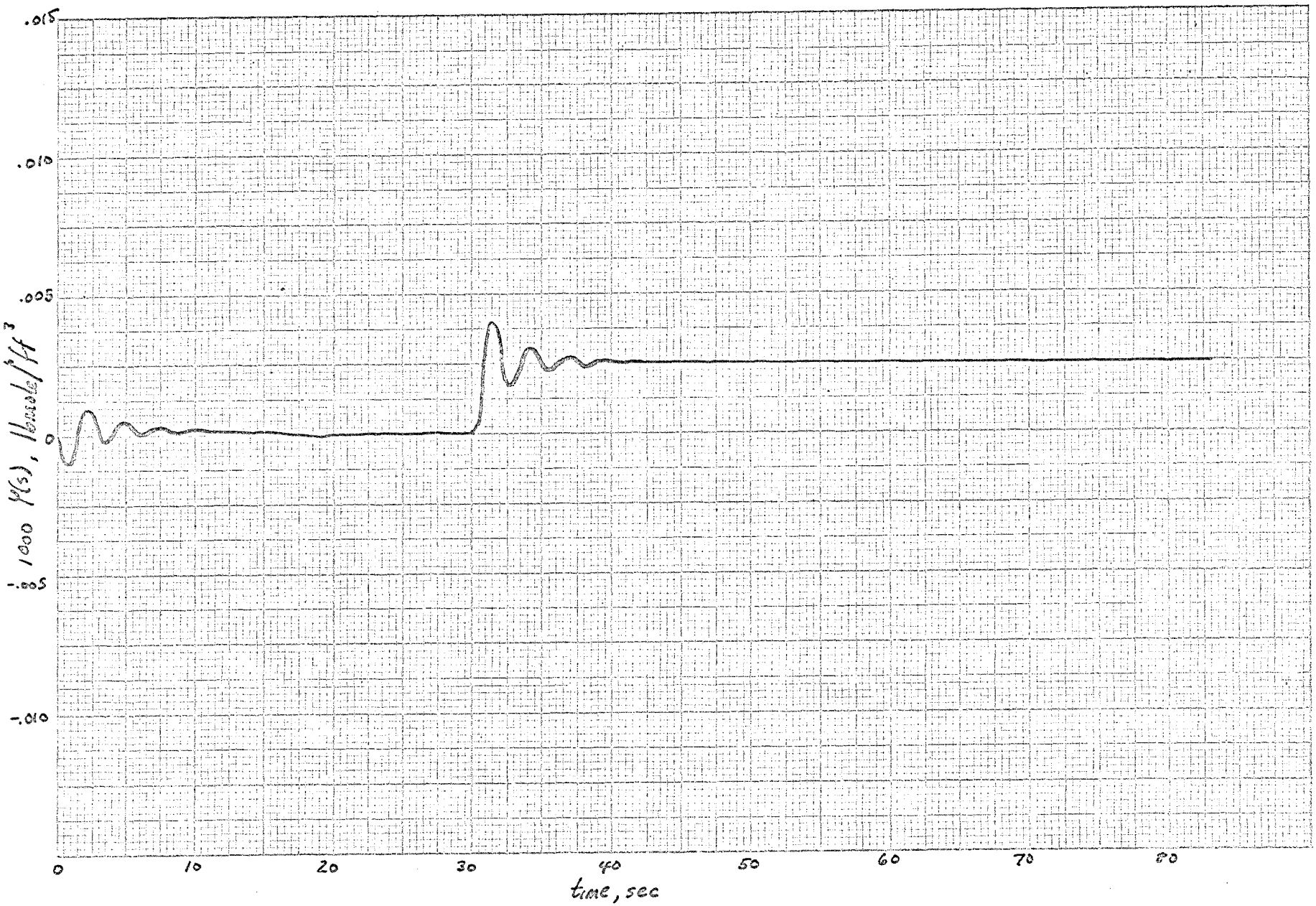

Figure 22 TRANSIENT RESPONSE for Feedforward-feedback Control, PI
$K_c = 4$ $\tau_I = .1$ Change in set-point

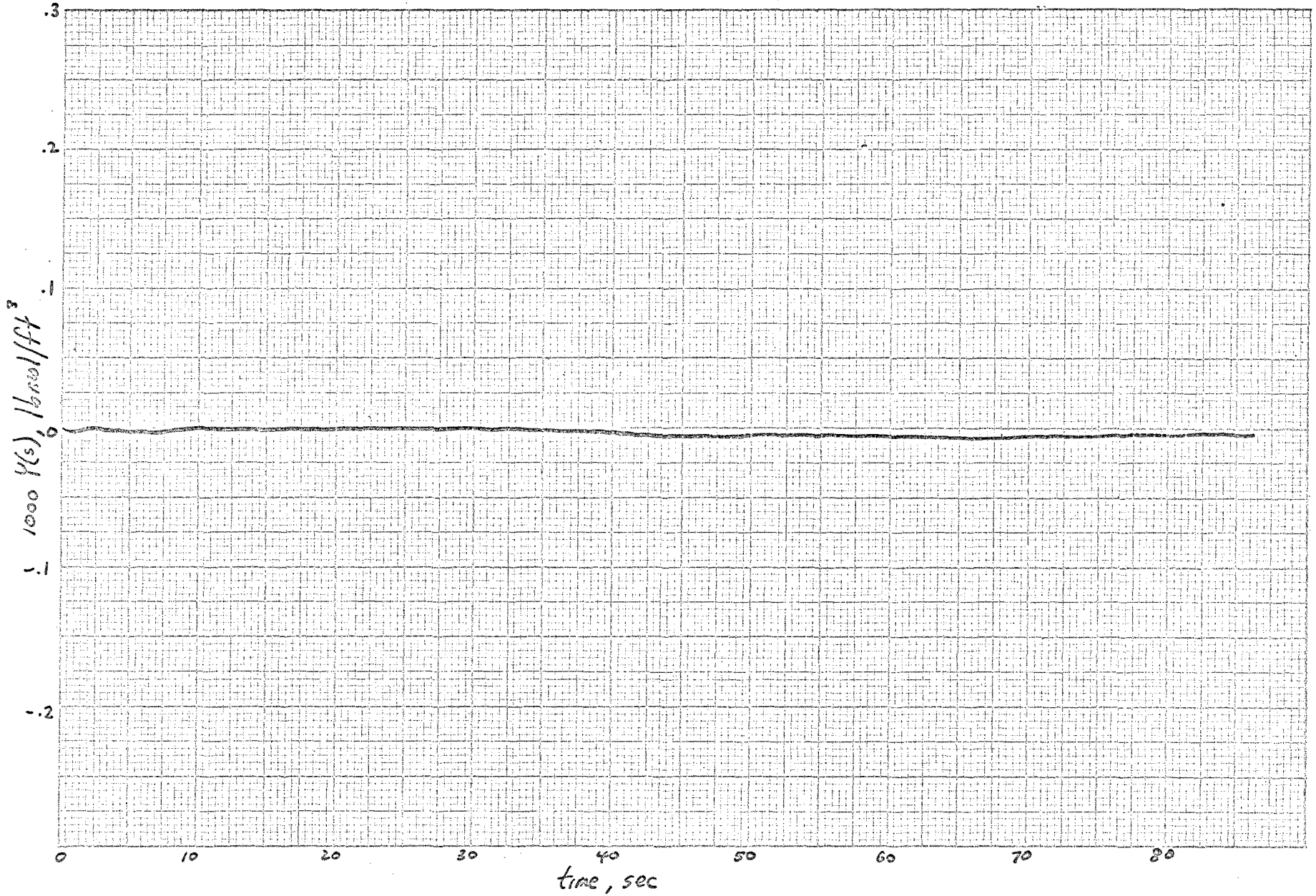

FIGURE 23 TRANSIENT RESPONSE FOR FEEDFORWARD-FEEDBACK CONTROL, PI: $K_C = 4$, $\tau_I = .1$ CHANGE IN LOAD

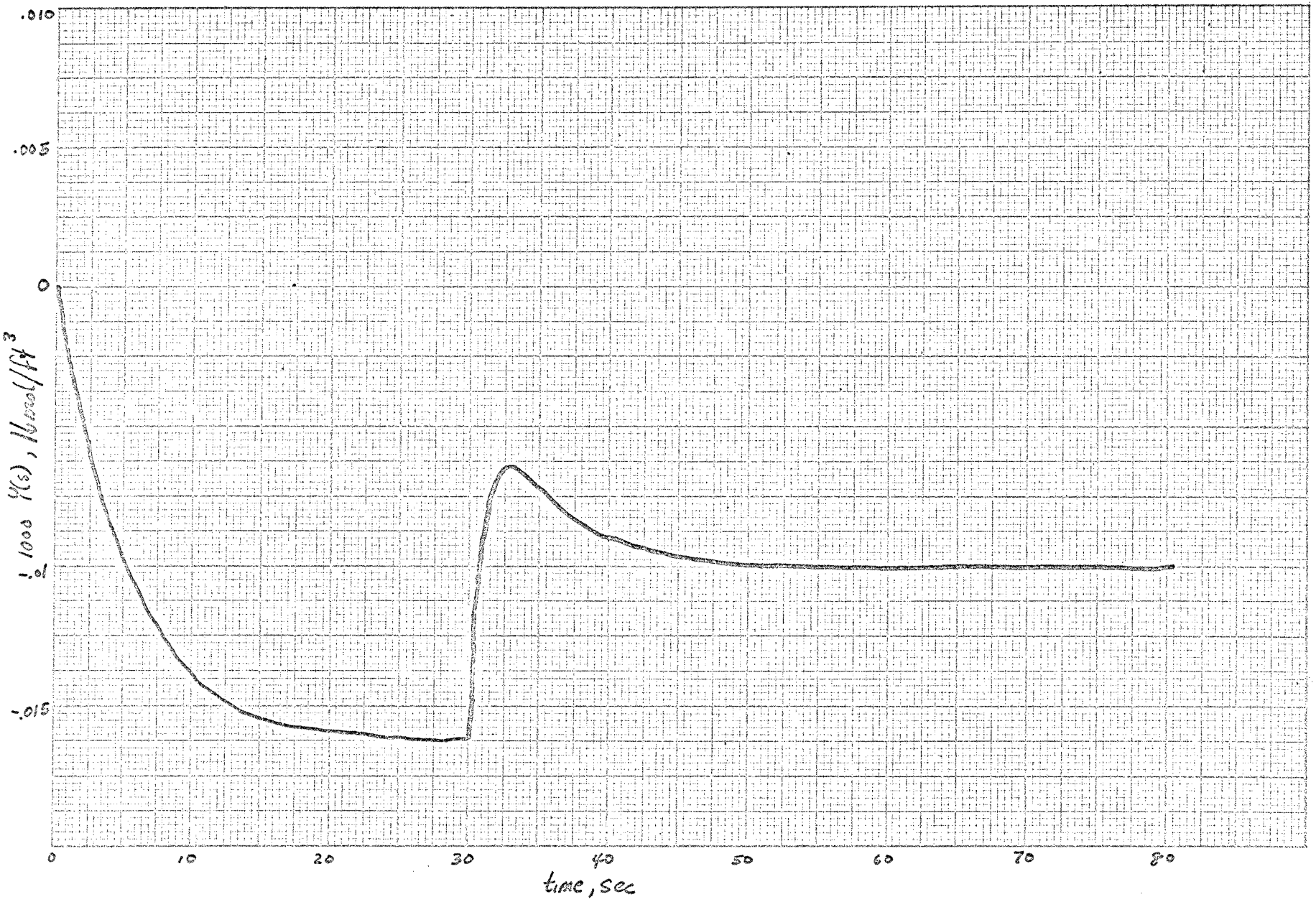

Figure 24 Transient Response for Feedforward-feedback Control, PD: $K_c = 4$ $\tau_D = 10$ Change in set-point.

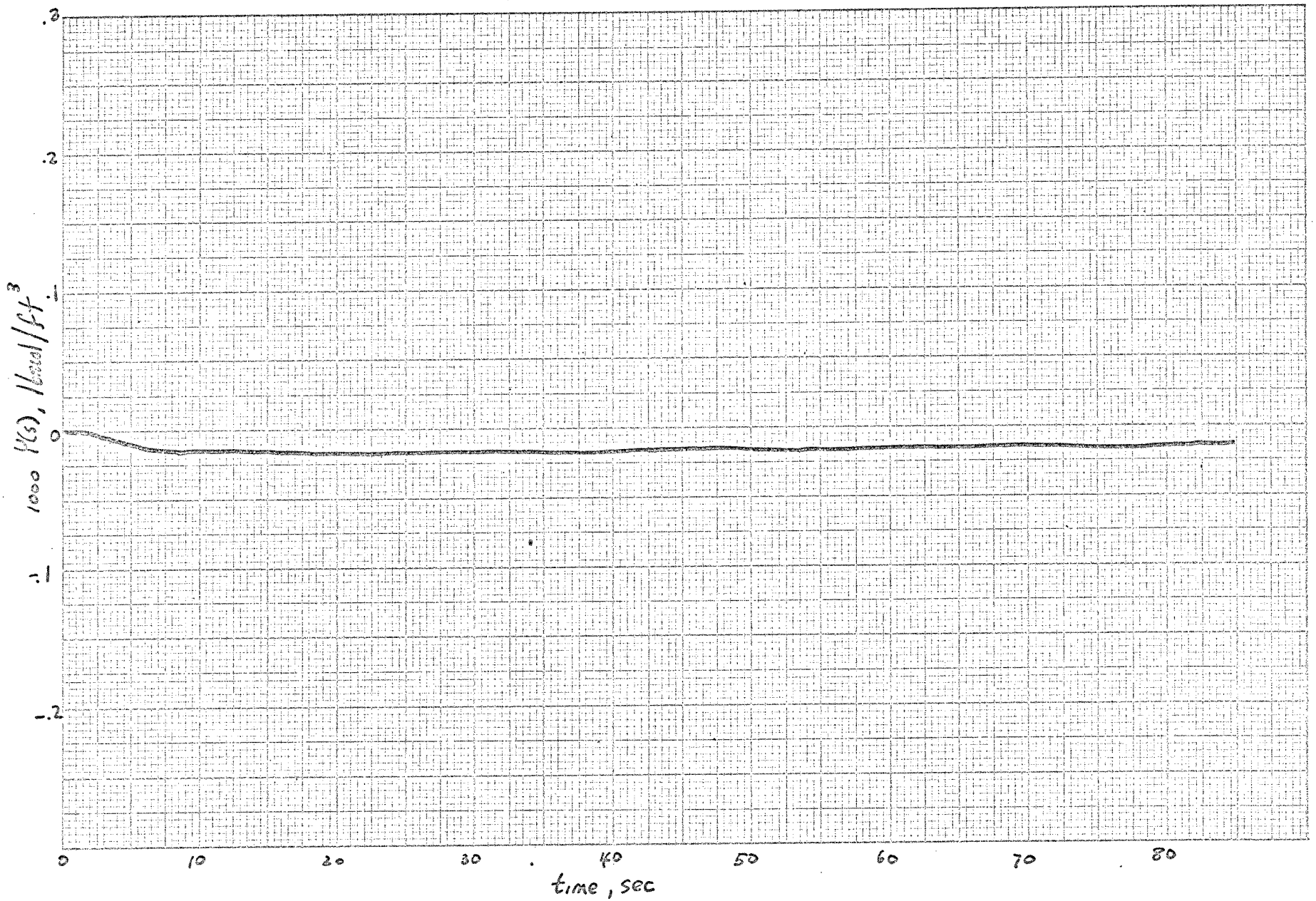

Figure 25 Transient Response for Feedforward-feedback Control, PD: $K_c = 4$ $\tau_D = 10$. Change in load.

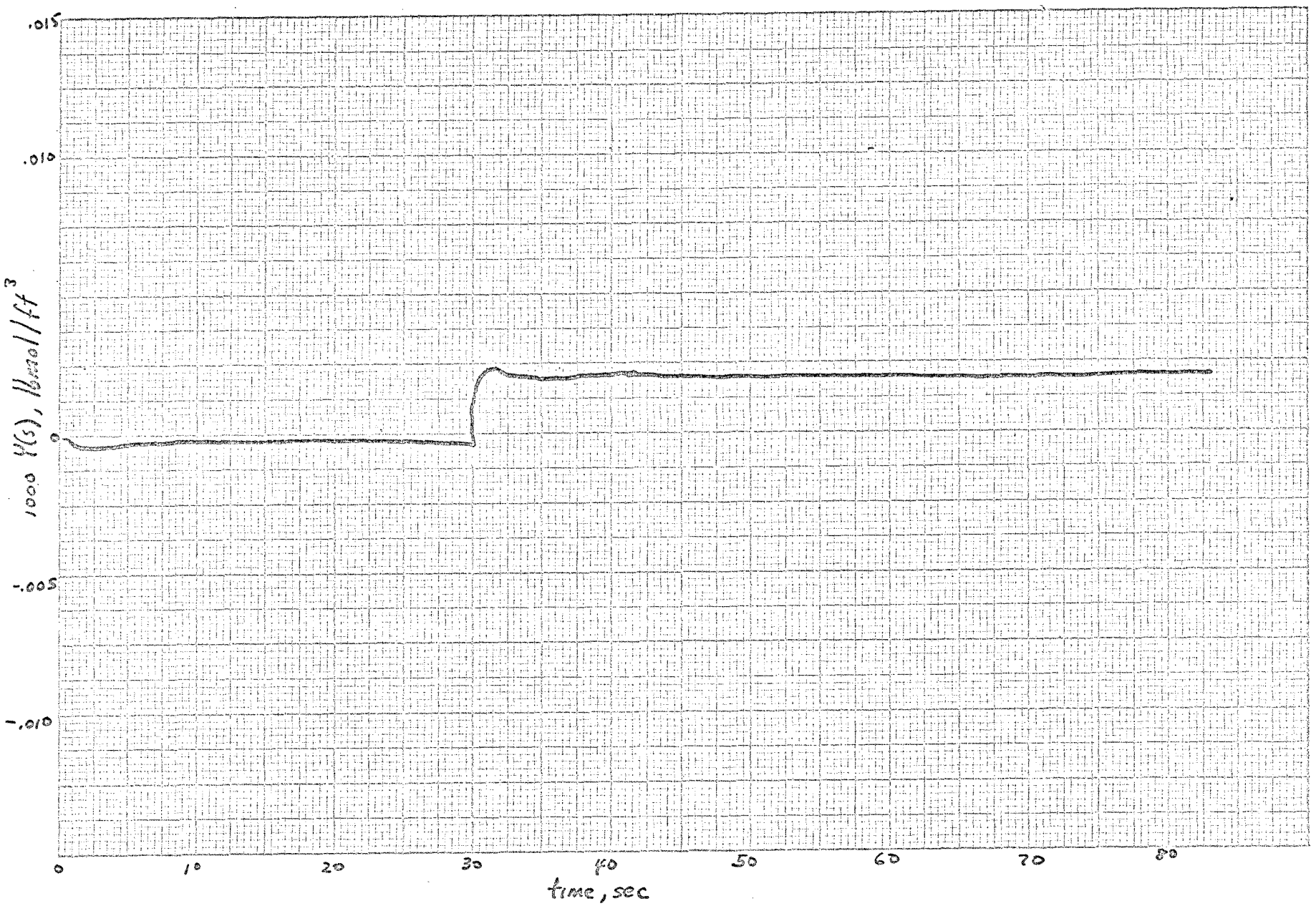

Figure 26 Transient Response for Feedforward-feedback Control
PID : $K_c = 4$, $\tau_I = .1$, $\tau_D = 10$ Change in set-point

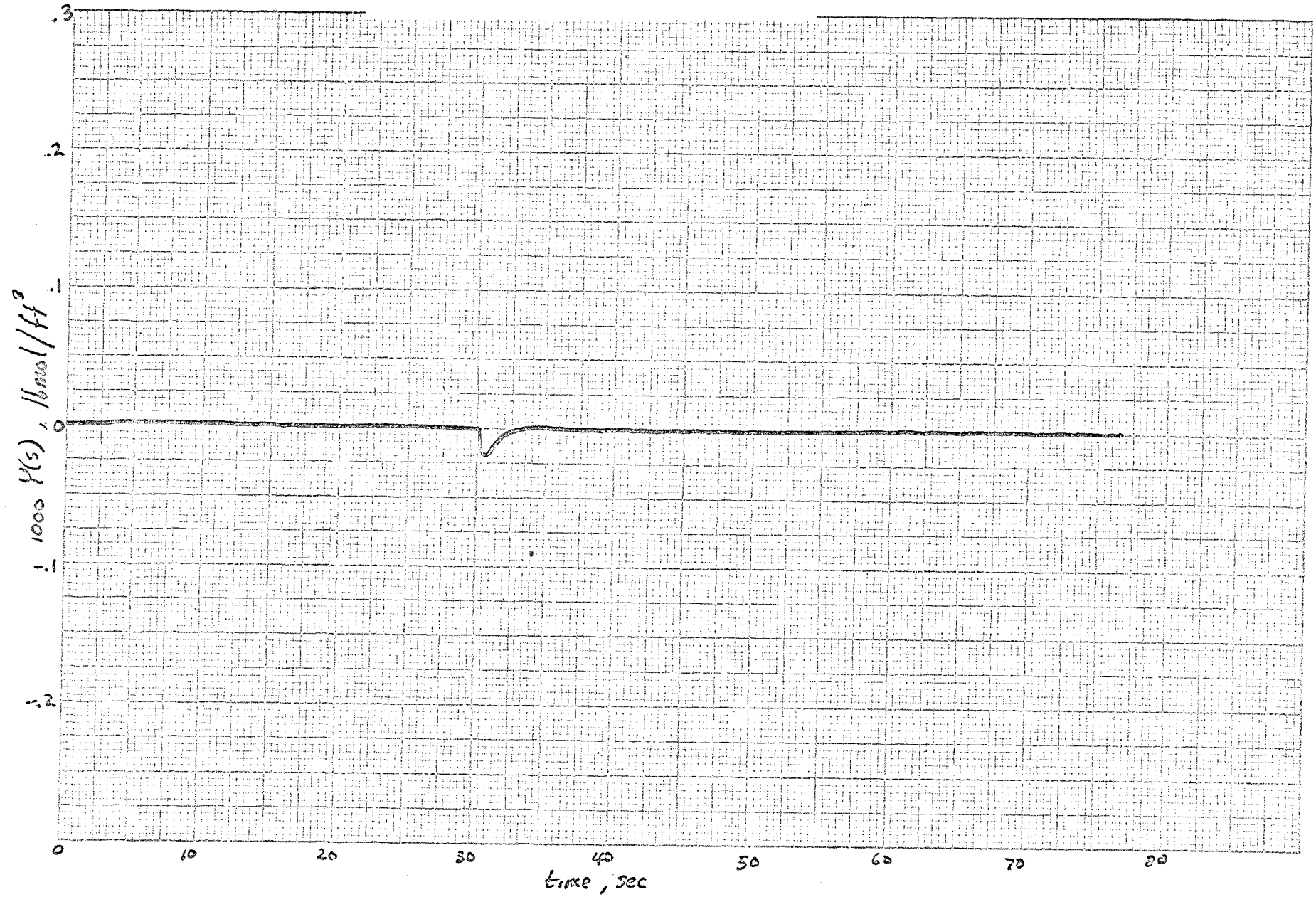

Figure 27 TRANSIENT Response for Feedforward-feedback Control, PID: $K_c = 4$, $\tau_I = .1$, $\tau_D = 10$ Change in load.

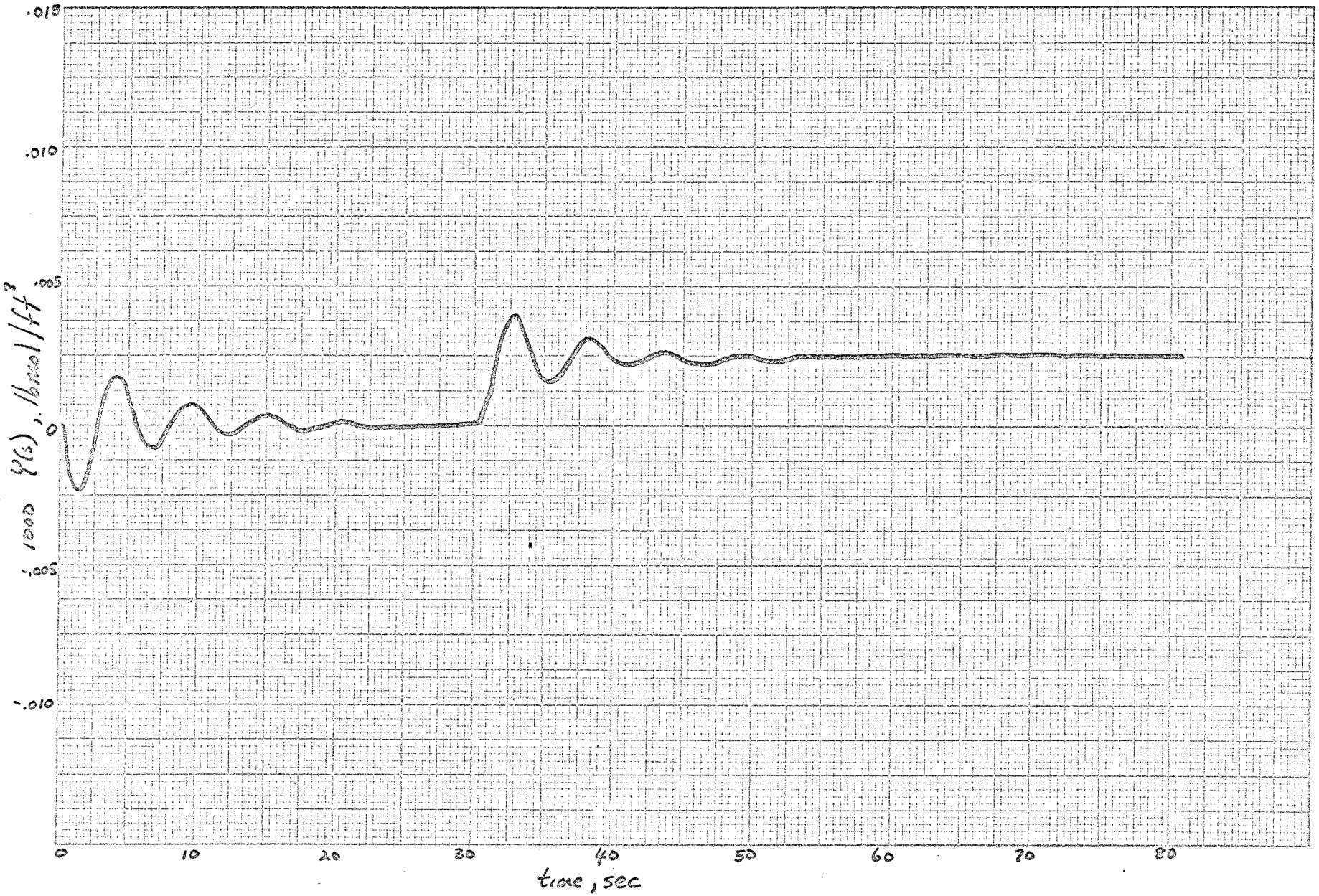

FIGURE 28 TRANSIENT Response for Feedforward-feedback Control, PI: $K_c = 1$, $\tau_I = .1$ Change IN set-point.

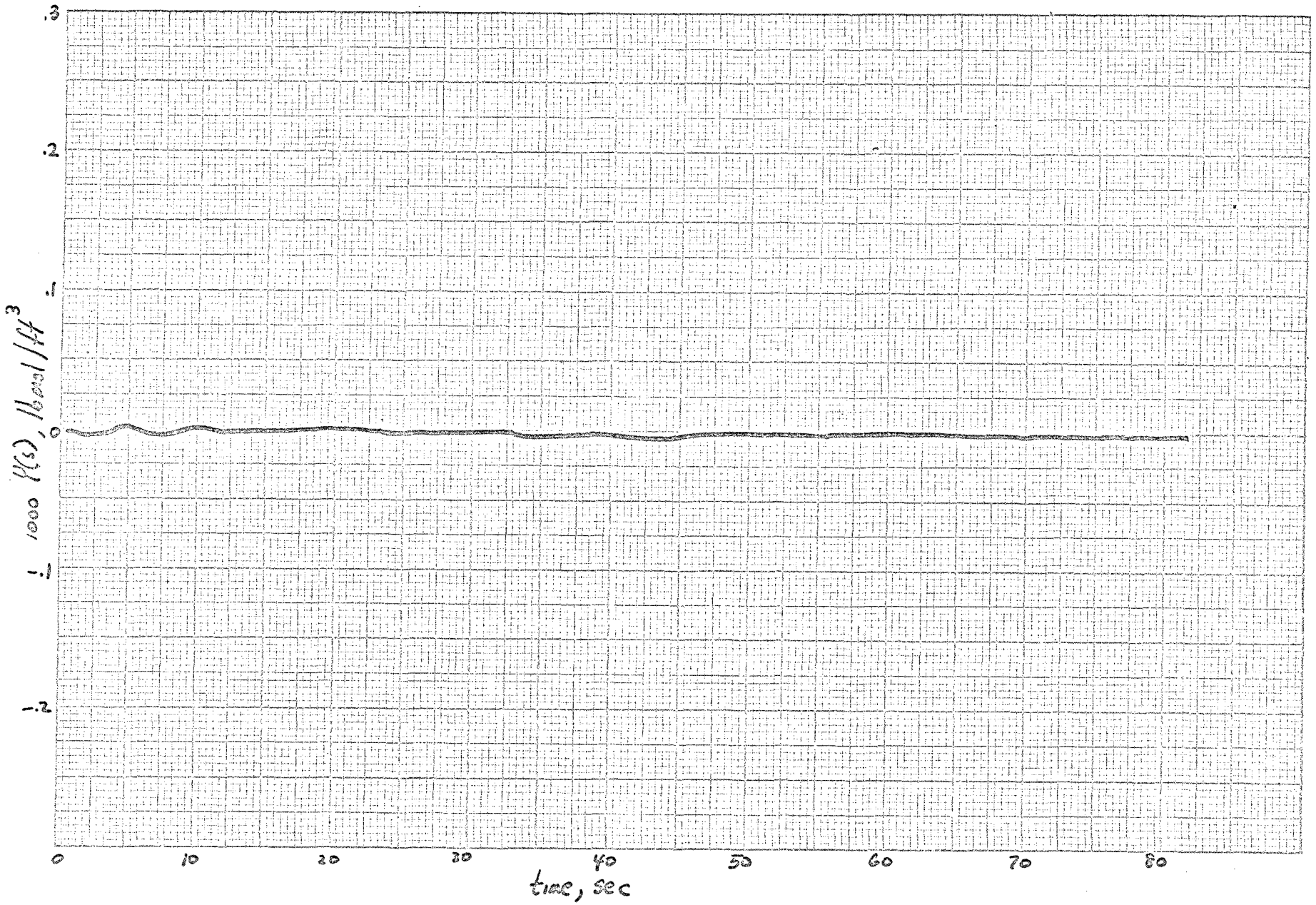

Figure 29 Transient Response for Feedforward-feedback Control, PI: $K_c = 1$, $\tau_I = .1$ Change in load.

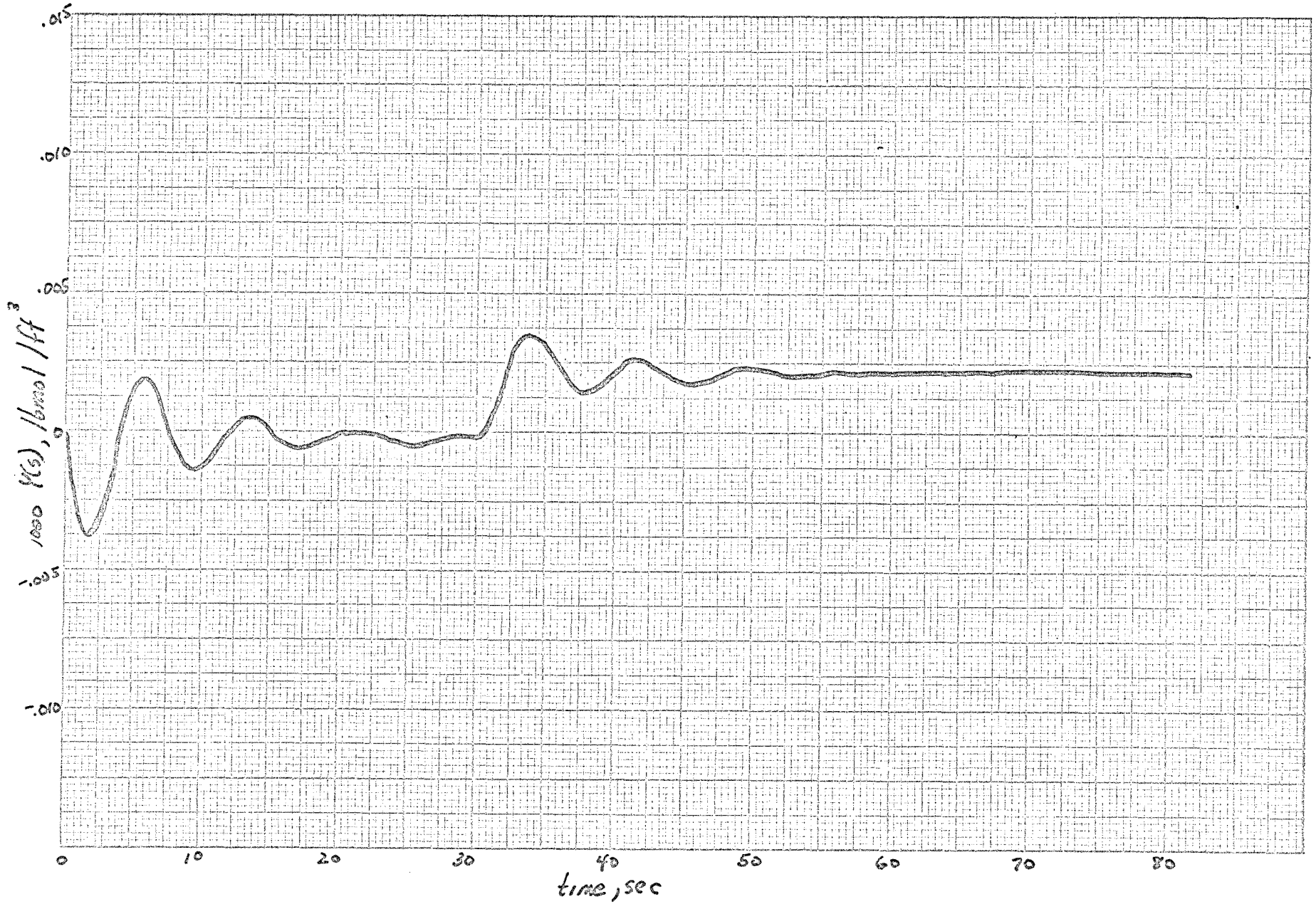

Figure 30 TRANSIENT Response for Feedforward-feedback Control.
PI: $K_c = .5$, $\tau_I = .1$ Change in set-point

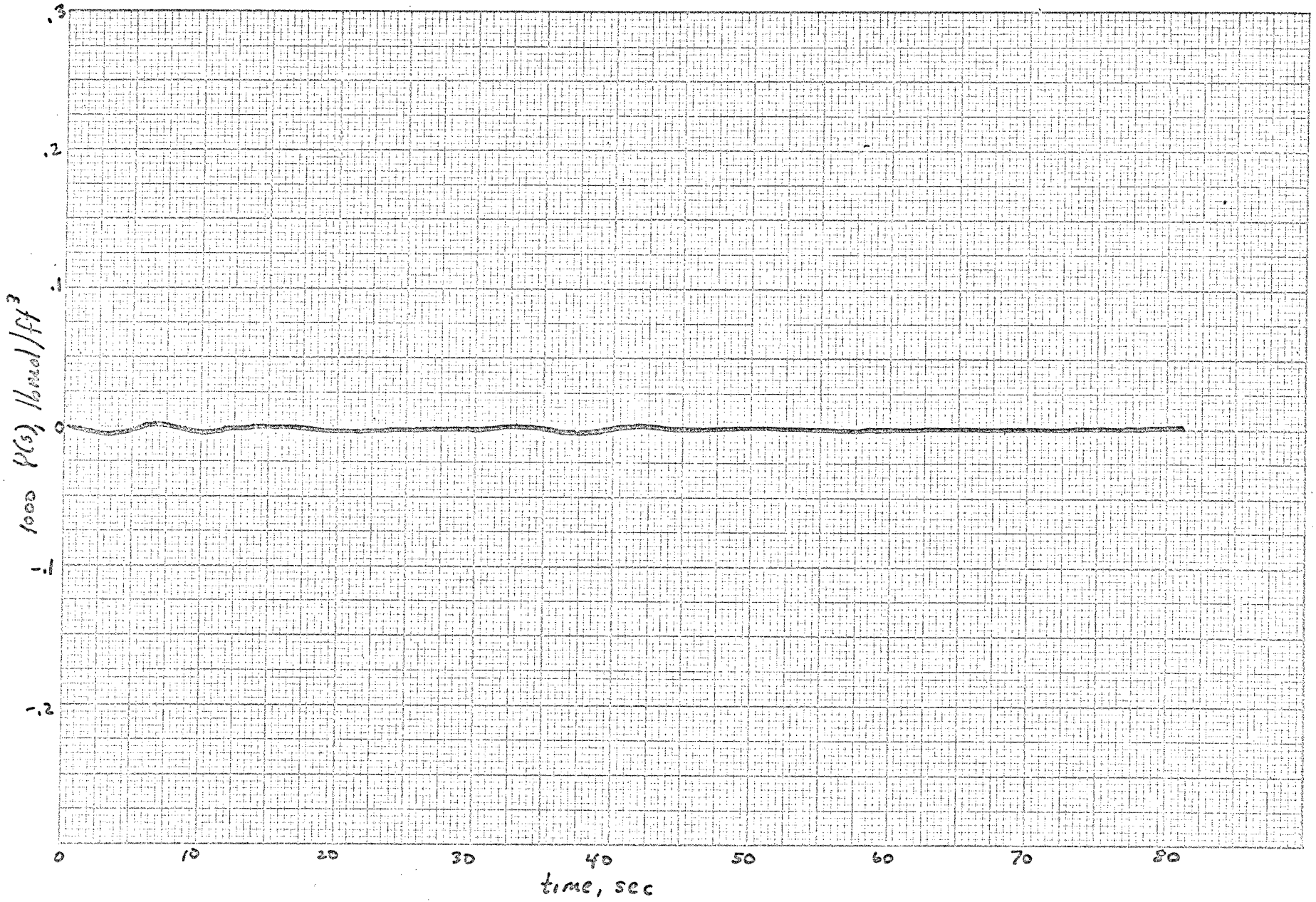

Figure 31 Transient Response for Feedforward-feedback Control, PI: $K_c = .5$, $\tau_I = .1$ Change in Load.

Figure 32 Ziegler-Nichols and Cohen-Coon Ultimate Controller Settings. Proportional: $K_c = 4$ Change in set-point

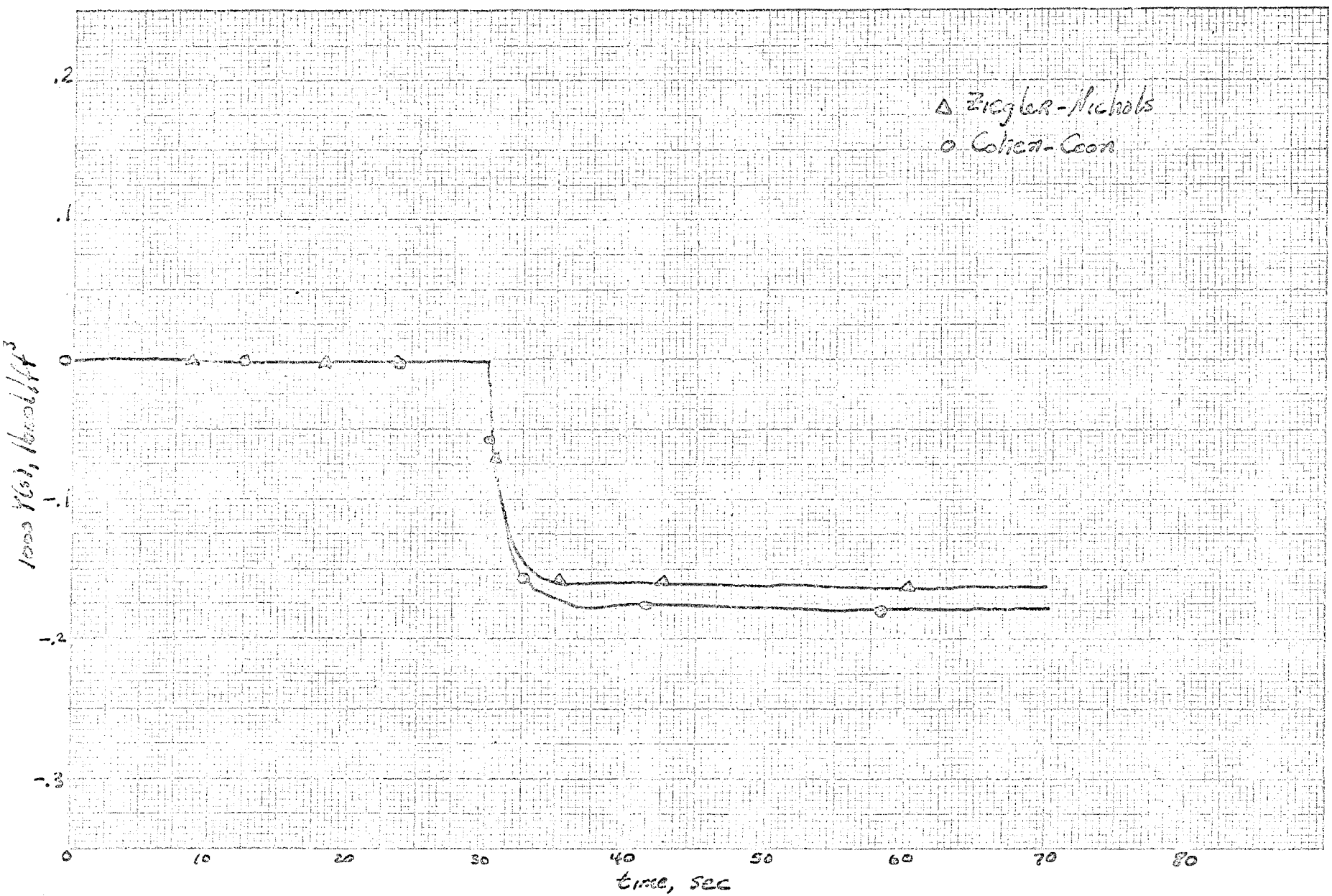

Figure 33 Ziegler-Nichols and Cohen-Coon Ultimate Controller Settings
Proportional: $K_c = 4$ Change in load

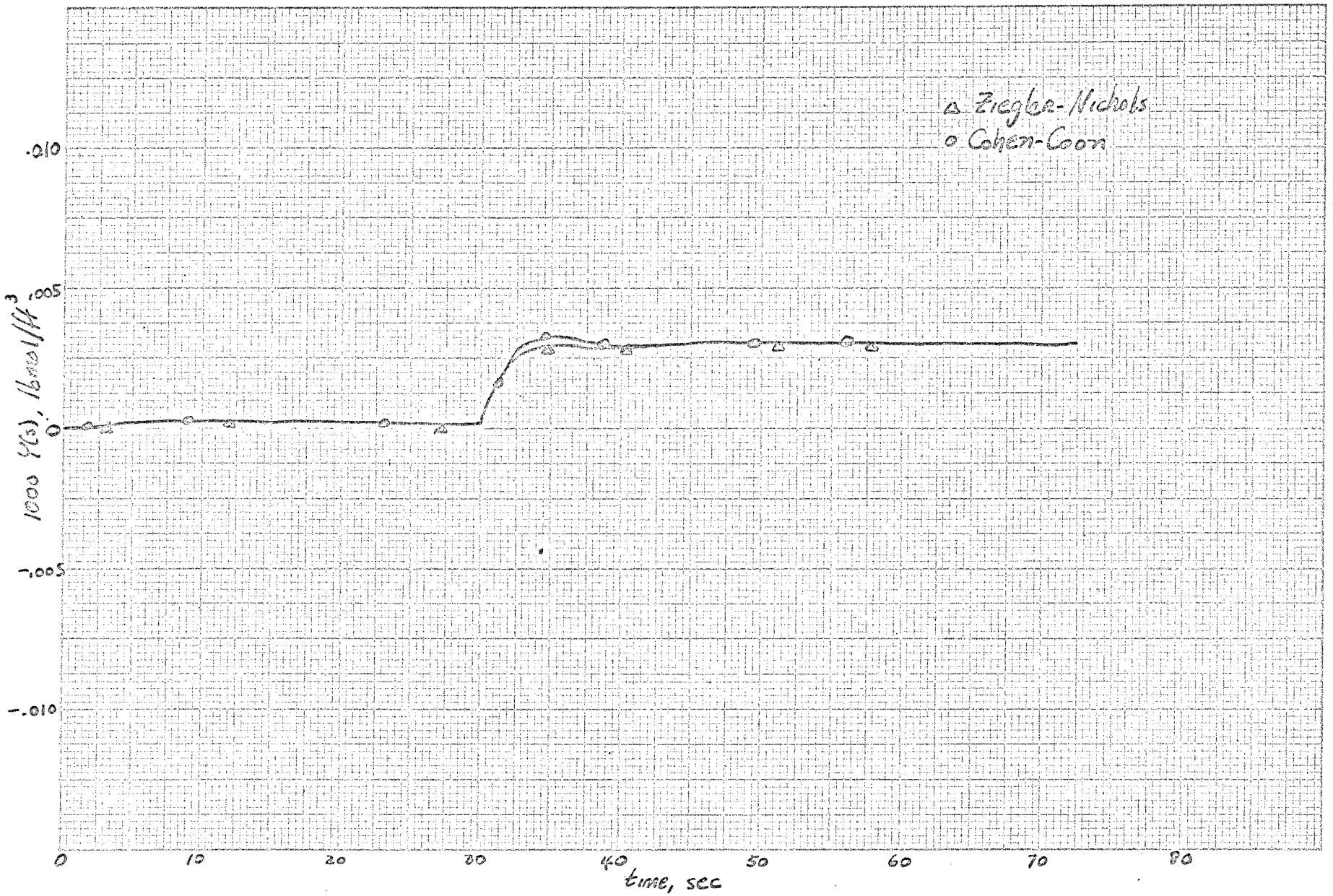

Figure 34 Ziegler-Nichols and Cohen-Coon Ultimate Controller Settings
PI: $K_c = 4$ Change in set-point

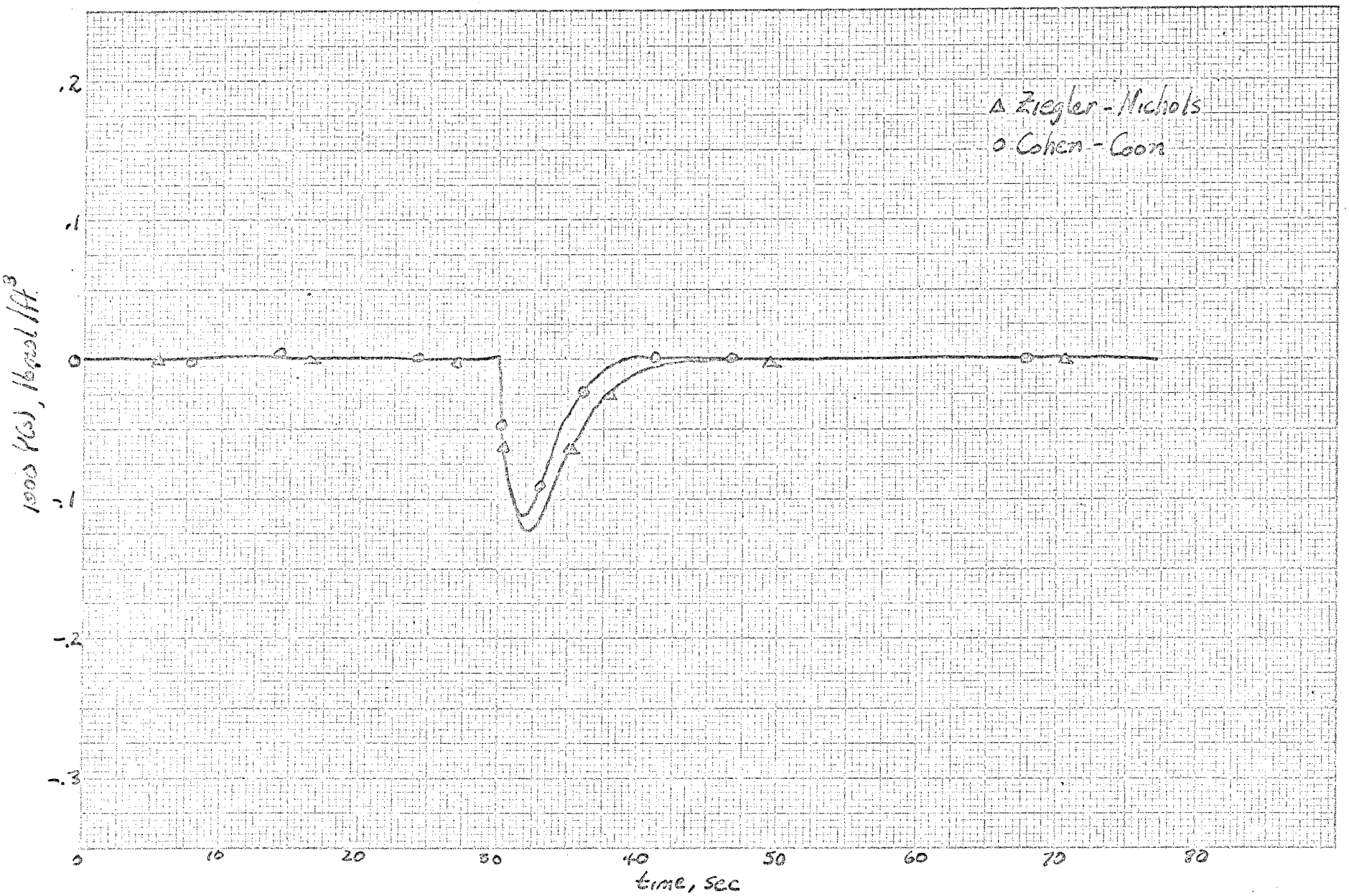

Figure 35 Ziegler-Nichols and Cohen-Coon Ultimate Controller Settings
PI: Change in load

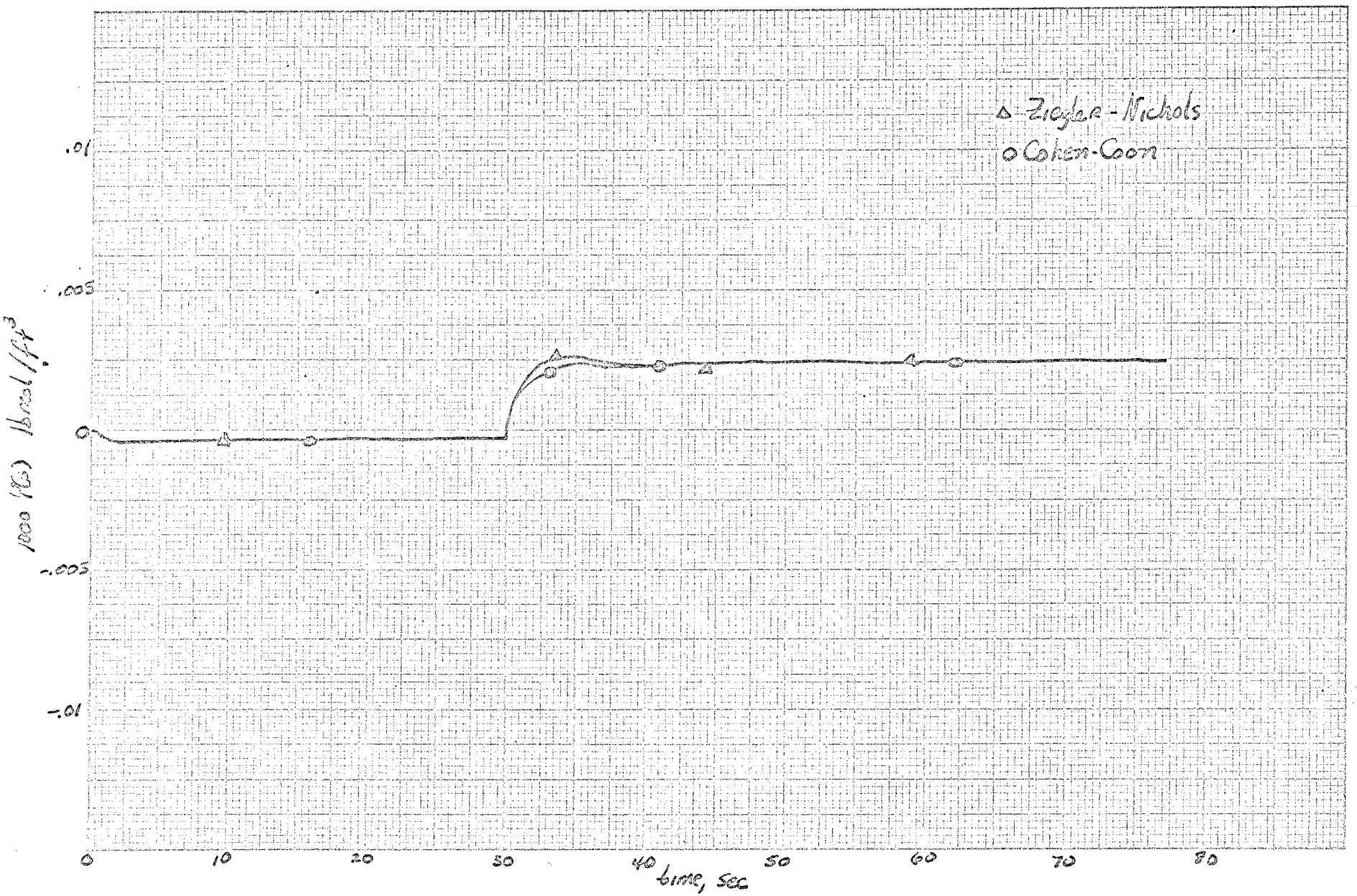

Figure 36 Ziegler-Nichols and Cohen-Coon Ultimate Controller Settings
PID: Change in set-point

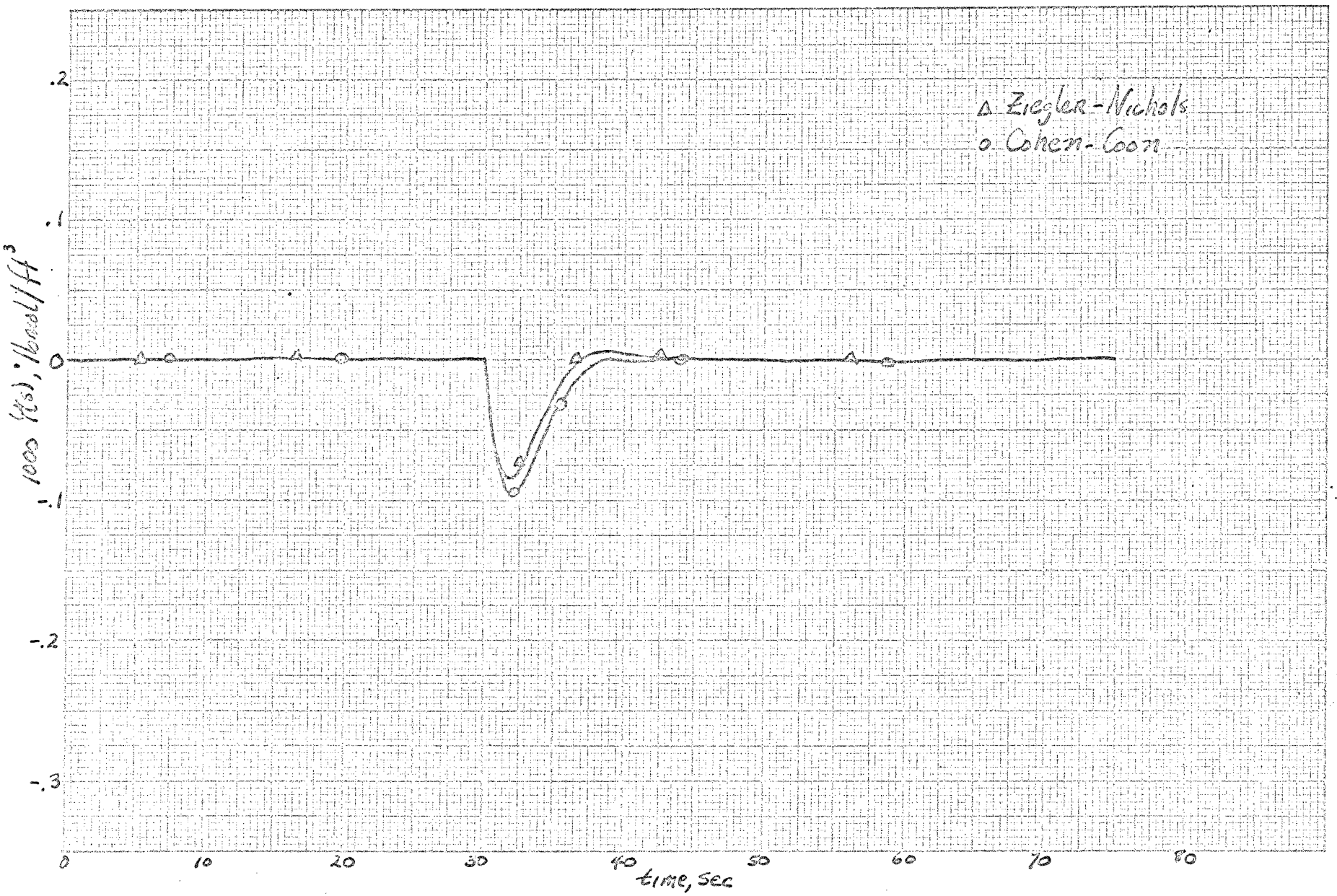

Figure 37 Ziglar-Nichols and Cohen-Coon Ultimate Controller Settings
PID: Change in Load

CONCLUSIONS

From the results of this study it can be concluded that:

1. Combined feedforward-feedback control systems bring about tighter control of a fluidized-bed reactor than either feedforward or feedback alone.

2. Both the Ziegler-Nichols and the Cohen and Coon reaction curve methods of determining values of K_c, T_i, and T_d for optimum control appear to be equally good in achieving tighter control.

3. Elimination of the lag time term from the process transfer function only shifts the curve to the left an amount equal to the reactor lag time.

RECOMMENDATIONS

The findings of this paper and those of the EAI Bulletin No. ALAC64075, (3), show that combined feedforward feedback control systems offer improvements in the performance of systems displaying large holdup times. Perhaps this would not be so with systems with relatively shorter holdup times. This should be investigated.

Other disturbances other than step changes in set-point and load should also be investigated.

NOMENCLATURE

A	Gain at the crossover frequency
C_c	Concentration of cumene, lbmol/ft^3
$G_c(s)$	Controller transfer function
$G_f(s)$	Ideal controller transfer function
$G_p(s)$	Process transfer function
G_v	Transfer function for valve, ft^3/sec psi
H_1	Transducer transfer function, psi sec/ ft^3
H_2	Transducer transfer function, psi ft^3/lbmol
j	Sqrt(-1)
K_c	Proportional Gain
K_u	$(\partial z/\partial u)_c$
K_u	Ultimate gain
K_x	$(\partial z/\partial x)_c$
M	Molecular weight of cumene
P_u	Ultimate period, sec/cycle
$R(t)$	Step change in set-point
s	Laplace transform variable
T_i	Integral time constant, sec
T_d	Derivative time constant, sec
T_o	Reactor lag time, sec
T_1	Transportation time delay, sec
u_{mf}	Minimum fluidization velocity, ft/sec
$u(t)$	Solvent flow rate, ft^3/sec
$U(t)$	Step change in load, ft^3/sec

w Frequency, radians

w_{co} Crossover frequency, radians

$x(t)$ Volumetric flow rate of cumene, ft^3/sec

y_c Mole fraction of cumene

$z(t)$ Total volumetric flow rate through bed, ft^3/sec

ϱ Molar density of cumene, $lbmol/ft^3$

π Total pressure, atm

APPENDIX

I. Ziegler-Nichols Ultimate Controller Settings

II. Analog Computer Diagrams

- A. Pade Circuit
- B. Feedforward Control System
- C. Feedback Control System
- D. Combined Feedforward-Feedback Control System

III. Bode Diagrams

IV. Digital Computer Program

I. ZIEGLER-NICHOLS ULTIMATE CONTROLLER SETTINGS

The Ziegler-Nichols settings are derived by determining the ultimate gain and the ultimate period. The ultimate gain is defined as:

$$K_u' = 1/A$$

where A is the gain at the crossover frequency, w_{co}. The ultimate period is defined as:

$$P_u = 2\pi / w_{co}$$

A method of determining K_u' and P_u is given below:

Let G(s) represent the gain of the final control element, the process, and the measuring element in series. This function is needed at the crossover frequency. Hence,

$$G(s) = G_v K_x H_2 G_p(s) \tag{46}$$

Now as previously stated,

$$G_p(s) = \frac{e^{-T_o s}}{T_1 s + 1} \tag{1}$$

and,

$$s = jw \tag{47}$$

Thus,

$$G_p(jw) = e^{-T_o jw} / T_1 jw + 1 \tag{48}$$

$$G(jw) = G_v K_x H_2 G_p(jw) \tag{49}$$

$$G(jw) = 0.635 \frac{e^{-T_o jw}}{T_1 jw + 1} \tag{50}$$

$$G(jw) = 0.635 \left[\frac{-T_1 jw + 1}{-T_1 jw + 1}\right] \left[\frac{\cos w - j \sin w}{T_1 jw + 1}\right] \tag{51}$$

$$G(jw) = \frac{0.635}{T_1^2 w^2 + 1} - j \frac{3.175w}{T_1^2 w^2 + 1} (\cos w - j \sin w) \tag{52}$$

Simplifying terms,

$$G(jw) = \frac{0.635\cos w - 3.175w \sin w}{25w^2 + 1} + j\frac{-3.175w \cos w - 0.635\sin w}{25w^2 + 1} \quad (53)$$

By definition,

$$\angle G(jw) = \tan^{-1} \frac{-3.175w \cos w - 0.635\sin w}{0.635\cos w - 3.175w \sin w} \quad (54)$$

The crossover frequency is that frequency at which the phase lag is 180°, i.e.,

$$G(jw) = 180^\circ = \tan^{-1} 0.0 \quad (55)$$

Thus,

$$\angle G(jw_{co}) = 0.0 = \frac{-3.175w_{co}\cos w_{co} - 0.635\sin w_{co}}{0.635\cos w_{co} - 3.175w_{co}\sin w_{co}} \quad (56)$$

Solving by trial

$$w_{co} = 0.0,\ 1.685 \text{ rad}$$

Now for the gain at the crossover frequency:

$$A = |G(jw_{co})| = 0.0836$$

Therefore,

$$\text{Ultimate Period} = P_u = 2\pi/w_{co} = 3.73 \text{ sec/cycle}$$

$$\text{Ultimate gain} = K_u' = 1/A = 12$$

II. ANALOG COMPUTER DIAGRAMS

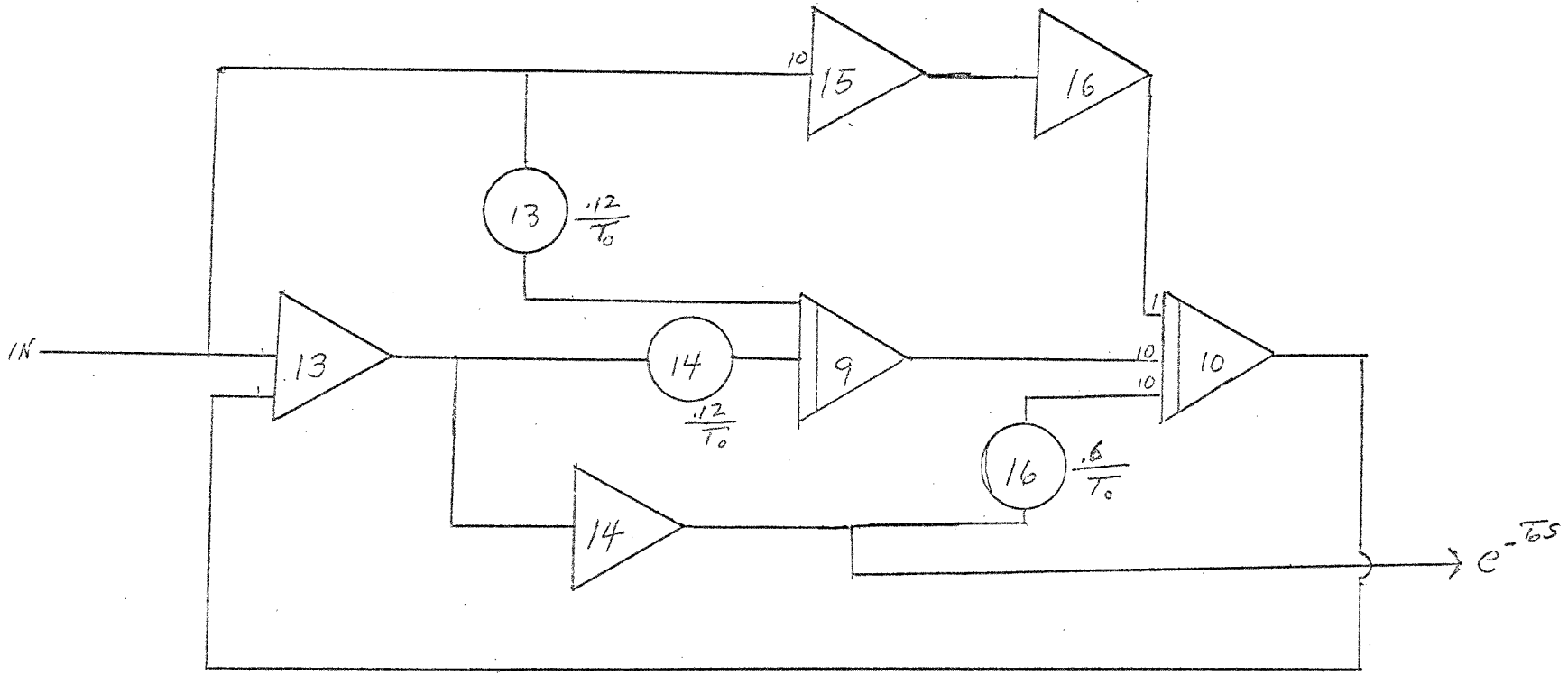

Figure 38 Analog Computer Diagram of Padé-Approximaton

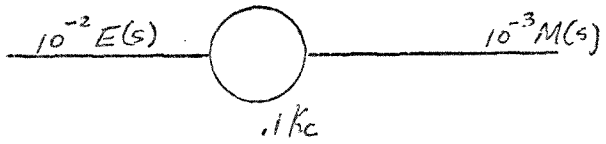

$M(s)/E(s) = K_c$

FIGURE 39 PROPORTIONAL CONTROLLER

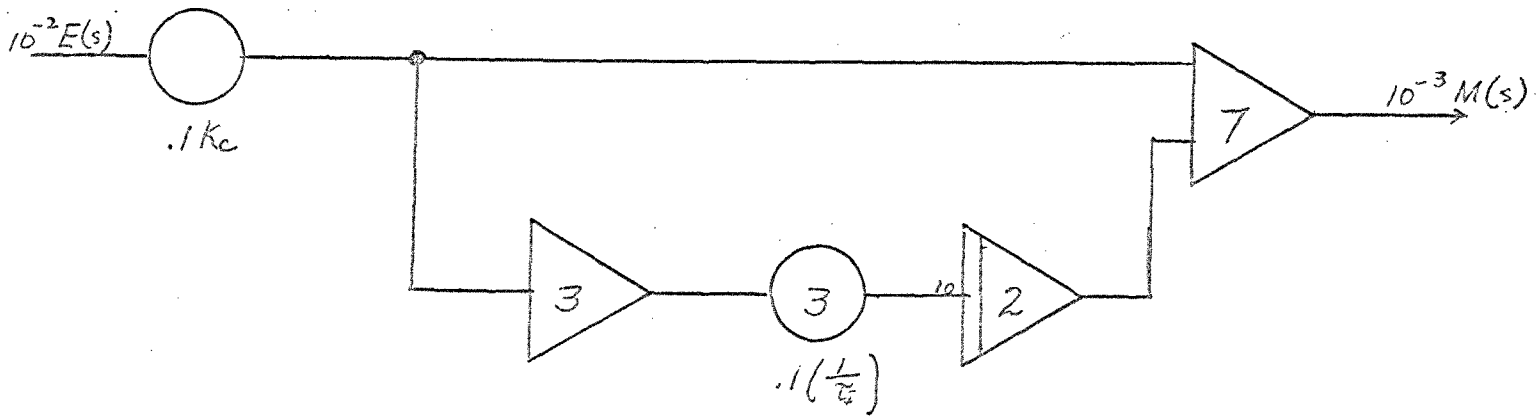

$$M(s)/E(s) = K_c\left(1 + \frac{1}{\tau_i s}\right)$$

FIGURE 40 PROPORTIONAL-INTEGRAL CONTROLLER

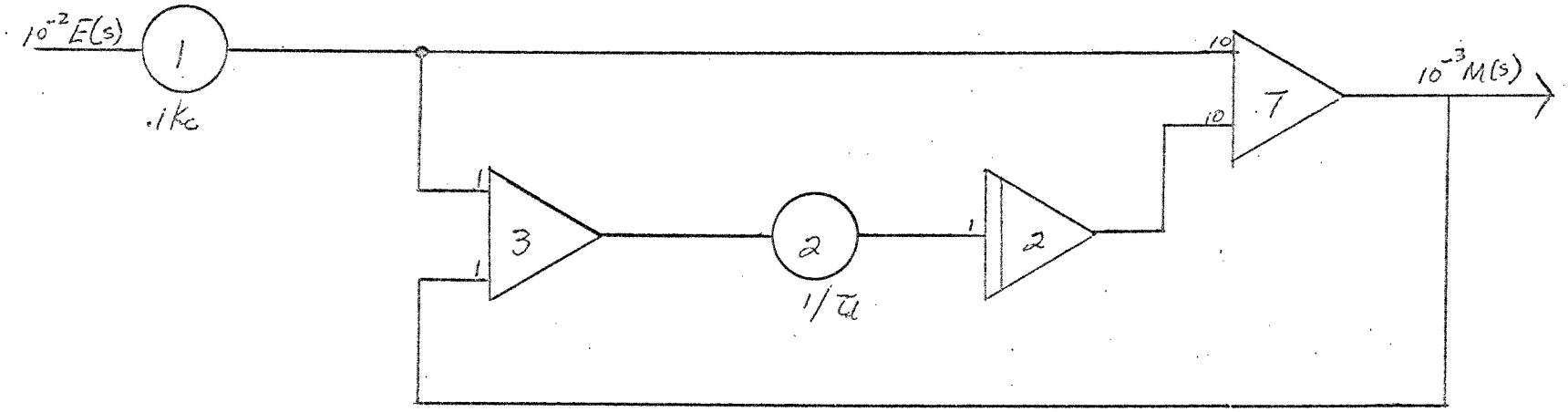

$$M(s)/E(s) = K_c(1 + \tau_d s)$$

FIGURE 41 PROPORTIONAL-DERIVATIVE CONTROLLER

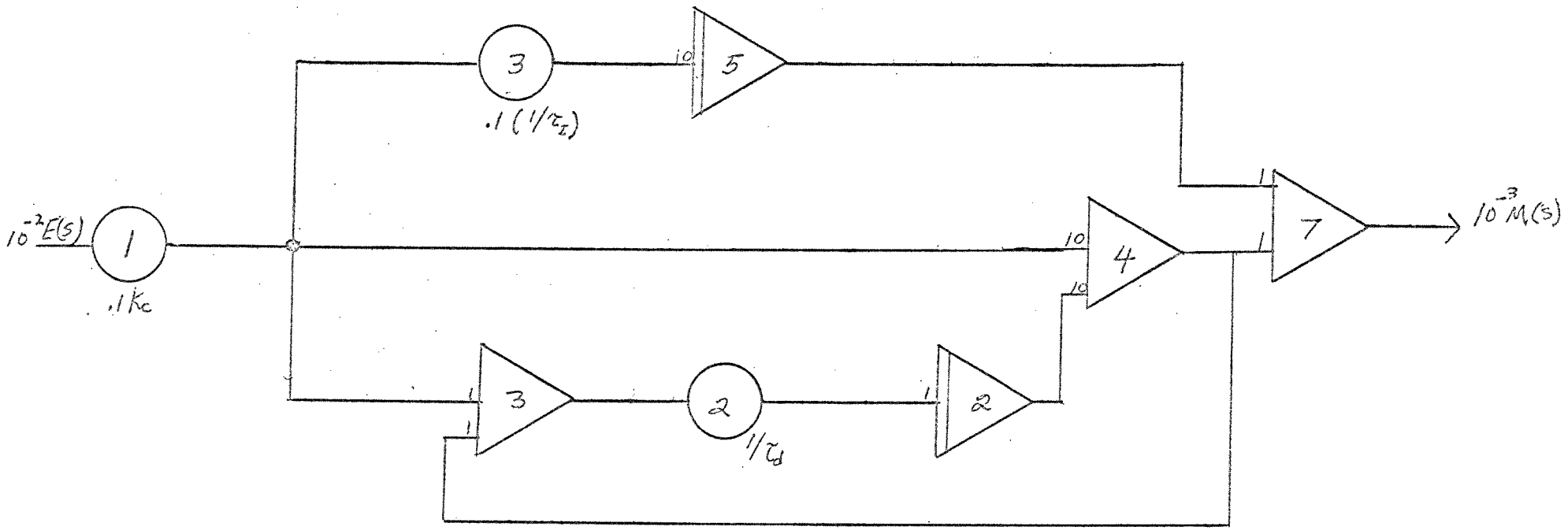

$$M(s)/E(s) = K_c\left(1 + 1/\tau_I s + \tau_d s\right)$$

FIGURE 42 PROPORTIONAL - INTEGRAL - DERIVATIVE CONTROLLER

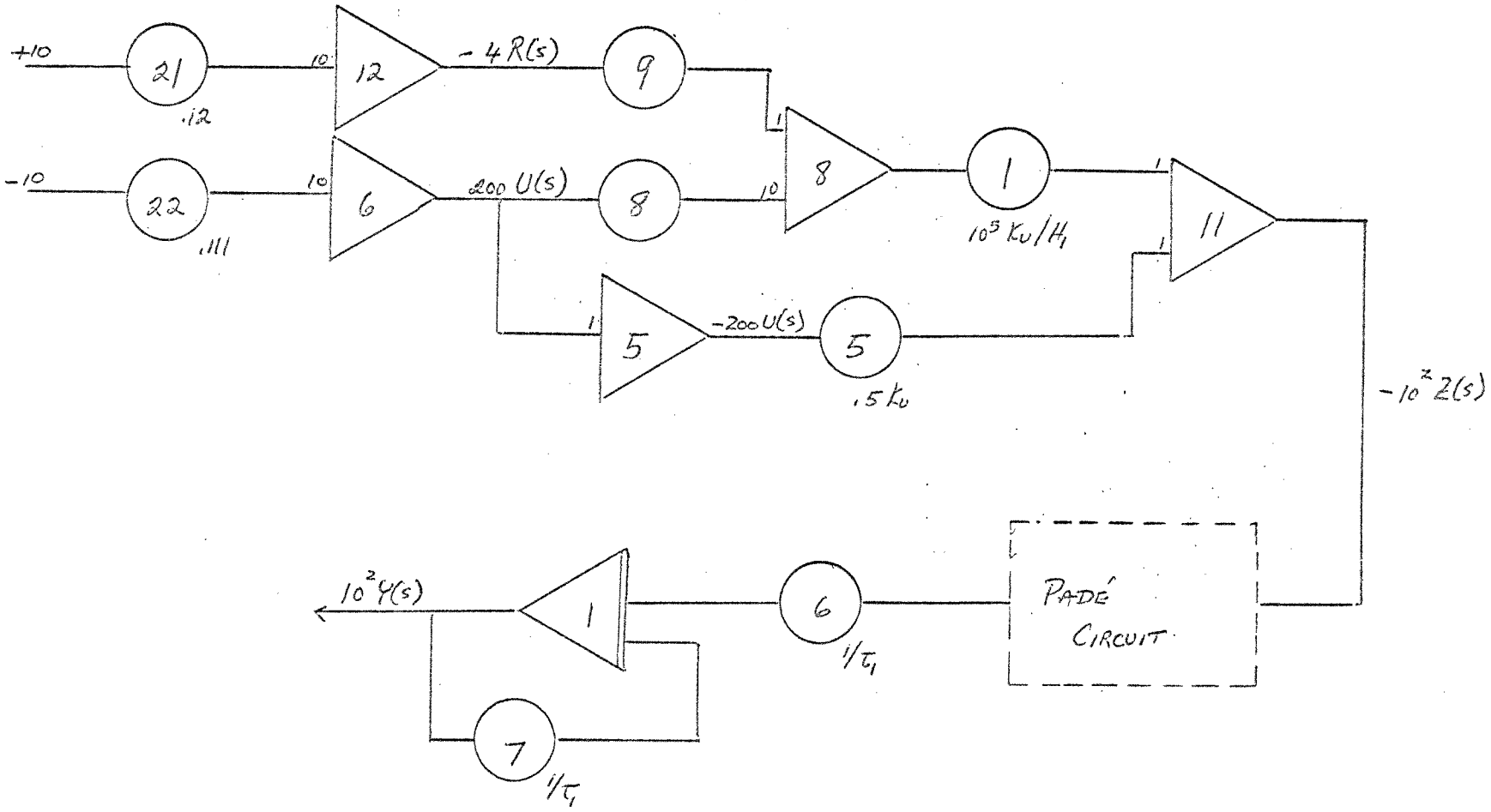

FIGURE 43 FEEDFORWARD CONTROL

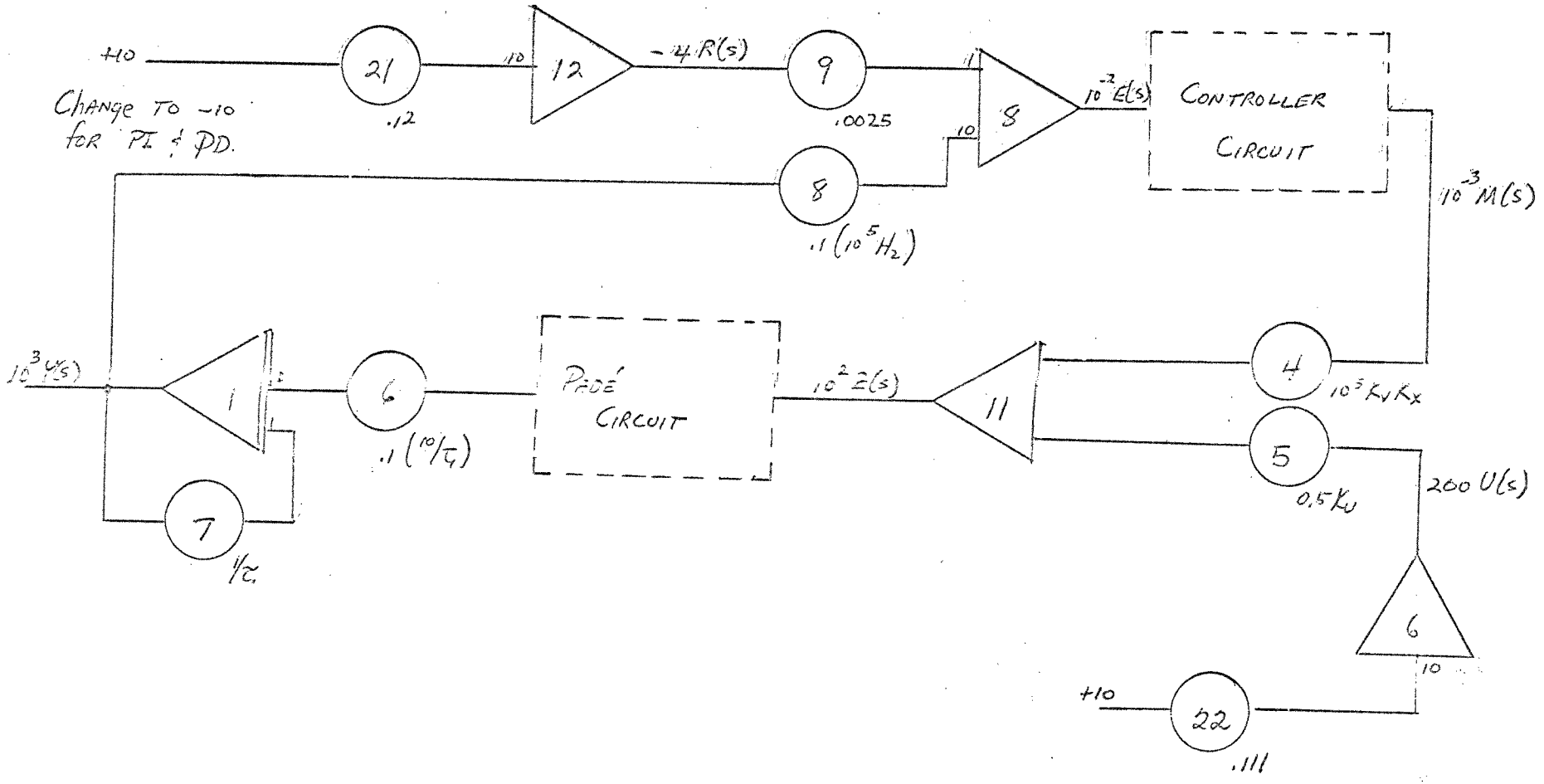

FIGURE 44 Feedback Control

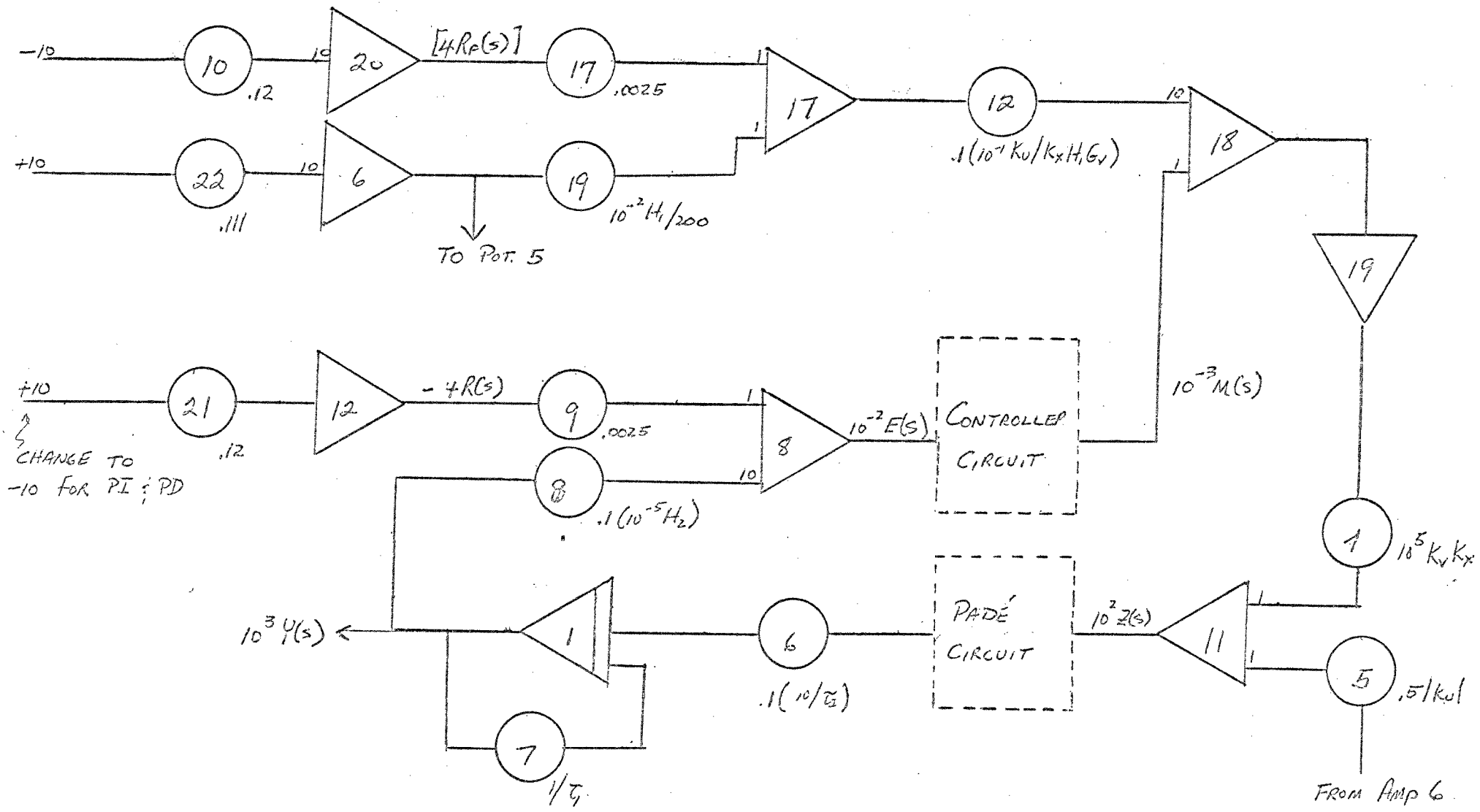

FIGURE 45 FEEDFORWARD - FEEDBACK CONTROL

III. BODE DIAGRAMS

A. Introduction

B. Figures 46-58: Changes in set-point

C. Figures 59-66: Changes in load

Introduction

The following Bode diagrams were obtained by programming the control equations 11, 16 and 25 on a digital computer. In the equations s was set equal to jw. The amplitude ratio was defined as follows:

$$AR = Y(jw)$$

The amplitude ratio is reported in decibels. The phase angle was defined as:

$$G = \tan^{-1} b/a$$

where a is the real part of the control equation and b the imaginary part.

SEMI-LOGARITHMIC
5 CYCLES X 10 DIVISIONS PER INCH
MADE IN U.S.A.

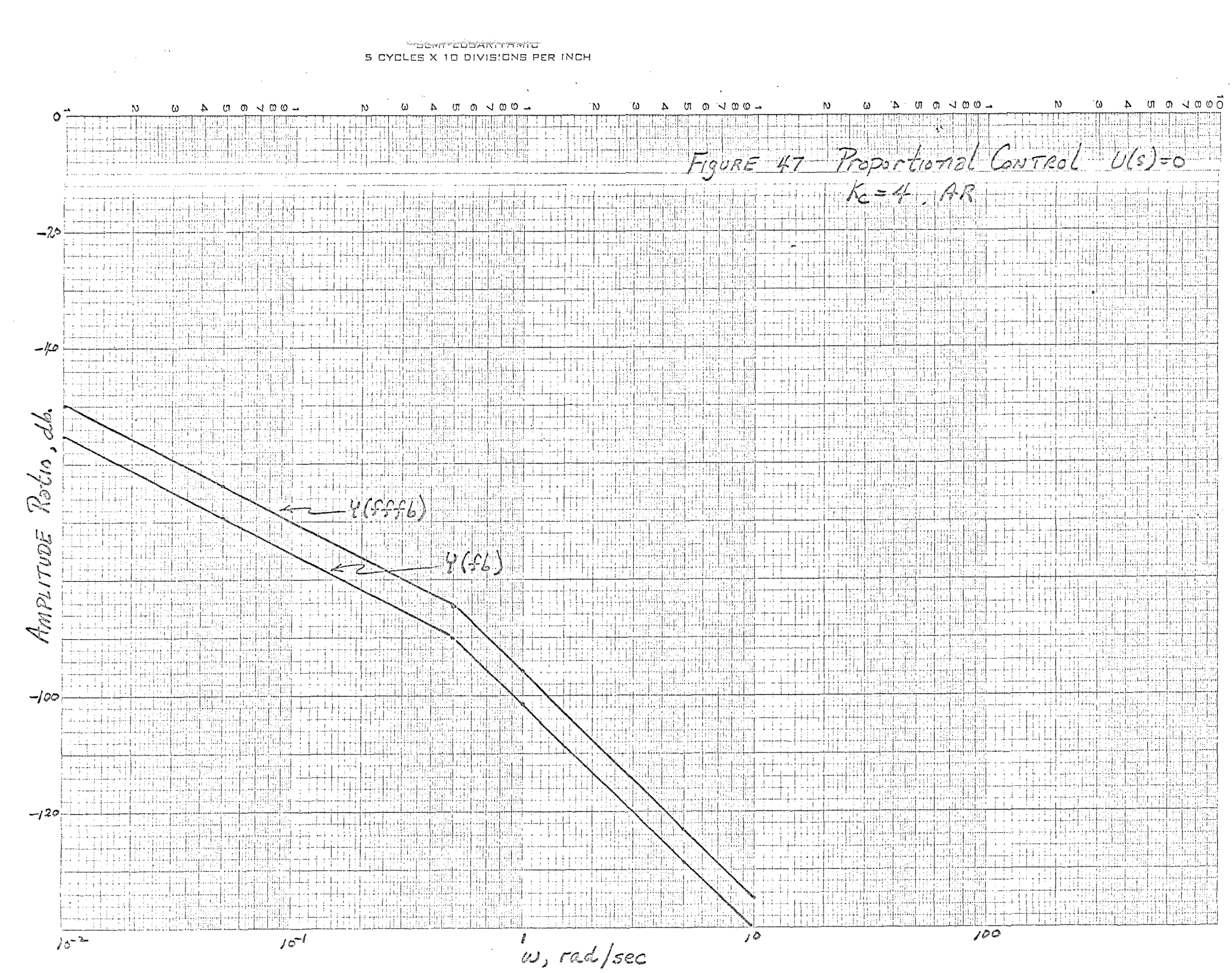

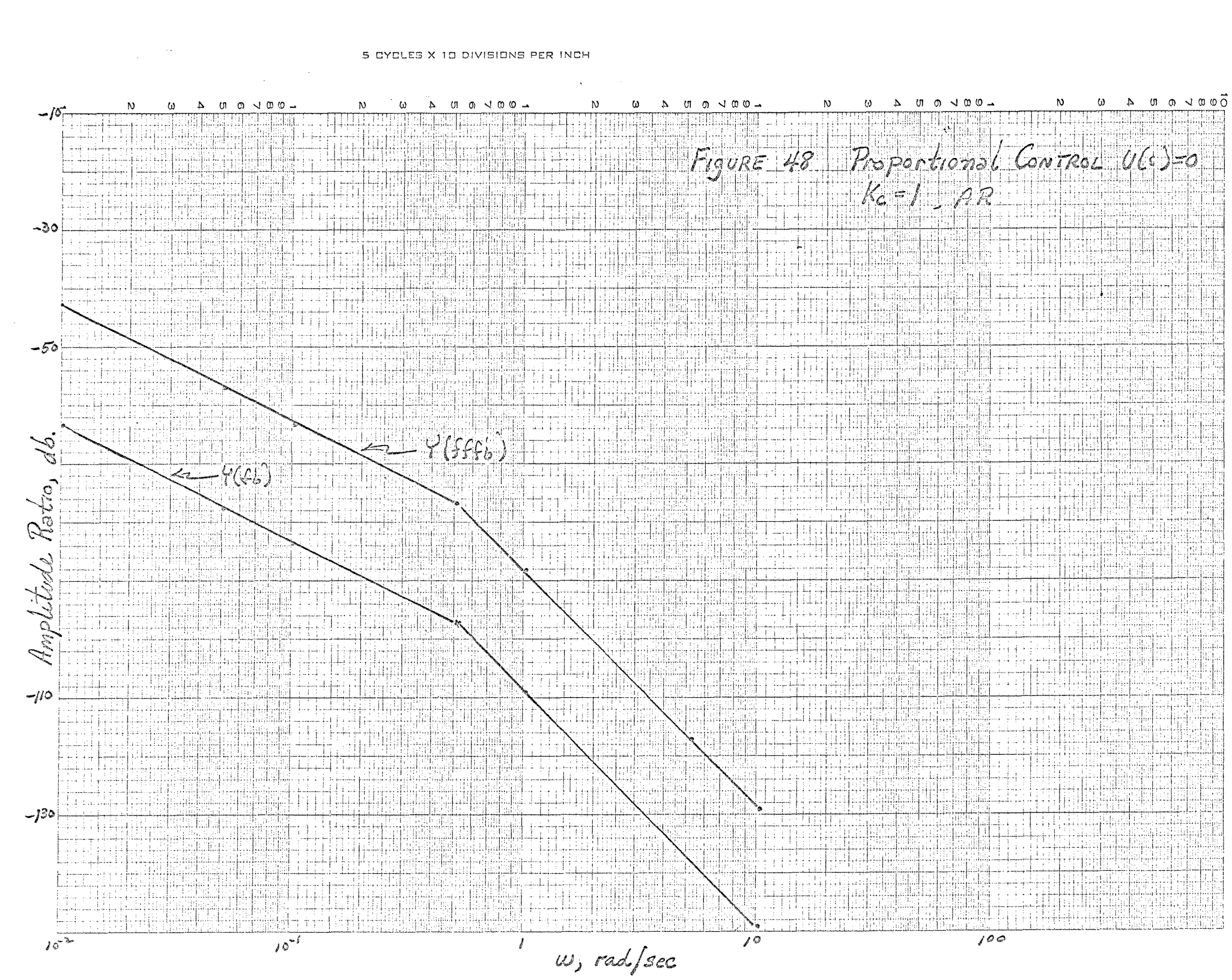
5 CYCLES X 10 DIVISIONS PER INCH
FIGURE 48 Proportional Control $G_c(s)=0$
$K_c = 1$ _ AR
$\Psi(\text{fff}b)$
$\Psi(fb)$
Amplitude Ratio, db.
-10
-30
-50
-110
-130
10^{-2}
10^{-1}
1
10
100
ω, rad/sec

SEMI-LOGARITHMIC
5 CYCLES X 10 DIVISIONS PER INCH

MADE IN U.S.A.

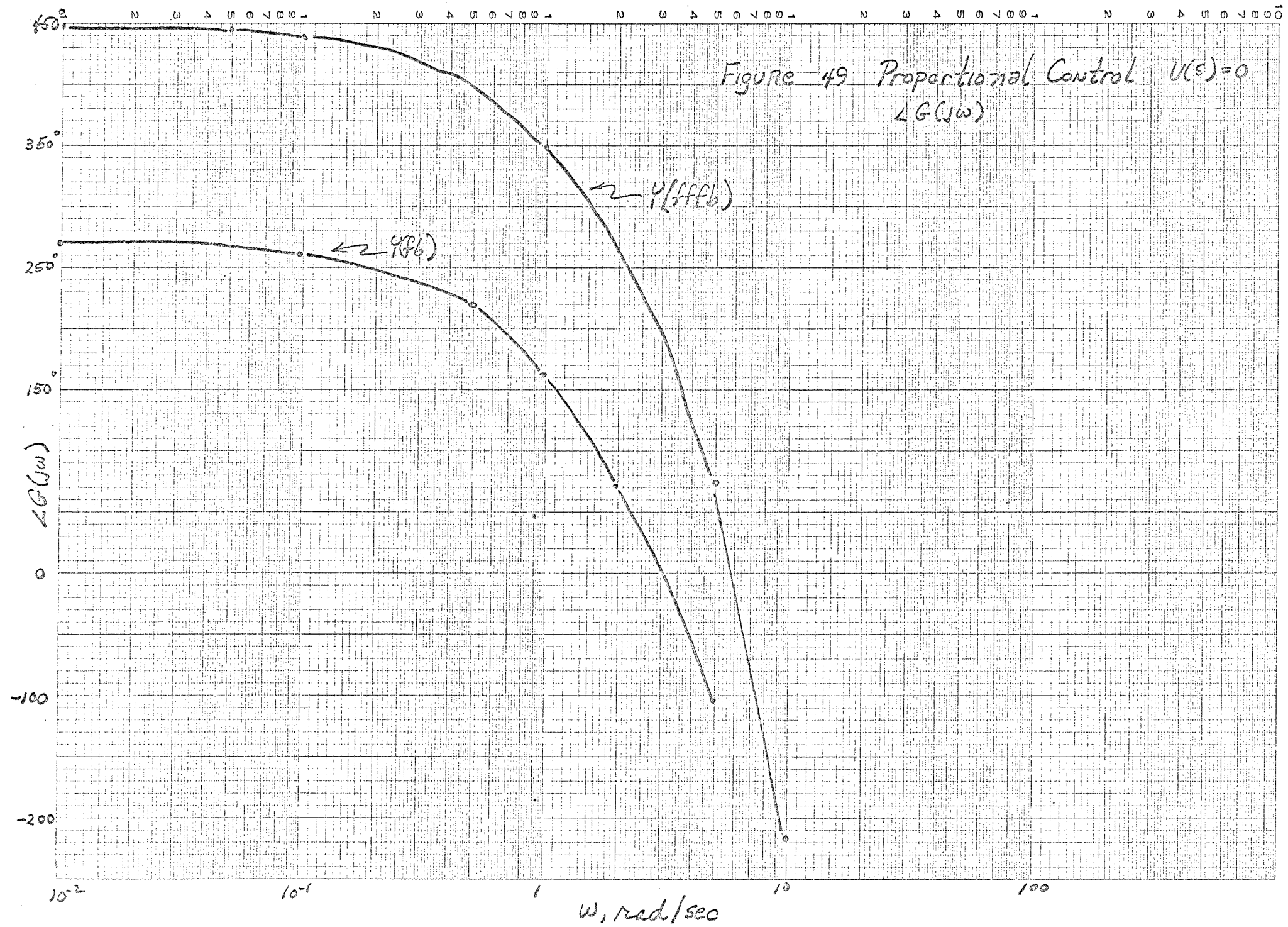

Figure 49 Proportional Control U(s)=0
∠G(jω)

5 CYCLES X 10 DIVISIONS PER INCH

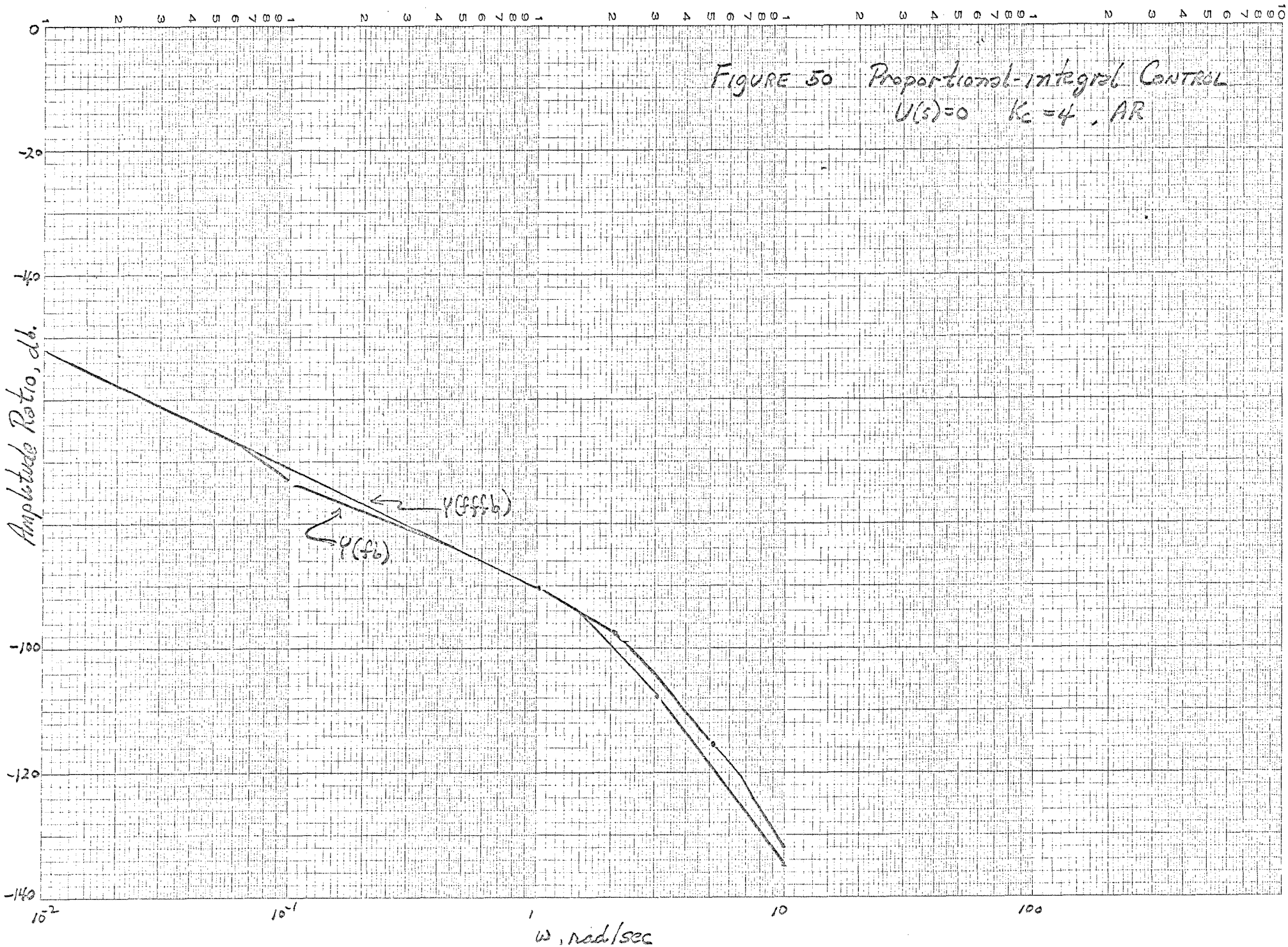

SEMI-LOGARITHMIC
5 CYCLES X 10 DIVISIONS PER INCH

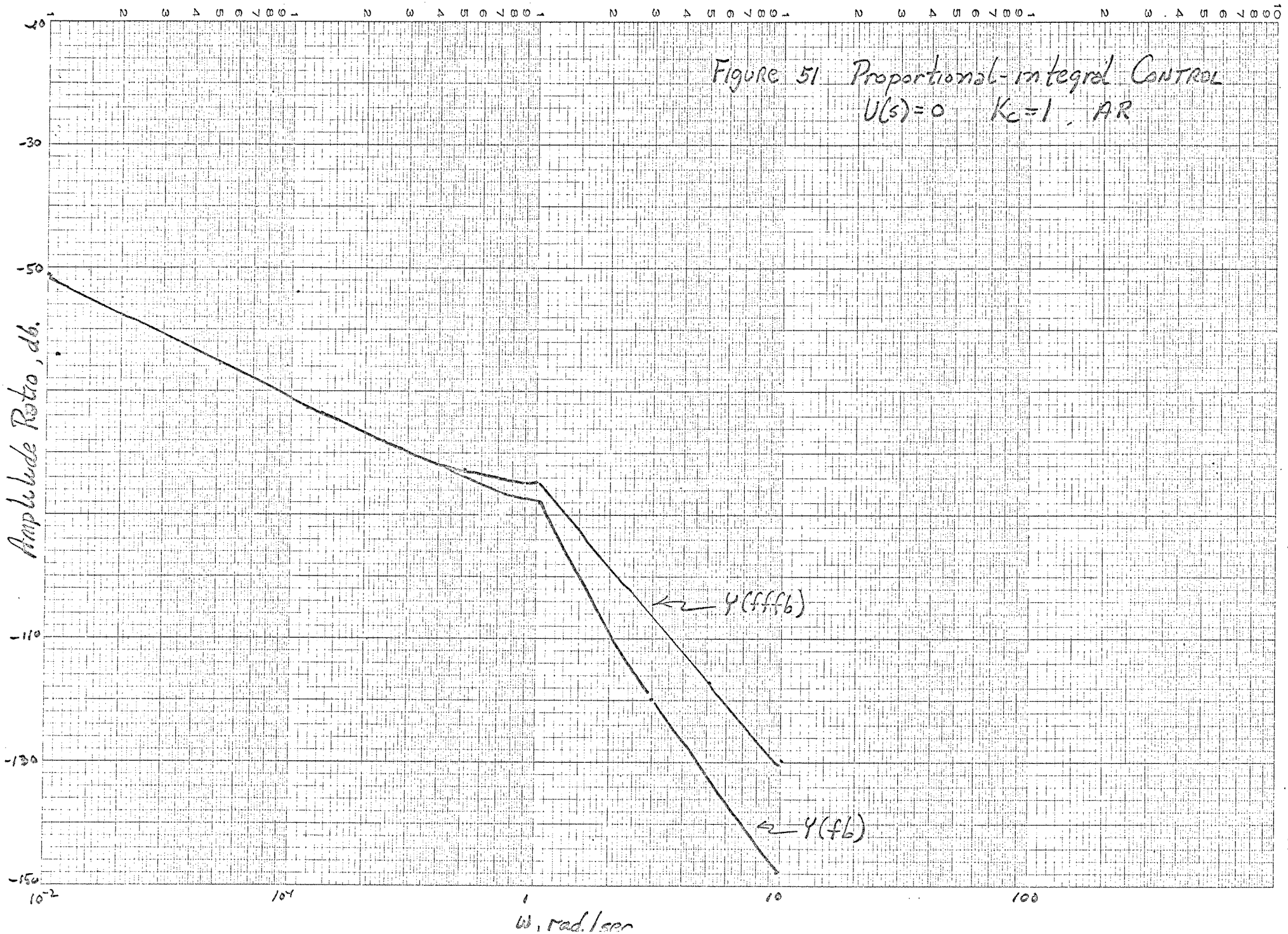

Figure 51 Proportional-integral Control
$U(s) = 0$ $K_c = 1$. AR

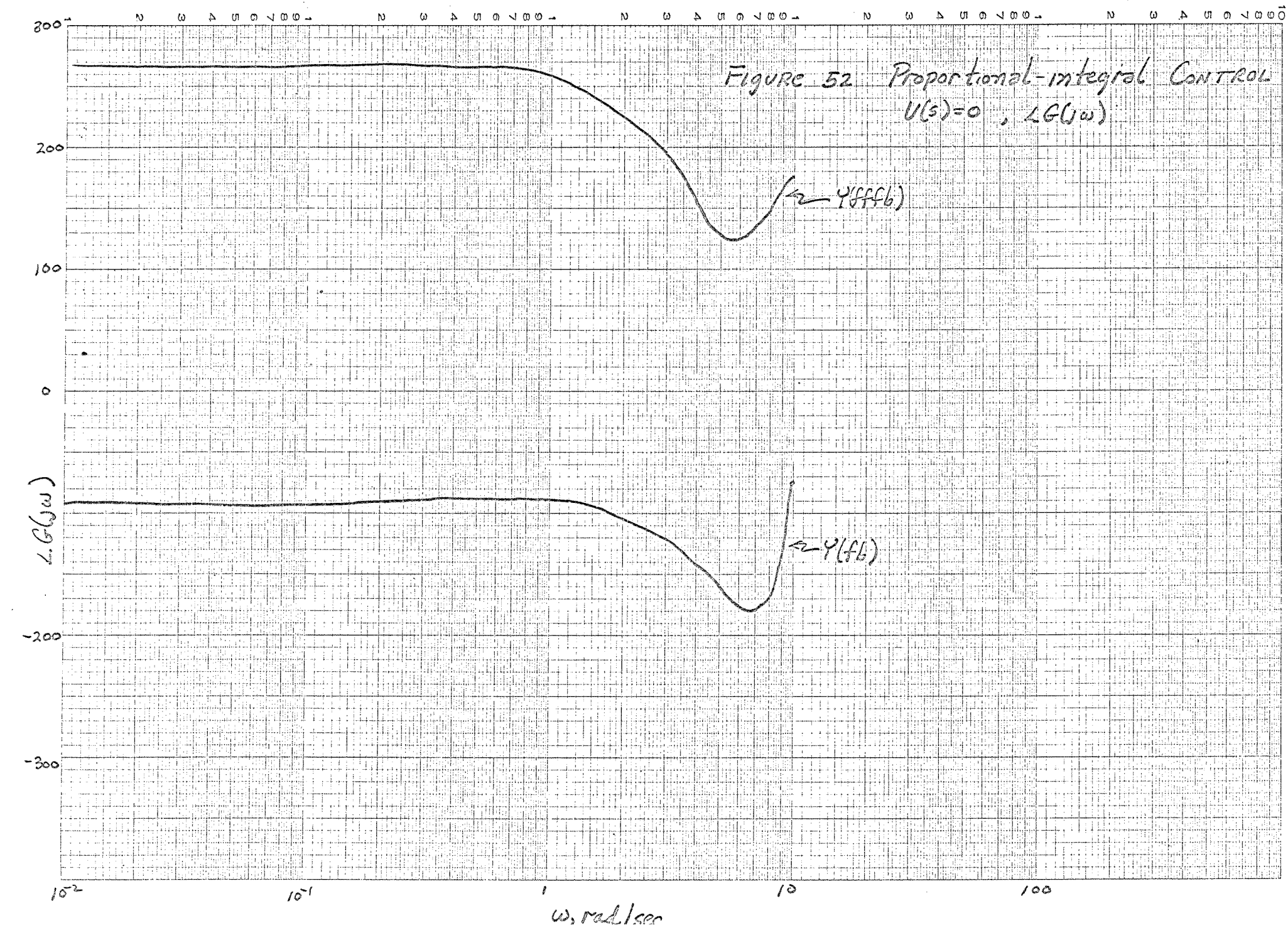
Figure 52 Proportional-integral Control
U(s)=0 , ∠G(jω)
Y(ffft)
Y(ft)
∠G(jω)
ω, rad/sec
800
200
100
0
-200
-300
10⁻²
10⁻¹
1
10
100

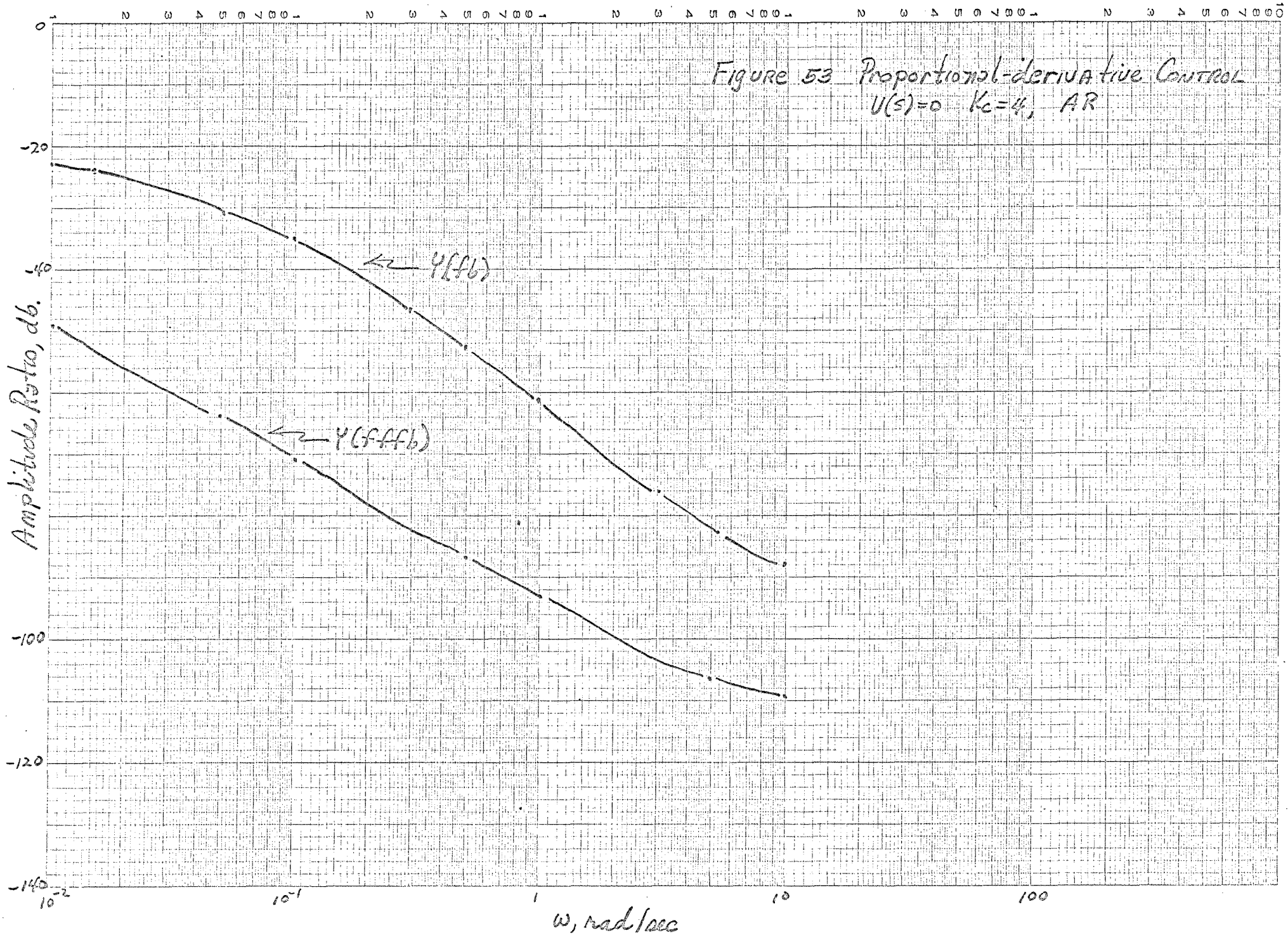

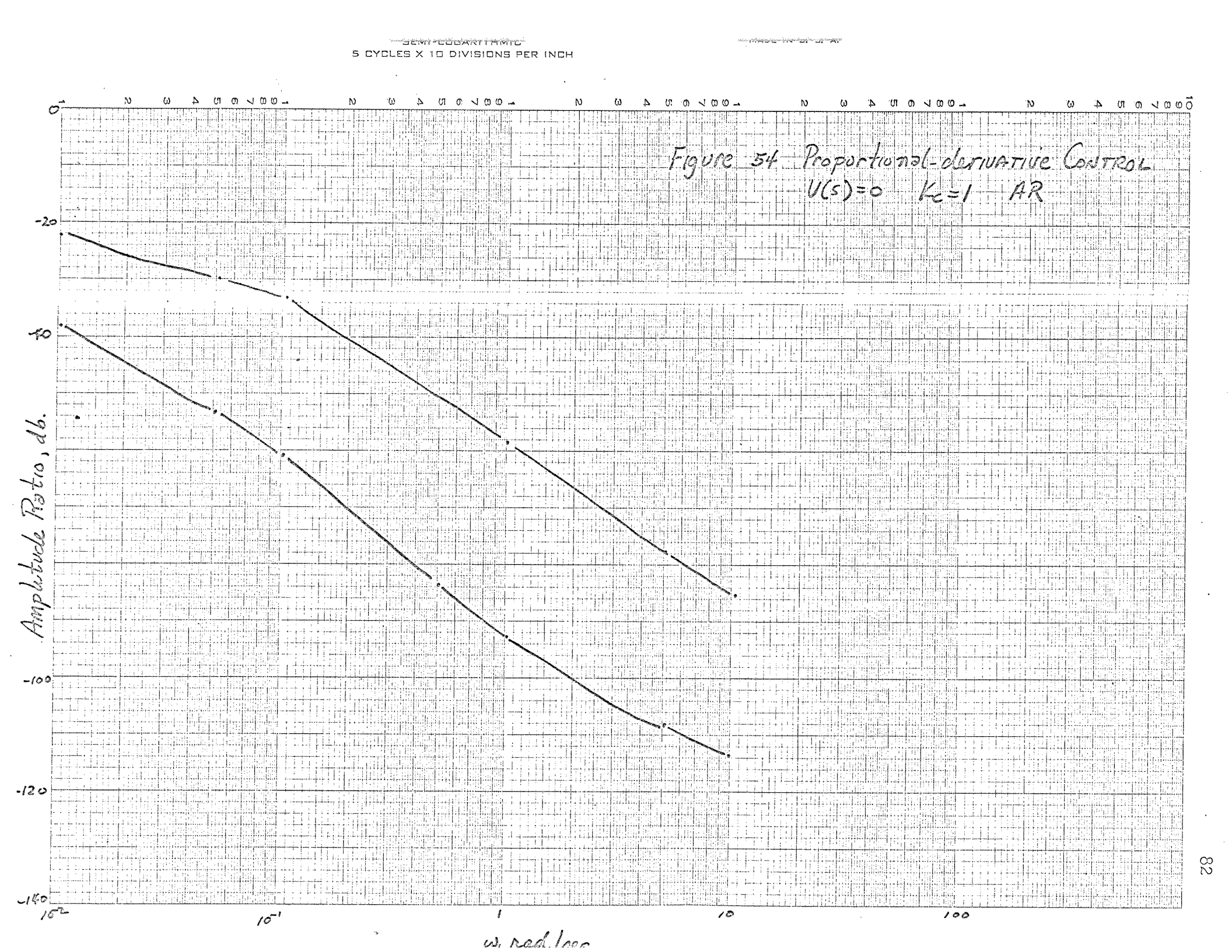
SEMI-LOGARITHMIC
5 CYCLES X 10 DIVISIONS PER INCH
MADE IN U.S.A.
Figure 54 Proportional-derivative Control
U(s)=0 Kc=1 AR
0
-20
-100
-120
-140
Amplitude Ratio, db.
10^2
10^1
1
10
100
w, rad/sec

SEMI-LOGARITHMIC
5 CYCLES X 10 DIVISIONS PER INCH

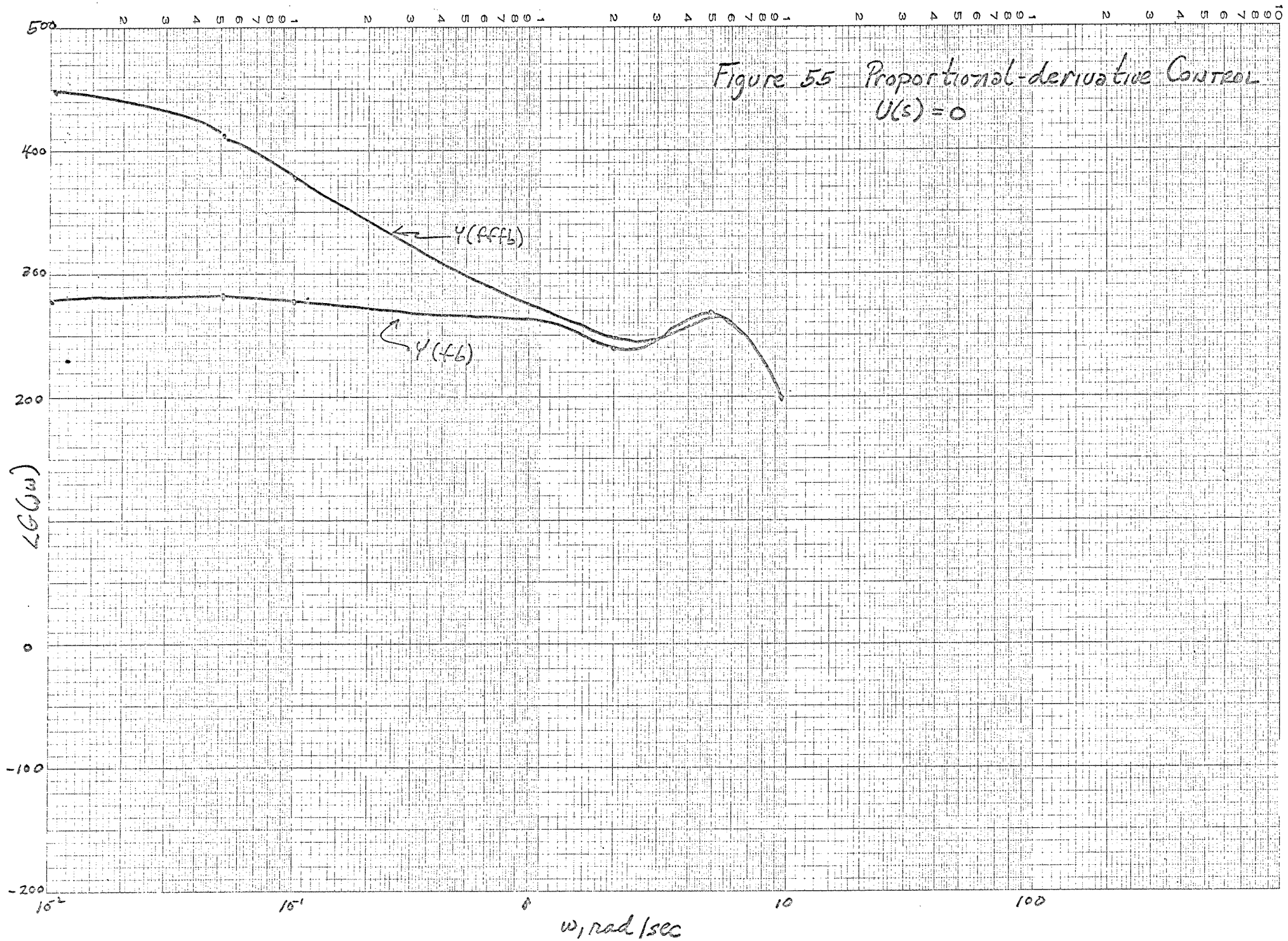

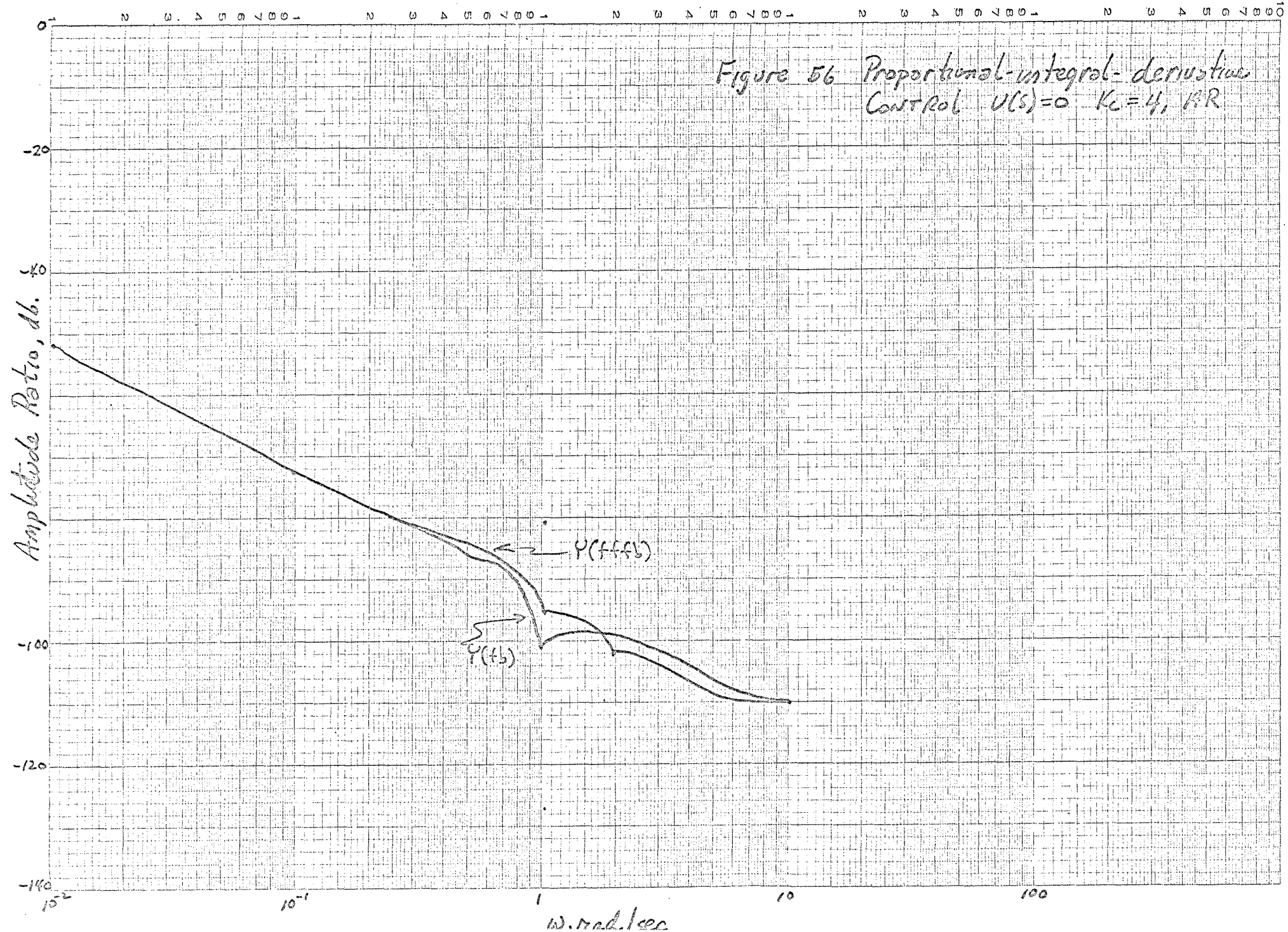
Figure 56 Proportional-integral-derivative Control U(s)=0 K_c=4, AR
Amplitude Ratio, db.
0
-20
-40
-100
-120
-140
Y(fffb)
Y(fb)
10^{-2}
10^{-1}
1
10
100
w, rad/sec

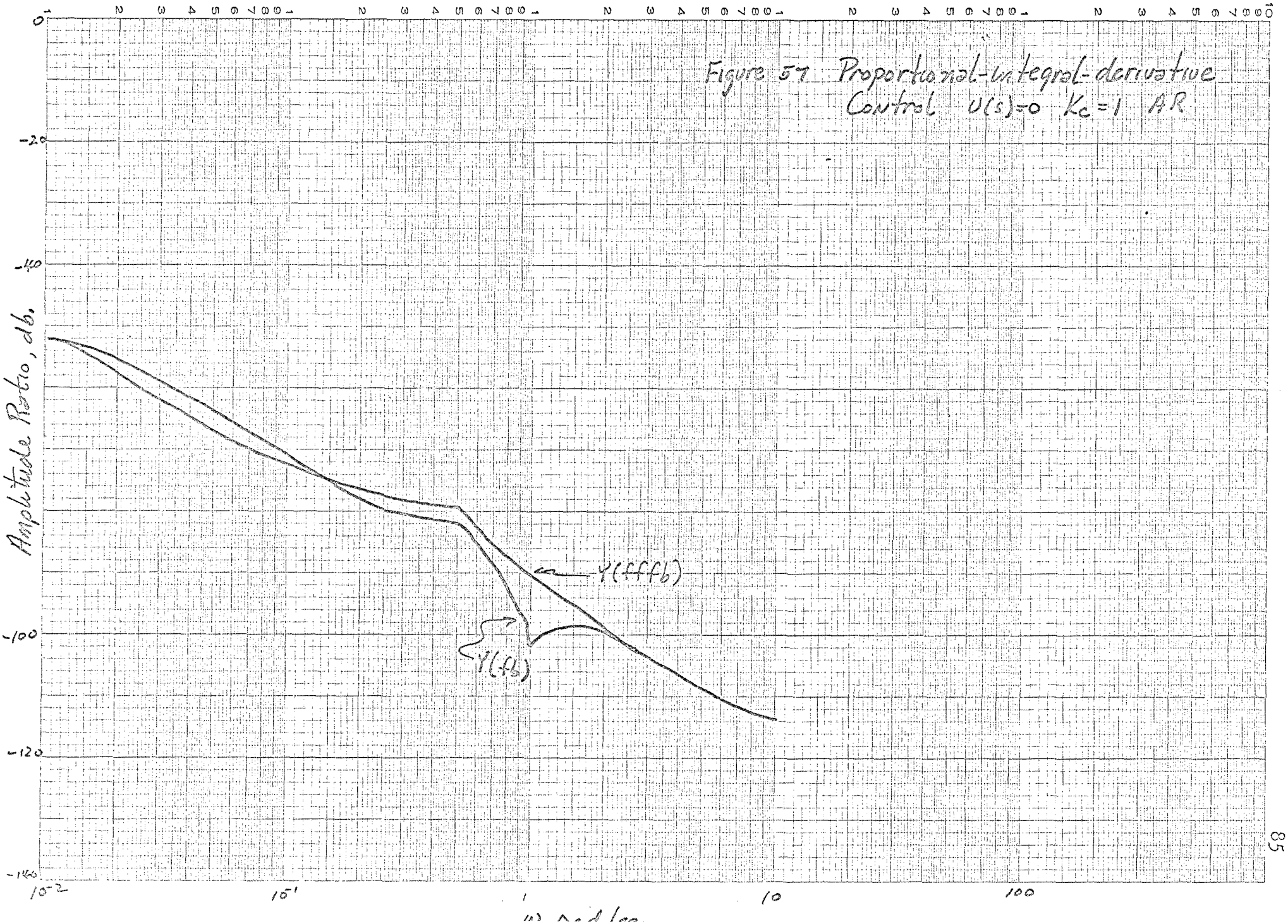

5 CYCLES X 10 DIVISIONS PER INCH

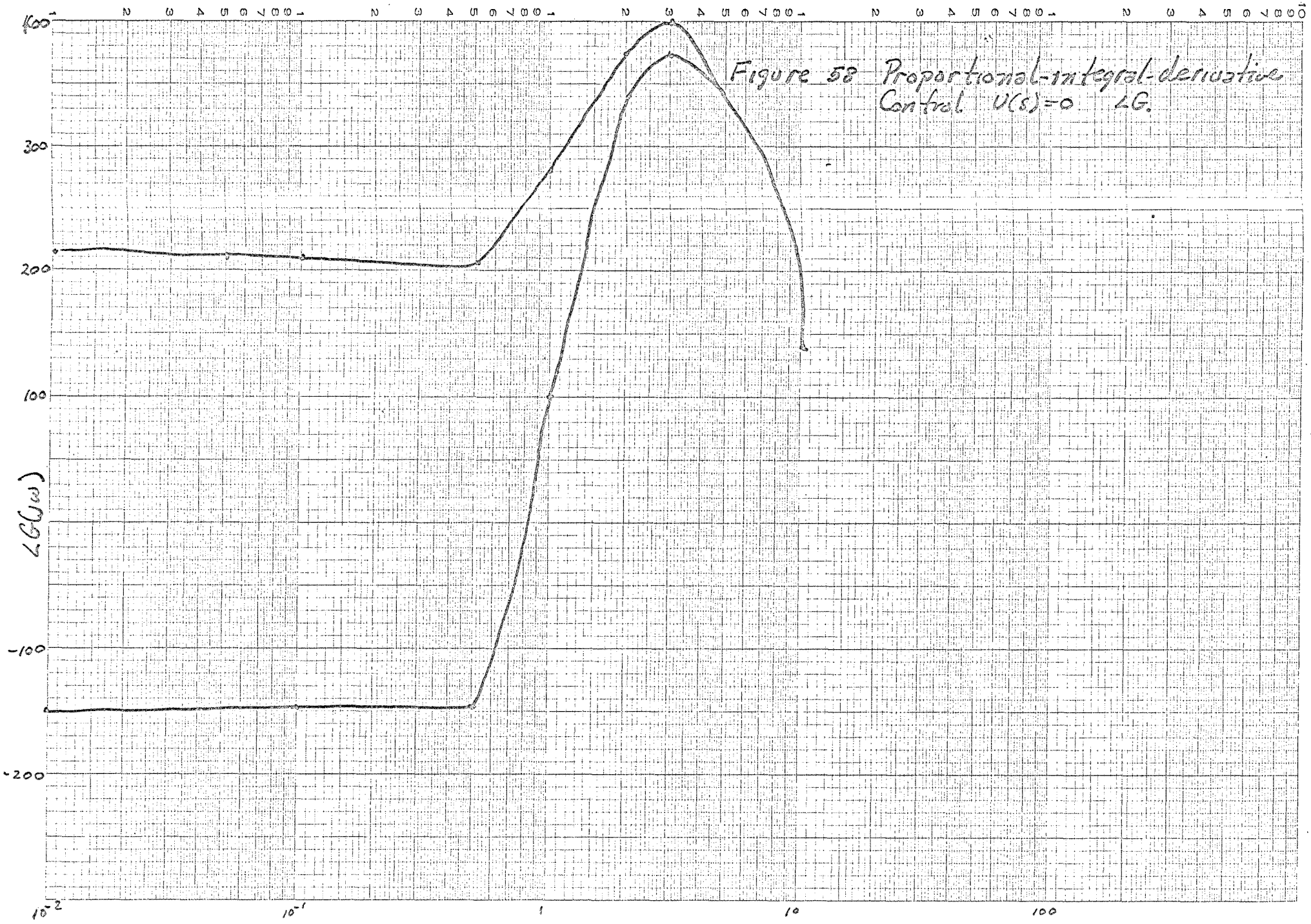

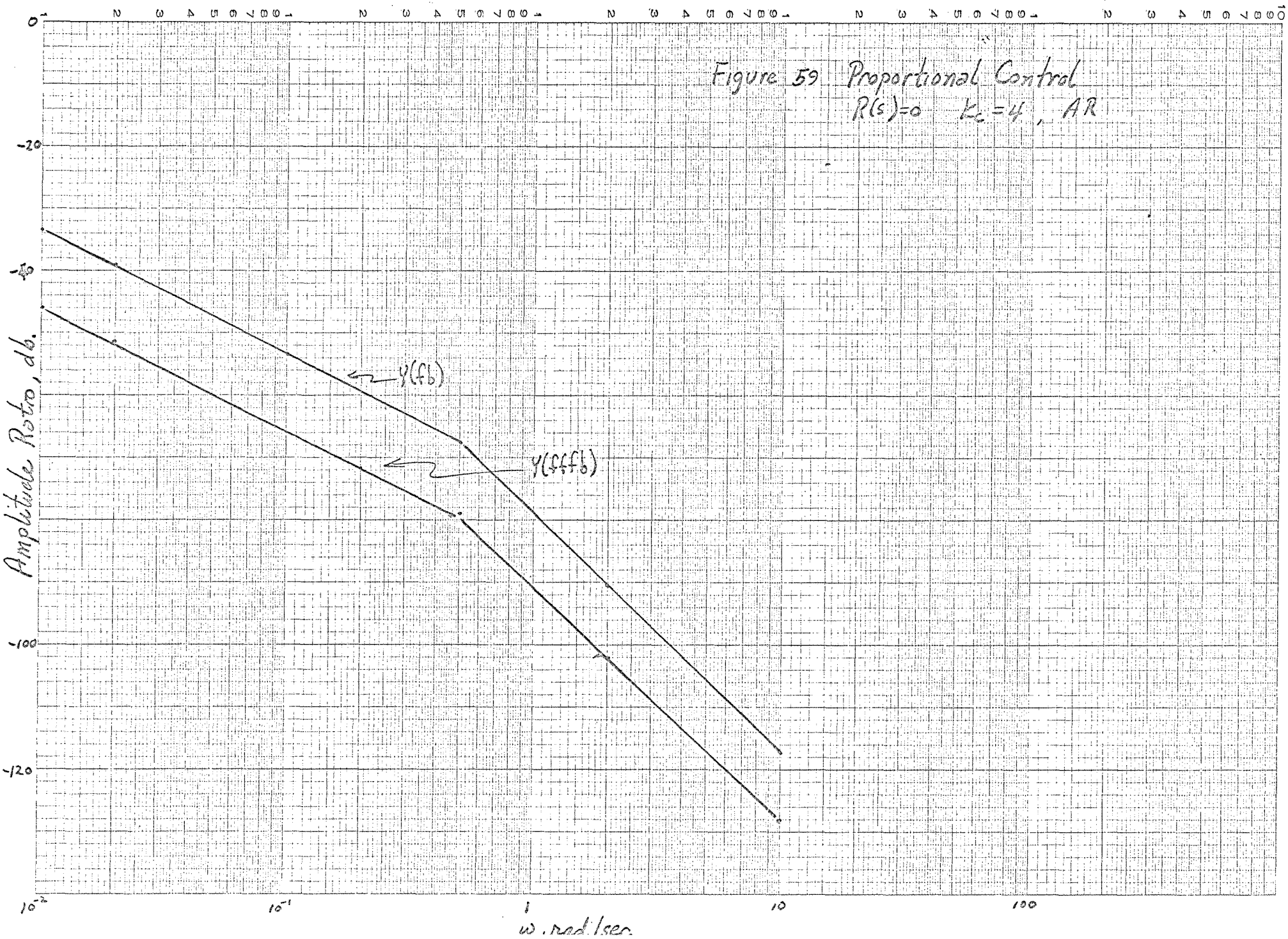

5 CYCLES X 10 DIVISIONS PER INCH

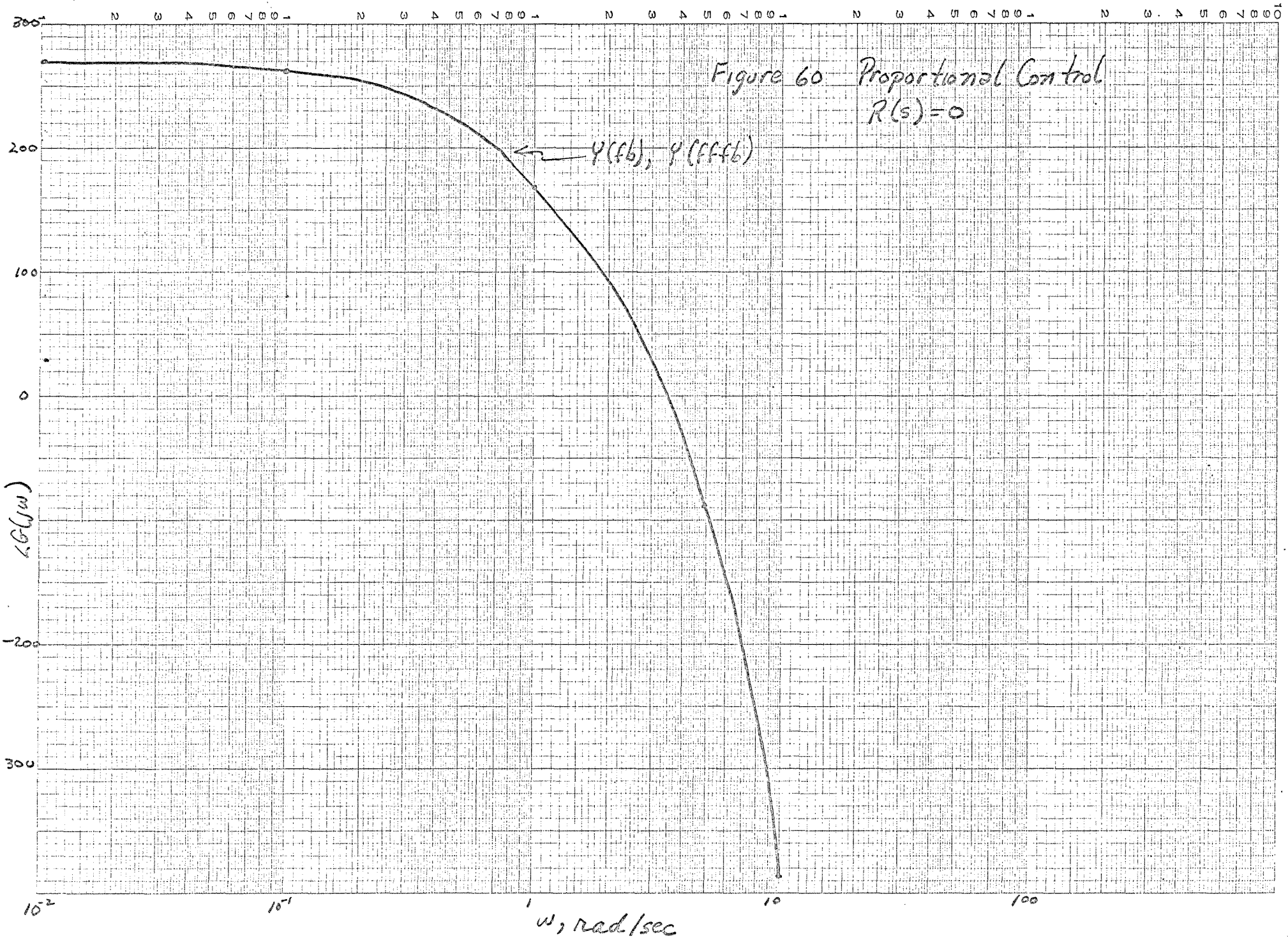

SEMI-LOGARITHMIC
5 CYCLES X 10 DIVISIONS PER INCH

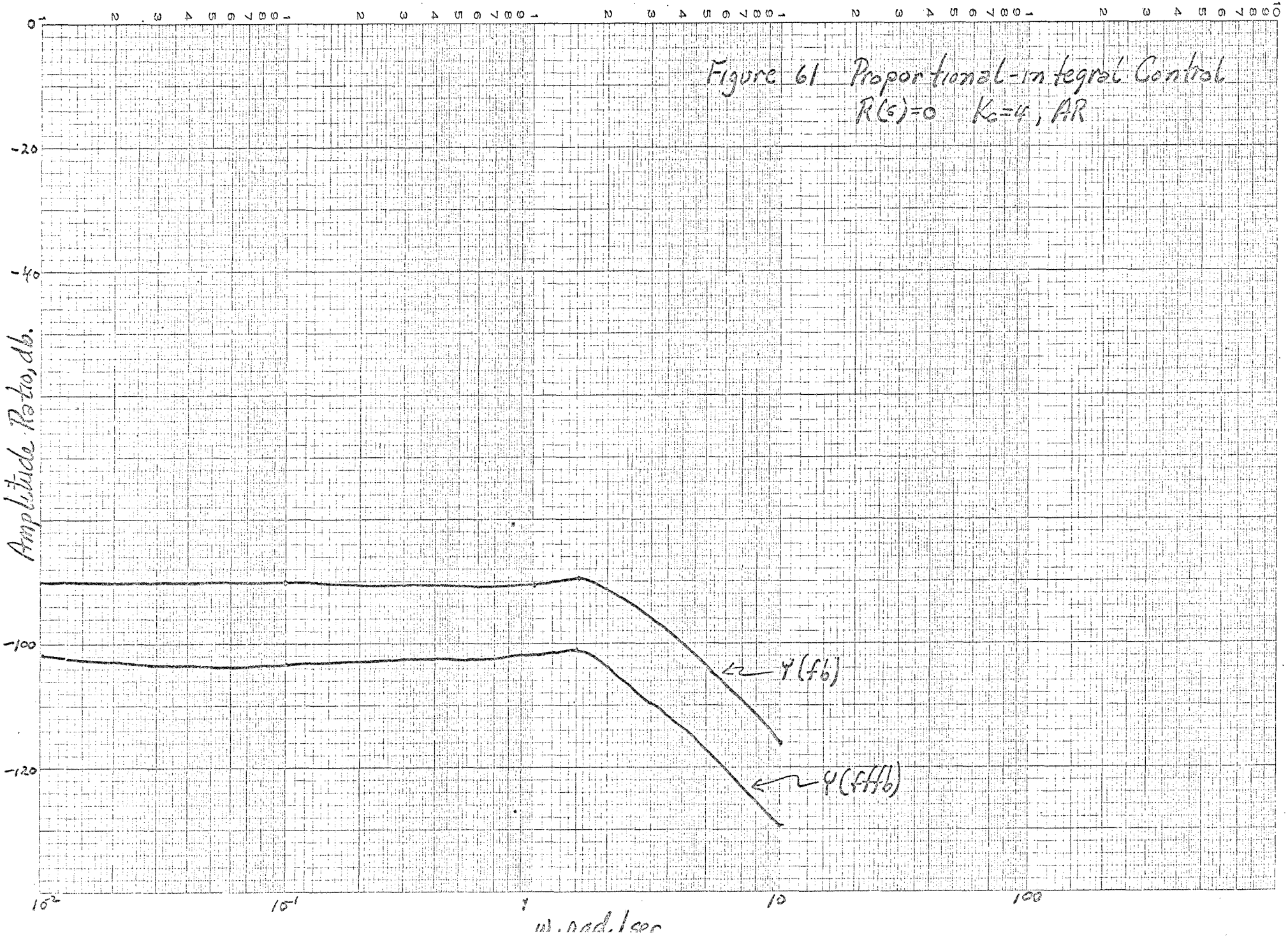

5 CYCLES X 10 DIVISIONS PER INCH

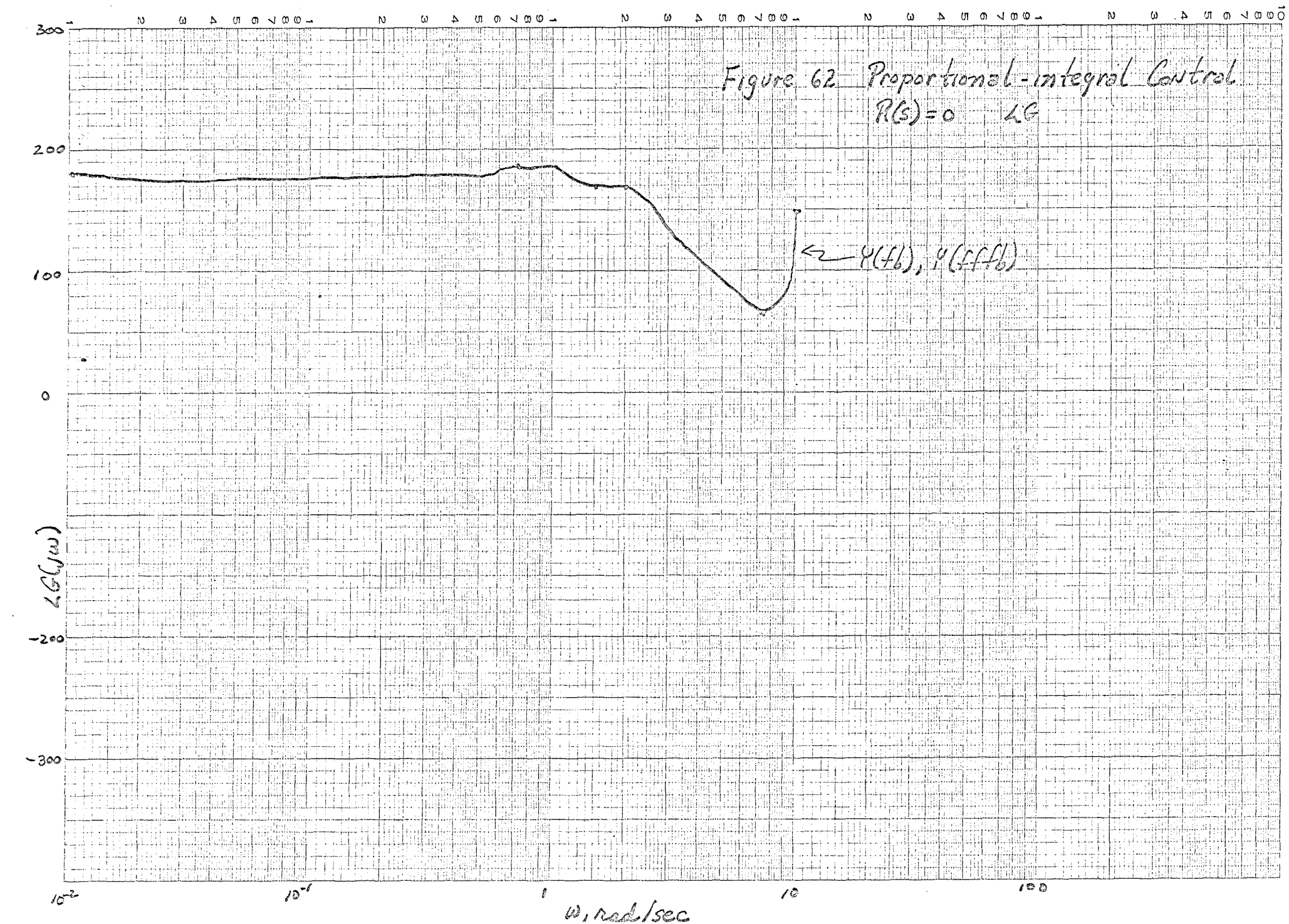

5 CYCLES X 10 DIVISIONS PER INCH

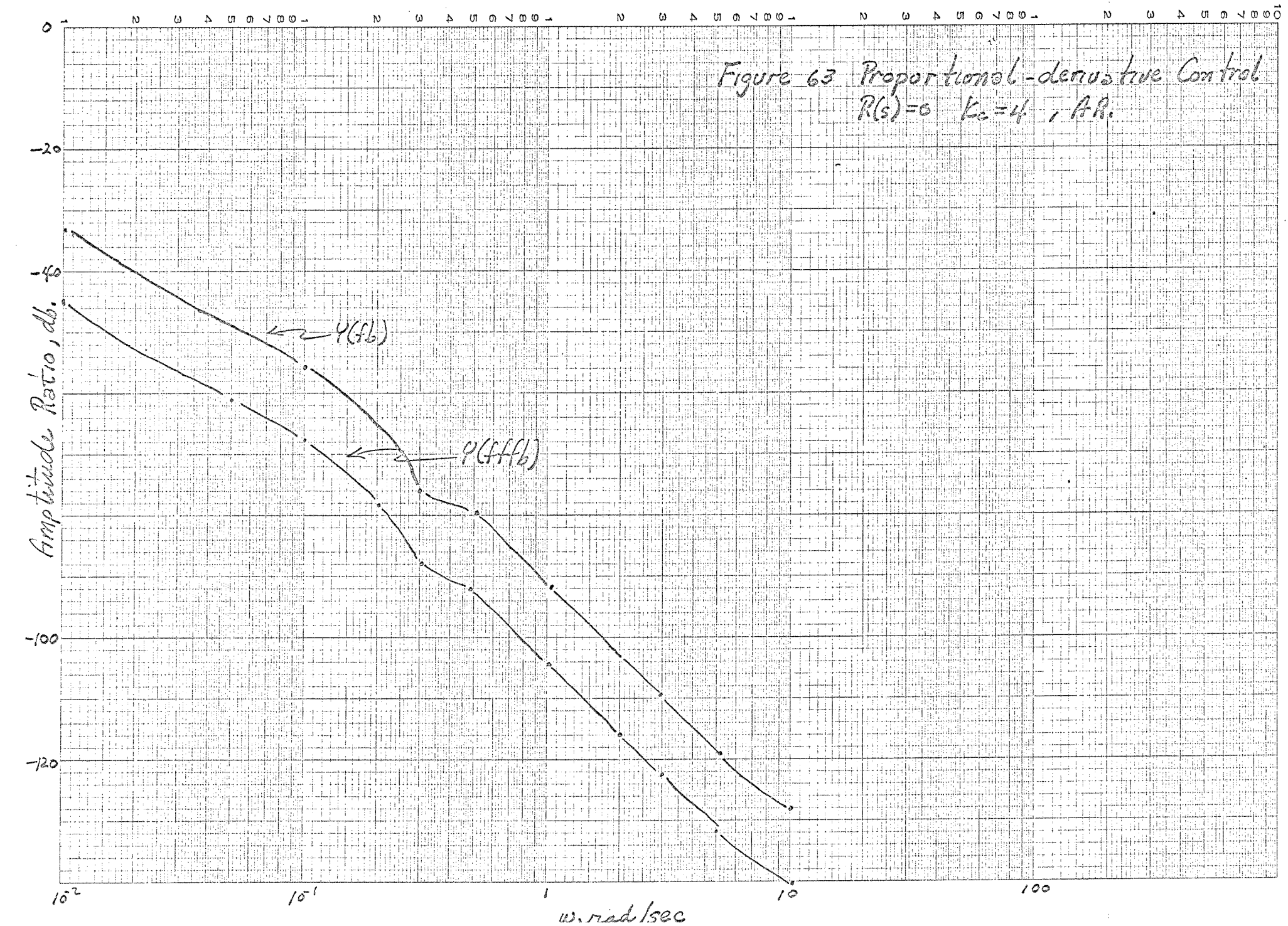

5 CYCLES X 10 DIVISIONS PER INCH

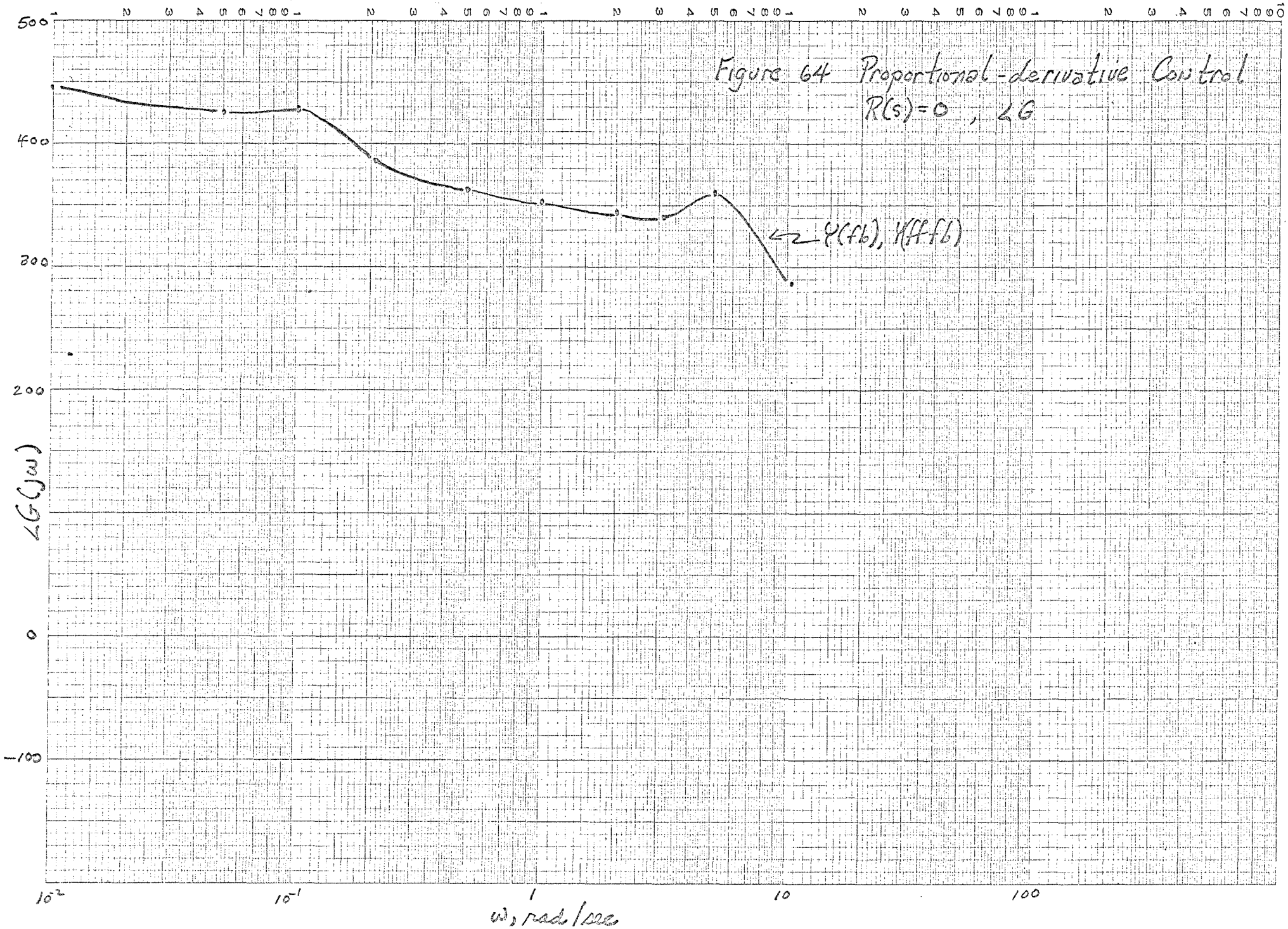

Figure 64 Proportional-derivative Control
$R(s) = 0$, $\angle G$

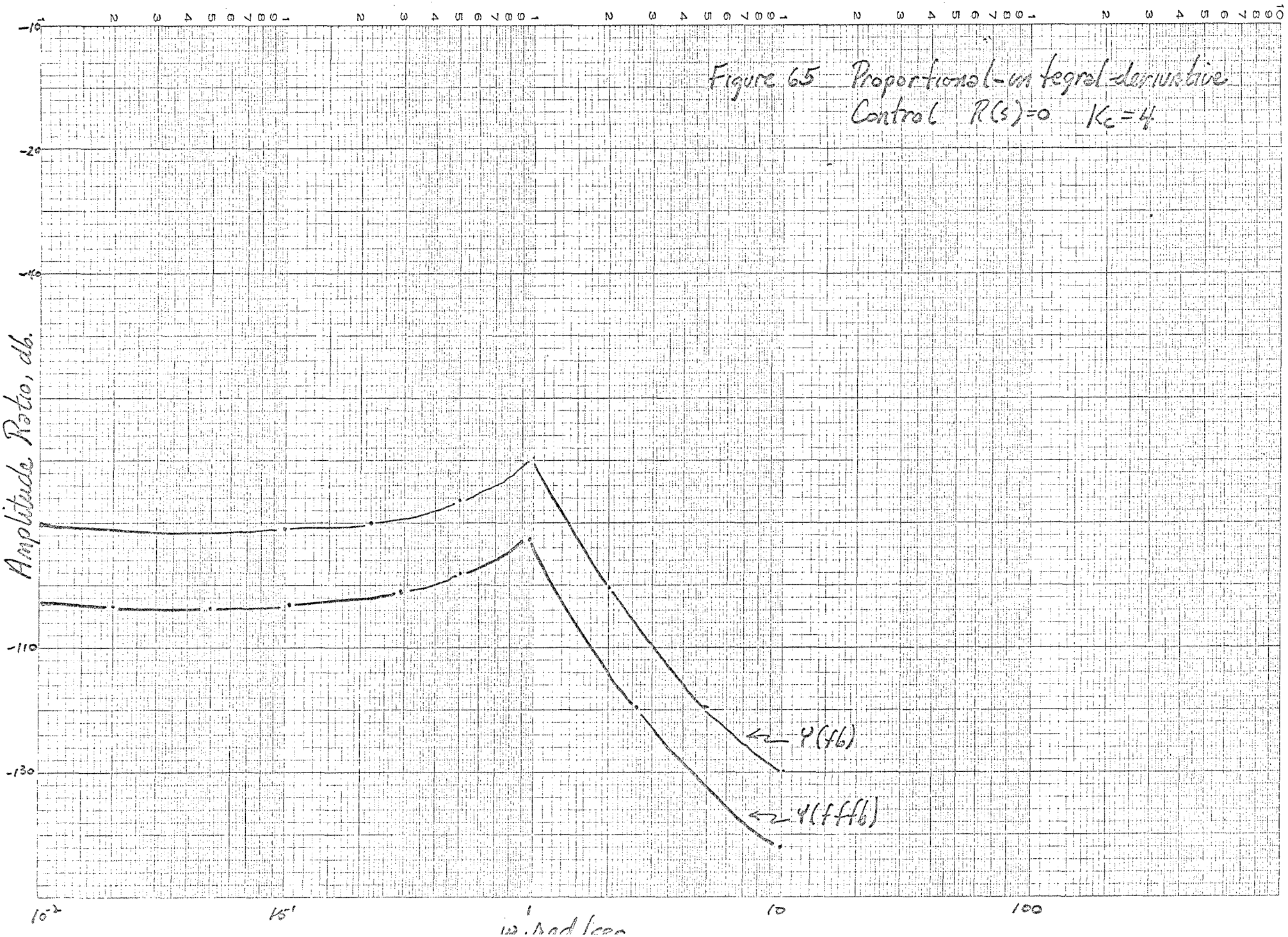

Fig 66 Proportional-entegral-derivative Control, R(s)=0 ∠G.

```
// JOB  R.E. MITCHELL CC51
// PARAM LIST=YES
// PARAM DEBUG=YES
// FORTRN
      PROGRAM R
      DIMENSION RYFF)100*,RYFB)100*,RYFFFB)100*,
      DIMENSION PYFF)100*,PYFB)100*,PYFFFB)100*
      DIMENSION XKC)3*,XTI)3*,XTD)3*
      REAL IYFF)100*,IYFB)100*,IYFFFB)100*
      REAL MYFF)100*,MYFB)100*,MYFFFB)100*
      REAL KC,KV,K1,K2,KX,KU,MAINH
      COMPLEX R,U,RF
      COMPLEX YFB)100*,FBN)100*,FBD)100*,YFF)100*
      COMPLEX FFL)100*,FFR)100*,YFFFB)100*,FFK)100*
      COMPLEX GP,S,GC
      RF)S* = 3./S
      R)S* = 0.
      U)S* = )5.56*)10.**)-3.***/S
      KV = 2.32*)10.**)-5.**
      K1 = 2160
      K2 = 1.142*)10.**5.*
      KX = 0.24
      KU = 0.1385
      T1 = 5.
      T0 = 1.
      XKC)1* = 4.
      XKC)2* = 1.
      XKC)3* = 0.5
      XTI)1* = 0.1
      XTI)2* = 10.
      XTD)1* = 0.1
      XTD)2* = 10.
      DO 100 IKC = 1,3
      DO 100 ITI = 1,2
      DO 100 ITD = 1,2
      KC = XKC)IKC*
      TI = XTI)ITI*
      TD = XTD)ITD*
      MAINH = 1.
      N = 100
      WRITE)6,10*
      WRITE)6,12* N,MAINH,KC,KV,K1,K2,T0,T1,TI,TD,KX,KU
      DO 1 I = 1,N
      X = I
      S = )0.0,1.0* *MAINH*X
      GP = )CEXP)-T0*S**/))T1*S*,1.*
      GC = KC*)1.,)1./)TI*S**  . )TD*S**
      GF = -)KU/)KX*K1*KV**
      FFL)I* = )GP*GF*KV*KX**RF)S*
      FFR)I* = )GP*))K1*KX*GF*KV*.KU**U)S**
      FFK)I* = KX*GC*KV*GP*R)S*
      YFF)I* = )FFL)I**R)S**/RF)S* - FFR)I*
      FBN)I* = GP*))KX*KV*GC*R)S**-KU*U)S**
      FBD)I* =  )1.,)KX*KV*K2*GC*GP**
      YFB)I* = FBN)I*/FBD)I*
      YFFFB)I* = )FFL)I* -FFR)I* . FFK)I**/FBD)I*
    1 CONTINUE
      DO 2 J = 1,N
      RYFF)J* = REAL)YFF)J**
      IYFF)J* = AIMAG)YFF)J**
      RYFB)J* = REAL)YFB)J**
      IYFB)J* = AIMAG)YFB)J**
      RYFFFB)J* = REAL)YFFFB)J**
```

```
      IYFFFB)J* = AIMAG)YFFFB)J**
      MYFF)J* = CABS)YFF)J**
      PYFF)J* = ATAN)IYFF)J*/RYFF)J**
      MYFB )J* = CABS)YFB)J**
      PYFB)J* = ATAN)IYFB)J*/RYFB)J**
      MYFFFB)J* = CABS)YFFFB)J**
      PYFFFB)J* = ATAN)IYFFFB)J*/RYFFFB)J**
    2 CONTINUE
      WRITE)6,16*
      DO 3 J = 1,N
      WRITE)6,18* J,RYFF)J*,IYFF)J*,RYFB)J*,IYFB)J*,RYFFFB)J*,IYFFFB)J*
    3 CONTINUE
      WRITE)6,20*
      DO 4 J = 1,N
      WRITE)6,18* J,MYFF)J*,PYFF)J*,MYFB)J*,PYFB)J*,MYFFFB)J*,PYFFFB)J*
    4 CONTINUE
  100 CONTINUE
   10 FORMAT)1H1,'N     MAINH       KC          KV          K1          K2
     1  TO          T1          TI          TD          KX          KU',/*
   11 FORMAT)8F10.0*
   12 FORMAT)1H ,I2,2X,10F12.4/1H ,10F12.4*
   16 FORMAT)1H ,'J     REAL YFF    IMAG YFF    REAL YFB    IMAG YFB    REAL
     1 YFFFB    IMAG YFFFB',/*
   18 FORMAT)1H ,I2,6)E10.4,2X*,///*
   20 FORMAT)1H ,'J    MAG YFF    PHS YFF    MAG YFB    PHS YFB    MAG YFFFB
     1 PHS YFFFB ',/*
   22 FORMAT)1H ,I2,6E10.4*
      STOP
      END
// EXEC
```

REFERENCES

1. Barnstone, L. A. and Harriott, P., "Frequency Response of Gas Mixing in a Fluidized - Bed Reactor", AICHE Journal Vol. 13, #3, May, 1967, pp. 465 - 475.

2. Caughonowr, D. R. and Koppel, L. B., Process System Analysis and Control, New York: McGraw - Hill, 1965.

3. EAI Application Study: 6.2.19a, "Combined Feedforward Feedback Control of a Chemical Reactor", EAI Bulletin #ALAC 64075.

4. EAI TR - 20 Computer Operator's Reference Handbook, Electronic Associates, Inc., 1964.

5. Echigoya, E., et al, "Method of Estimating Chemical Reaction Conversion Rate in Fluidized-beds--Heterogeneous Phase System: First Order Reaction", Kagaku Kogaku 29, 1965, pp. 892 - 898.

6. Johnson, E., Automatic Process Control, New York: McGraw - Hill, 1965.

7. Holst, Per A., "Pade-Approximations and Analog Computer Simulations of Time Delay", Simulations, June, 1969.

8. Perlmutter, D. D., Introduction to Chemical Process Control, New York: John Wiley & Sons, Inc., 1965.